THE BASAL PENGUIN (AVES: SPHENISCIFORMES) *PERUDYPTES DEVRIESI* AND A PHYLOGENETIC EVALUATION OF THE PENGUIN FOSSIL RECORD

DANIEL T. KSEPKA

Department of Marine, Earth, and Atmospheric Sciences
North Carolina State University, Raleigh, NC 27695
(daniel_ksepka@ncsu.edu)

JULIA A. CLARKE

Division of Paleontology
American Museum of Natural History, and
Department of Geological Sciences
Jackson School of Geosciences
The University of Texas at Austin
1 University Station C1100 Austin, TX 78713
(Julia_Clarke@jsg.utexas.edu)

BULLETIN OF THE AMERICAN MUSEUM OF NATURAL HISTORY
Number 337, 77 pp., 30 figures, 2 tables
Issued June 3, 2010

 ISSN 0003-0090

CONTENTS

ABSTRACT

We present the first detailed description of *Perudyptes devriesi*, a basal penguin from the middle Eocene (~42 Ma) Paracas Formation of Peru, and a new analysis of all published extinct penguin species as well as controversial fragmentary specimens. The *Perudyptes devriesi* holotype includes key regions of the skull and significant postcranial material, thus helping to fill a major phylogenetic and stratigraphic (~20 million year) gap between the earliest fossil penguins (*Waimanu manneringi* and *Waimanu tuatahi*, ~58–61.6 Ma) and the next oldest partial skeletons. *Perudyptes devriesi* is diagnosable by five autapomorphies: (1) an anteroventrally directed postorbital process, (2) marked anterior expansion of the parasphenoid rostrum, (3) posterior trochlear ridge of the humerus projecting distal to the middle trochlear ridge and conformed as a large, broadly curved surface, (4) convex articular surface for the antitrochanter of the femur, and (5) extremely weak anterior projection of the lateral condyle of the tibiotarsus. The skull of *Perudyptes* is characterized by deep temporal fossae and an elongate, narrow beak that differs from other reported stem penguins in its short mandibular symphysis. The wing skeleton of *Perudyptes* preserves a combination of plesiomorphic features also observed in the basal penguin *Waimanu* and derived features shared with more crownward penguins. Features of the wing optimized as primitive for Sphenisciformes include retention of a discrete dorsal supracondylar tubercle on the humerus and presence of a modestly projected pisiform process on the carpometacarpus. Derived features present in *Perudyptes* and all more crownward penguins, but absent in *Waimanu*, include a more flattened humerus, development of a trochlea for the tendon of m. scapulotriceps at the distal end of the humerus, and bowing of the anterior face of the carpometacarpus.

A combined molecular and morphological dataset for Spheniciformes was expanded by adding 25 osteological and soft tissue characters as well as 11 taxa. In agreement with previous results, *Perudyptes devriesi* is identified as one of the most basal members of Sphenisciformes. This analysis also confirms the placement of the middle/late Miocene (~11–13 Ma) fossil *Spheniscus muizoni* as a member of the *Spheniscus* clade and places the late Miocene (~10 Ma) *Madrynornis mirandus* as sister taxon to extant *Eudyptes*. These two species, known from relatively complete partial skeletons, are the oldest crown clade penguin fossils and represent well-corroborated temporal calibration points for the *Spheniscus*-*Eudyptula* divergence and *Megadyptes*-*Eudyptes* divergence, respectively. Our results reaffirm that the Miocene penguin taxon *Palaeospheniscus*, recently proposed to represent a member of the crown radiation, belongs outside of the crown clade Spheniscidae.

The phylogenetic positions of small Eocene Antarctic penguin taxa (*Delphinornis*, *Marambiornis*, and *Mesetaornis*) recently proposed as possible direct ancestors to crown Spheniscidae were further evaluated using alternate coding strategies for incorporating scorings from isolated elements that preserve critical morphologies and are thought to represent these taxa, although they cannot yet be reliably assigned to individual species. Under all scoring regimes, *Delphinornis*, *Marambiornis*, and *Mesetaornis* were recovered as distantly related to Spheniscidae.

Using synapomorphies identified in the primary analysis, we evaluated the phylogenetic position of fragmentary specimens, including the holotypes of valid but poorly known species, specimens currently unassignable to the species level, and morphologically distinct specimens that have not yet been named. All pre-Miocene specimens can be excluded from Spheniscidae based on presence of plesiomorphies lost in all crown penguins, consistent with a recent radiation for the penguin crown clade. This study provides additional support for a scenario of penguin evolution characterized by an origin of flightlessness near the K-T boundary, dispersal throughout the Southern Hemisphere during the early Paleogene, and a late Cenozoic origin for the crown clade Spheniscidae. Stratigraphic distribution and phylogenetic relationships of fossil penguins are consistent with distinct radiations during the Eocene, Oligocene, and Miocene. While the Eocene and Oligocene penguin faunas are similar in many respects, the Miocene fauna is characterized by smaller average size and novel cranial morphologies, suggesting that an ecological shift in diet occurred close to the origin of crown Spheniscidae.

INTRODUCTION

Sphenisciformes (penguins) are a charismatic group of flightless aquatic birds, distributed broadly throughout the Southern Hemisphere. Fossil material is abundant for the clade, owing largely to the marine habits and dense bone structure of these birds. Penguins first appear in the fossil record in the early Paleocene (~60.5–61.6 Ma) of New Zealand (Slack et al., 2006) and expand their range to nearly the entirety of their present-day geographical distribution by the late Eocene. Fossils indicate that stem penguins reached Antarctica by the late Paleocene (Tambussi et al., 2005), South America by the middle Eocene (Clarke et al., 2003, 2007), and Australia by the late Eocene (Simpson, 1957; Jenkins, 1974). Peruvian fossils reveal that these Paleogene dispersals included multiple incursions into low latitude waters by the late Eocene (Clarke et al., 2007). The middle Eocene (~42 Ma) *Perudyptes devriesi*, collected from rocks deposited at ~14°S paleolatitude, is the oldest penguin known from equatorial waters (Clarke et al., 2007).

Prior to the discovery of *Perudyptes devriesi*, penguins were poorly represented in the fossil record for the ~20-million-year interval between the age of *Waimanu tuatahi* from the Paleocene (Slack et al., 2006) and the age of the next oldest partial skeletons from the late Eocene (Marples, 1952; Fordyce and Jones, 1990). Penguin specimens known from this early Paleocene–late Eocene interval were limited to fragmentary remains. Such material includes the holotype of *Crossvalia unienwillia*, comprising three incomplete bones from the late Paleocene of Seymour Island, Antarctica (Tambussi et al., 2005), a single partial femur from the ?middle Eocene of New Zealand (Marples, 1952; see Simpson [1972] regarding stratigraphic uncertainty), a partial hindlimb and pelvis from the middle Eocene of South America (Clarke et al., 2003), and ~70 almost exclusively isolated postcranial elements and a single beak fragment from the early-middle Eocene deposits of Seymour Island, Antarctica (Jadwiszczak, 2006a, 2006b). The limited nature of this material has obscured understanding of the morphological changes that took place in the early evolution of penguins. The holotype of *Perudyptes devriesi*, by contrast, includes a well-preserved skull associated with significant postcranial material, providing new insight into this poorly understood interval of penguin evolution. In this paper, we present a detailed anatomical description of this species and a comprehensive evaluation of the penguin fossil record.

Seventy-five fossil penguin species have been named over time, but many of these were later found to be nomina dubia or synonyms of previously named species (Simpson, 1946, 1971a, 1972a; Jenkins, 1985; Myrcha et al., 2002; Acosta Hospitaleche, 2004; Jadwiszczak, 2006b; Ando, 2007). Fifty-two fossil species are provisionally considered valid in this paper, although some of these await more detailed reevaluation (see discussion in Ksepka, 2007). Additionally, two taxa have been erected based on subfossil remains interpreted as belonging to recently extinct penguin species. *Megadyptes waitaha* represents the extinct sister taxon of the extant *Megadyptes antipodes* (Yellow-eyed Penguin) based on morphological features and ancient molecular data recovered from subfossil bones from New Zealand (Boessenkool et al., 2009). *Tasidyptes hunteri* was also originally identified as a recently extinct species based on remains recovered from a midden in Tasmania (van Tets and O'Conner, 1983), although as discussed below at least some of these bones may represent extant *Eudyptes* sp. The true total of extinct species is certainly higher than those formally recognized here, as several fossils representing unique species have been mentioned in the literature (Fordyce and Jones, 1990) but are not yet formally described and named (Ando, 2007). A conservative estimate places the total number of pre-Quaternary fossil penguin specimens in scientific repositories at well over 5000 (Ksepka, personal obs.), ranging from articulated skeletons to isolated bones. Subfossil remains are even more abundant, with many thousand specimens collected from Holocene beach deposits, abandoned breeding colonies, and middens throughout the world (e.g., McEvey and Vestjens, 1973; van Tets and O'Conner, 1983; Worthy, 1997; Lambert et al., 2002; Worthy and Grant-Mackie, 2003; Emslie and Woehler, 2005; Emslie et al., 2007; Emslie and Patterson, 2007). Although the

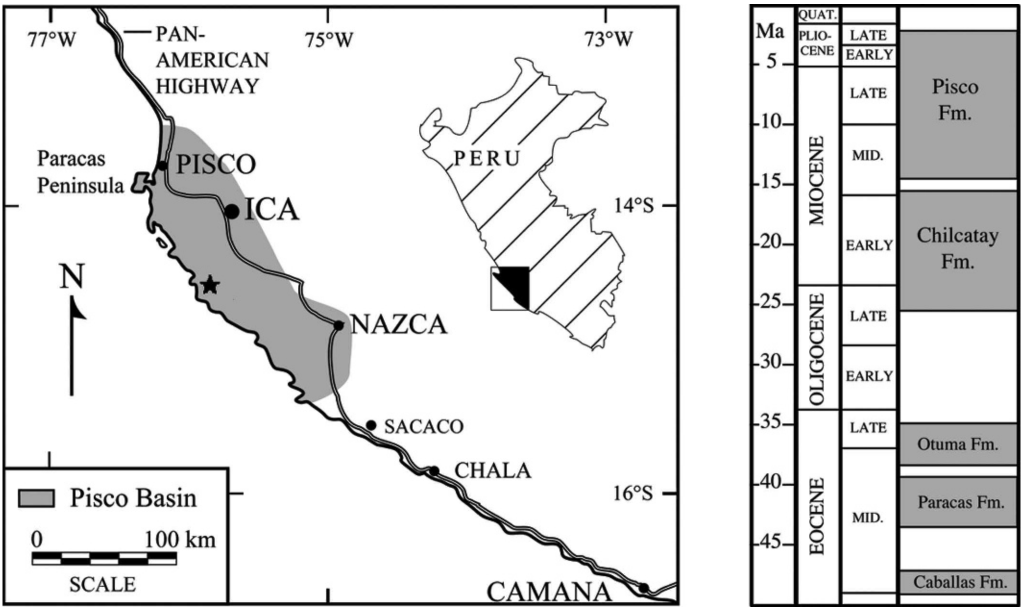

Fig. 1. Map showing the type locality of *Perudyptes devriesi* (star) and the extent of the Pisco Basin, with simplified stratigraphic column reflecting our current understanding of stratigraphy within the Pisco Basin (after Devries et al., 2006).

fossil record of penguins is rich, many species are known with certainty from only a single element. These incomplete specimens pose a challenge to phylogenetic analysis (discussed by Fordyce and Jones, 1990) and have hindered the incorporation of biogeographical, temporal, and morphological data from such taxa into the emerging synthesis of penguin evolution. Herein, we undertake an evaluation of the phylogenetic position of all fossil penguin taxa and multiple sets of remains recognized as representing as yet unnamed taxa, with the goal of improving our understanding of the tempo of penguin evolution and contributing to the debate regarding the timing of the radiation of crown Spheniscidae (Bertelli and Giannini, 2005; Baker et al., 2006; Ksepka et al., 2006; Jadwiszczak, 2006b; Clarke et al., 2007).

Geological Context of the *Perudyptes* Type Locality

Cenozoic marine sediments are exposed throughout the Pisco Basin of coastal southern Peru (fig. 1). The stratigraphy of the Pisco Basin was described in detail by Dunbar et al. (1990) and DeVries (1998). Marine deposits were laid down over the course of the Cenozoic during six major transgressions (DeVries, 1998) and preserve a wealth of fossil marine vertebrates (e.g., Muizon, 1981, 1984, 1988, 1993; Muizon et al., 2003, 2004; Stucchi, 2002, 2003, 2007; Stucchi and Urbina, 2004; Stucchi and Emslie, 2005; Stucchi et al., 2003; Clarke et al., 2007; Esperante et al., 2008; Ksepka et al., 2008; Lambert et al., 2008) and invertebrates (e.g., Rivera, 1957; de Muizon and DeVries, 1985; DeVries, 2007). *Perudyptes devriesi* is known from a single specimen collected from the middle Eocene Paracas Formation (Choros Formation of Dunbar et al., 1990). The Paracas Formation directly overlies crystalline basement rocks and is separated by an unconformity from the overlying middle-upper Eocene Otuma Formation (DeVries et. al., 2006; DeVries, 2007). The Paracas Formation comprises a basal transgressive sandstone member representing a comparatively nearshore paleoenvironment and grading upward into a fine-grained, tuffaceous, and diatomaceous silty sandstone member representing a more distal shelf paleoenvironment (DeVries, 2007). The *Per-*

udyptes devriesi holotype (MUSM 889) was collected from the southern wall of the Quebrada Perdida locality (14°34′S, 75°52′W) in an orange, coarse-grained, thick-bedded, siliciclastic sandstone bed that has been identified as part of the basal member of the Paracas Formation (DeVries, 1998). The beds containing the *Perudyptes devriesi* holotype are located a few tens of meters above the rugged platform of crystalline basement rock. Based on the presence of late middle Eocene radiolarians (*Cryptocarpium ornatum*, *Lithocyclia aristotelis*, *Lithocyclia ocellus*) higher in the section and the gastropod *Turritella lagunillasensis* in correlative sandstone beds, the age of these beds is ~42 Ma (DeVries et al., 2006).

Littoral invertebrate remains support deposition of the basal Paracas sandstone at Quebrada Perdida as close to the paleoshoreline. During the Eocene, Quebrada Perdida would have been located at a paleolatitude nearly equivalent to the 14°34′S present-day latitude, as there has been essentially no latitudinal translation of the area since the late Jurassic (Jesinkey et al., 1997; Somoza and Tomlinson, 2002; Hartley et al., 2005). Cold-water upwelling along the western coast of Peru appears to have been in place by the Late Cretaceous or early Tertiary (Keller et al., 1997), and this "proto-Humboldt" current may have influenced low-latitude penguin diversity by cycling cold, nutrient-rich water into the ecosystem (Clarke et al., 2007). Sedimentary evidence indicates that land adjacent to the coast was continuously arid or semiarid from the Jurassic to present day (Hartley et al., 2005).

Additional fossils from the Paracas Formation currently awaiting description suggest that a minimum of three penguin taxa occupying a range of body sizes occurred in the middle Eocene of Peru. Based on the size of preserved limb bones, the holotype individual of *Perudyptes devriesi* was comparable in size to the King Penguin (*Aptenodytes patagonicus*), the second largest extant penguin species. A smaller penguin (~75% the size of *Perudyptes devriesi*) is represented by a partial tibiotarsus and a partial tarsometatarsus (MUSM 890). Three large specimens significantly surpassing comparable elements of *Perudyptes devriesi* in size have also been collected (MUSM 891, 892, 894), but because of incomplete preservation it remains uncertain whether all specimens belong to the same taxon or multiple species are represented. However, these materials indicate that a diverse penguin fauna was well established in Peru by the middle Eocene (Clarke et al., 2007). Only one extant species of penguin (*Spheniscus humboldti*, Peruvian Black-footed Penguin) occurs regularly along the coast of Peru today, and only this species plus *Spheniscus mendiculus* (Galapagos Penguin) occur at latitudes below 20°S (Williams, 1995). While time averaging must be taken into account, the presence of at least three distinct taxa in a relatively narrow stratigraphic interval suggests greater sphenisciform diversity in Peru, and at low latitudes in general, during the Eocene than in the present.

Taxonomic Background

Clarke et al. (2003) proposed phylogenetic definitions for higher taxa within the penguin total group. Under these definitions, Pansphenisciformes is applied to the clade including all taxa more closely related to Spheniscidae than any other extant avian lineage. Sphenisciformes is applied in a more exclusive sense to the clade including all Pansphenisciformes that share the apomorphic loss of aerial flight. These taxa currently include the same set of known species. However, volant basal members of the penguin lineage (not yet reported in the fossil record) would be placed within Pansphenisciformes but excluded from Sphenisciformes. Spheniscidae is applied to the crown clade of penguins, comprising the most recent common ancestor of all living penguin species and its descendants. We employ this recommended taxonomy throughout this paper.

Institutional Abbreviations

AMNH, American Museum of Natural History; CADIC, Centro Austral de Investigaciones Científicas, Tierra del Fuego, Argentina; CM, Canterbury Museum, Christchurch, New Zealand; IB/P/B, Prof. A. Myrcha University Museum of Nature, University of Bialystok, Bialystok, Poland; MLP, Museo de La Plata, La Plata, Argentina; MNZS, Museum of New Zealand Te Papa Tongarewa, Wellington, New Zealand; MUSM, Museum of San Marcos University, Lima, Peru; NMV, National Museum of Victoria, Melbourne, Australia; OM, Otago Museum, Dunedin, New Zealand; OU, Otago University Geology Museum, Dunedin, New Zealand; SAM, South African Museum, Cape Town, South Africa; SAMA, South Australian Museum, Adelaide, Australia; UCMP, University of California Museum of Paleontology, Berkeley, CA; USNM, National Museum of Natural History, Smithsonian Institution, Washington, DC.

SYSTEMATIC PALEONTOLOGY

AVES LINNAEUS, 1758 (SENSU GAUTHIER, 1986)
NEOGNATHAE PYCRAFT, 1900
SPHENISCIFORMES SHARPE, 1891 (SENSU CLARKE ET AL., 2003)
PERUDYPTES DEVRIESI CLARKE ET AL., 2007

DESCRIPTION AND COMPARISONS

SKULL: The cranium of the *Perudyptes devriesi* holotype (figs. 2–3) is nearly complete posterior to the nasal-lacrimal contact, although it lacks palatal elements. The quality of preservation of the skull roof is high, but crushing has obscured much of the occipital region. A portion of the premaxilla was also recovered disarticulated from the remainder of the cranium.

The preserved portion of the premaxilla shows that the internarial bar is suboval in cross-section, as in *Archaeospheniscus lopdelli*. Most extant penguins also present a similar premaxilla shape in cross-section. However, the ventral surface of the internarial bar in *Spheniscus* is more flattened and possesses slight ventral projections along the lateral margins, giving the internarial bar an inverted U-shaped cross-section. The sutures between the left and right premaxillae, as well as those between the premaxillae and nasals, are completely obliterated on the dorsal surface in *Perudyptes devriesi*. Ventrally, the premaxillae are convex and share a sutural contact demarcated by a shallow depression.

A salt gland fossa embays the supraorbital margin of the frontals and extends ventrally along the anterior surface of the postorbital process to near the tip of the process. In extant penguins and *Paraptenodytes antarcticus* this fossa varies in development on the frontals, but it does not extend along the anterior face of the postorbital process. The surface occupied by the salt gland is unusually smooth compared to extant penguins and other fossil taxa, where this surface is rough and deeply pitted. Although a smoother surface is characteristic of juvenile extant penguins, MUSM 889 shows full fusion of all preserved elements and does not exhibit unfinished texturing of the limb bones, suggesting that the holotype individual represents an adult. A lateral shelf of bone bounds the salt gland fossa in extant *Pygoscelis*, *Megadyptes*, and most exemplars of *Eudyptes* as well as some outgroup taxa (Diomedeidae), but this shelf is absent in *Perudyptes devriesi* and most other stem Sphenisciformes (Ksepka and Bertelli [2006] inferred the presence of a shelf in a single interorbital fragment from the late Eocene of Antarctica). The postorbital process of *Perudyptes devriesi* is anteriorly deflected, a proposed apomorphy of the species. The relative width of the frontals between the orbits is narrow, comparable to the width in *Waimanu tuatahi* (Slack et al., 2006: fig. 1).

Deep temporal fossae incise the posterior portion of the skull roof. A clearly defined sagittal crest is formed where the crests bounding these fossae meet at midline. The sagittal crest meets the nuchal crest at a nearly 90° angle. The edges of the temporal fossae are particularly well demarcated anteriorly. A small foramen for the external ophthalmic artery perforates the squamosal in the caudoventral area of the temporal fossa. The sharp, anteroposteriorly elongate sagittal crest of *Perudyptes devriesi* most closely resembles that of *Paraptenodytes antarcticus*. In *Waimanu tuatahi*, skulls assigned to *Palaeospheniscus*, and extant and extinct species of *Spheniscus*, the sagittal crest tends to be wider, with greater separation of the temporal fossae (Zusi, 1975; Acosta Hospitaleche and Canto, 2005; Slack et al., 2006). Intraspecific variation in the separation of the temporal fossae occurs within

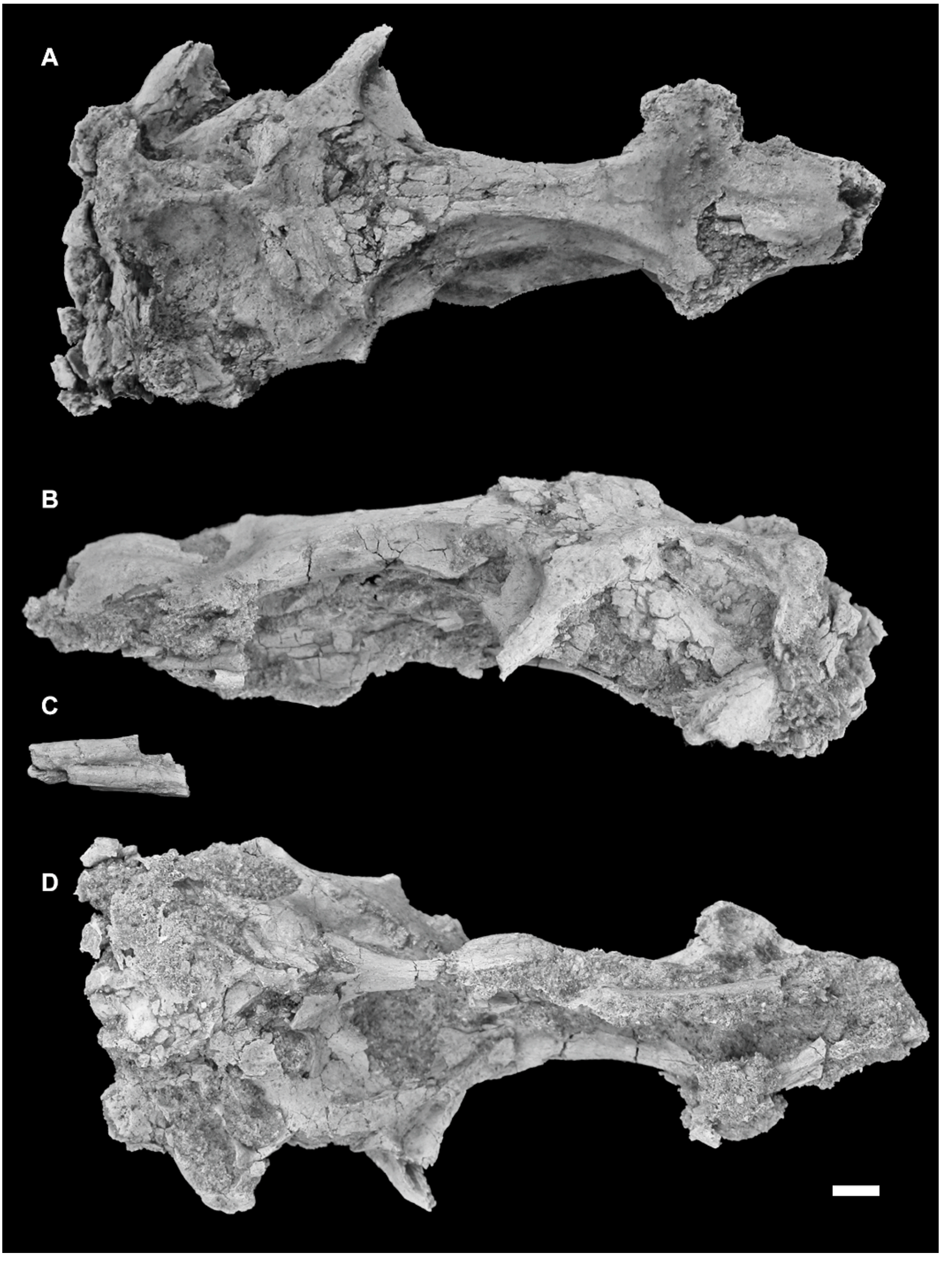

Fig. 2. Cranium of MUSM 889 in (**A**) dorsal view, (**B**) left lateral view, and (**D**) ventral view. Fragment of upper beak (**C**) in lateral view. Scale bar = 1 cm.

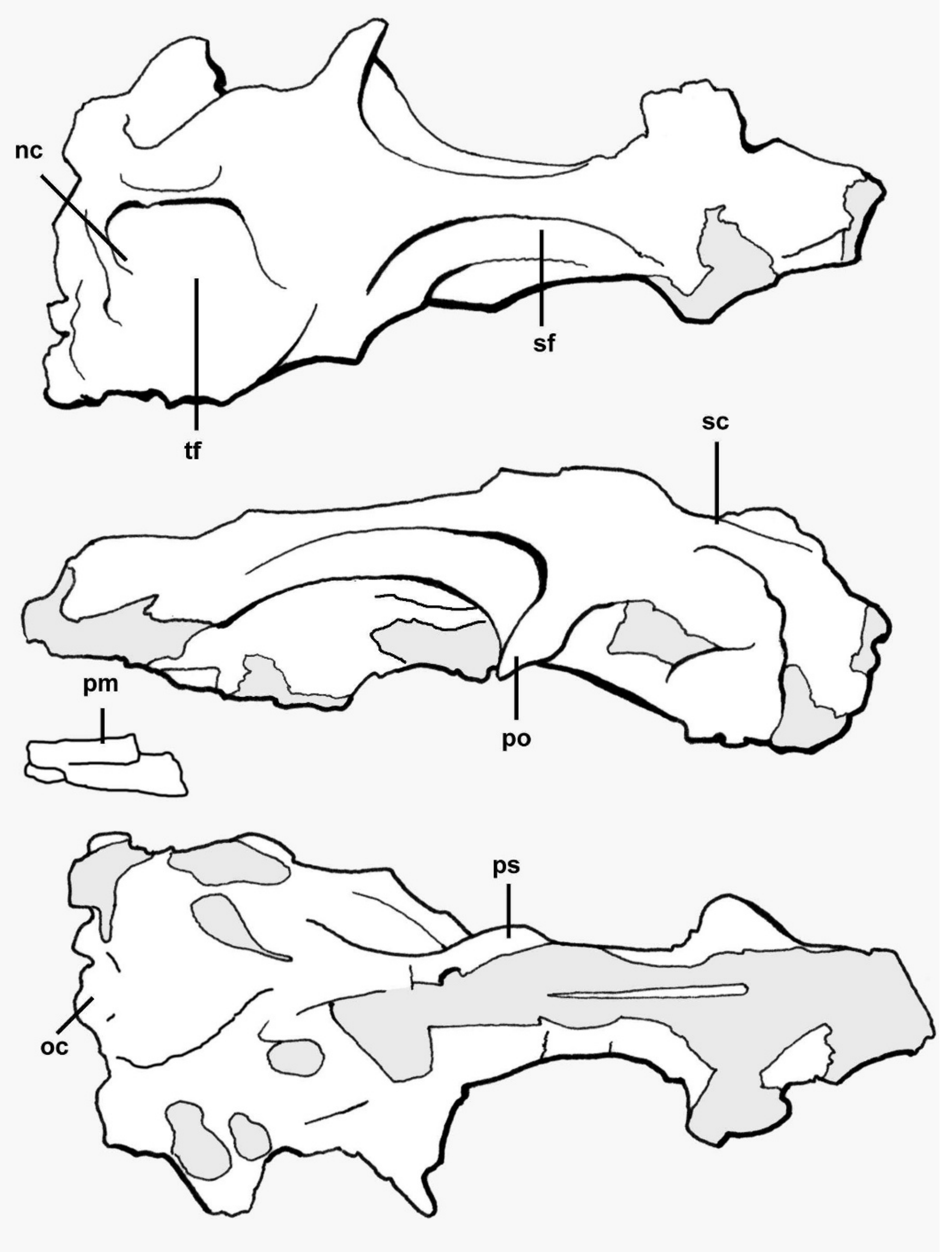

Fig. 3. Line drawings of the cranium of MUSM 889 in same views as figure 2. See appendix 5 for abbreviations.

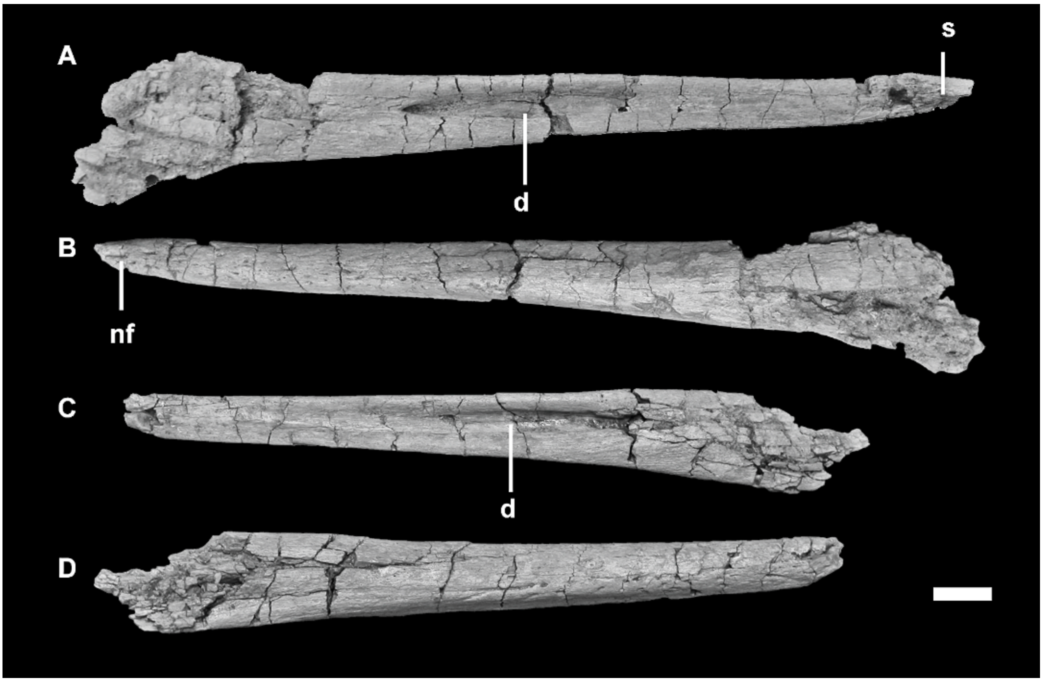

Fig. 4. Mandible of MUSM 889: (**A**) left mandibular ramus in medial view, (**B**) left mandibular ramus in lateral view, (**C**) right mandibular ramus in medial view, and (**D**) right mandibular ramus in lateral view. Scale bar = 1 cm. See appendix 5 for abbreviations.

extant *Spheniscus* species (Ksepka and Bertelli, 2006), but sample sizes in fossil taxa remain too small to evaluate variation in extinct taxa.

A portion of the mesethmoid is intact. This element attaches to the frontals along the midline, but there is no trace of the thin lateral expansion for the olfactory chamber present in extant penguins. The delicate nature of the mesethmoid leaves it susceptible to damage, but as we were unable to identify a broken edge, the absence of the expansion appears to be real.

The dorsal tympanic recess is located in a circular fossa that is posteriorly bounded and distinct from the basicranium-quadrate articulation. The parasphenoid rostrum flares laterally, forming a well-developed shelflike surface near its anterior end. Small ridges that bound the ventral surface of the parasphenoid rostrum are especially visible in this slightly expanded region. We interpret this surface as a support for the palatines near the palatine-pterygoid articulation, although a skull preserving the complete palate is necessary to confirm this hypothesis. The occipital condyle is wider than high. As in other penguins, the supraoccipital projects caudally to form a hood over the occipital condyle. Dorsoventral compression at the posterior part of the cranium distorts the shape of the foramen magnum and obscures the morphology of surrounding elements.

The mandible (fig. 4) is preserved from the symphysis to the caudal tip of the dentary. It is elongate and narrow, although it does not exhibit the extreme spearlike morphology of *Icadyptes salasi* (Clarke et al., 2007; Ksepka et al., 2008). The symphysis is short, contrasting with the extensive symphysis in the stem sphenisciforms *Waimanu tuatahi*, *Icadyptes salasi*, and *Archaeospheniscus lowei*. The rostral tip is not entirely intact, but the beak is tapering at the most distal preserved point, indicating that at most a small fragment has been lost. The mandibular ramus is very straight with no noticeable deepening at the midpoint. A rostral mandibular fenestra is absent. A conspicuous elongate depression is present on the lingual surface of the dentary. As noted by Clarke et al. (2007), a similar depression is present in an isolated Eocene penguin beak from Antarctica and also occurs in Gaviidae (loons), but it is absent in extant penguins. The dentary of *Perudyptes devriesi* is forked posteriorly as in other penguins. Because the mandible is incomplete posteriorly and the upper bill is preserved only as a small fragment, the precise proportions of the rostrum to the rest of the skull cannot be assessed.

HUMERUS: The humerus (fig. 5) exhibits the flattening typical of wing-propelled diving birds. However, the shaft is less flattened and more narrow than in all other penguin taxa save *Waimanu* (table 1). Livezey (1989) reported that the humerus was more flattened and/or longer in 11 stem fossils than in extant Spheniscidae, while the stem taxon *Palaeospheniscus* was similar in proportions to extant taxa. Our values are not directly comparable because we collected measurements from midshaft while Livezey (1989) calculated flatness from minimum and maximum dimensions of the shaft. However, our calculations broadly agree with those of Livezey (1989) in that basal penguins (e.g., *Waimanu tuatahi*, *Palaeeudyptes gunnari*, *Icadyptes salasi*) possess less strongly flattened humeri.

The broken left humerus of the *Perudyptes* holotype reveals a dense, osteosclerotic bone structure, also observable in the bones of the hindlimb. The humeral head is reniform, but it is less strongly kidney-shaped than in extant penguins. In proximal view, the ligament insertion pit (Ksepka et al., 2006: fig. 8) observed in many extant penguins is absent. The apex of the humeral head is located close to the midpoint of the head. The dorsal tubercle is nearly level with the apex of the humeral head. A similar morphology is seen in *Pachydyptes ponderosus*, *Waimanu tuatahi*, and *Anthropornis nordenskjoeldi*, while the dorsal tubercle is located more distally relative to the humeral head in *Paraptenodytes antarcticus*, *Archaeospheniscus lowei*, and Spheniscidae. The transverse sulcus and capital incisura are confluent. The tricipital fossa is a single chamber and lacks a pneumatic foramen. Compared to that of extant penguins, the tricipital fossa is smaller in proportion to the size of the humerus. A deep secondary tricipital fossa is developed on the posterior face of the humerus and excavates a significant portion of the humeral head. This secondary tricipital fossa is not bounded distally by a ridge of bone.

An oblong depression marks the insertion of m. pectoralis on the anterior face of the humerus. This depression is noticeably shallower than in all other penguins, with the exception that *Waimanu tuatahi* has a similarly shallow depression. On the posterior face of the humerus, the insertion of m. supracoracoideus is elongated proximodistally as is typical for penguins and other wing-propelled diving birds such as alcids and diving petrels. A small, round, slightly raised scar for the insertion of m. latissimus dorsi arises just proximal to the midpoint of the shaft and is widely separated from the scar for m. supracoracoideus. Overall, the shaft has a moderately sigmoid shape similar to the humeri of *Palaeeudyptes gunnari* and *Palaeeudyptes klekowskii* (Jadwiszczak, 2006a: figs.7–8), although it is less strongly sigmoid than in *Anthropornis nordenskjoeldi* or *Archaeospheniscus lowei* (e.g., Marples, 1952; Jadwiszczak, 2006a). The preaxial angle is prominent and located on the distal half of the shaft. Dorsoventral width remains nearly constant for the length of the shaft. A compact tubercle is present near the distal end on the posterior face, close to the dorsal margin. The position of this tubercle suggests that it represents the dorsal supracondylar tubercle, particularly when the oblique flattening of the sphenisciform distal humerus is taken into account (Clarke et al., 2007). This tubercle has not been described in any other penguin, although it appears to be present in *Waimanu tuatahi* (Slack et al., 2006: fig. 1).

At the distal end of the humerus, the radial condyle projects far beyond the dorsal margin of the shaft. The ulnar condyle is damaged, but preservation is consistent with prominent projection and a rounded shape. A prominent shelf also extends anteriorly from the edge of the ulnar condyle. The width of this shelf varies in penguins from wider than the ulnar condyle in some stem taxa (e.g., *Icadyptes salasi*, *Pachydyptes ponderosus*) to extremely narrow in Sphenis-

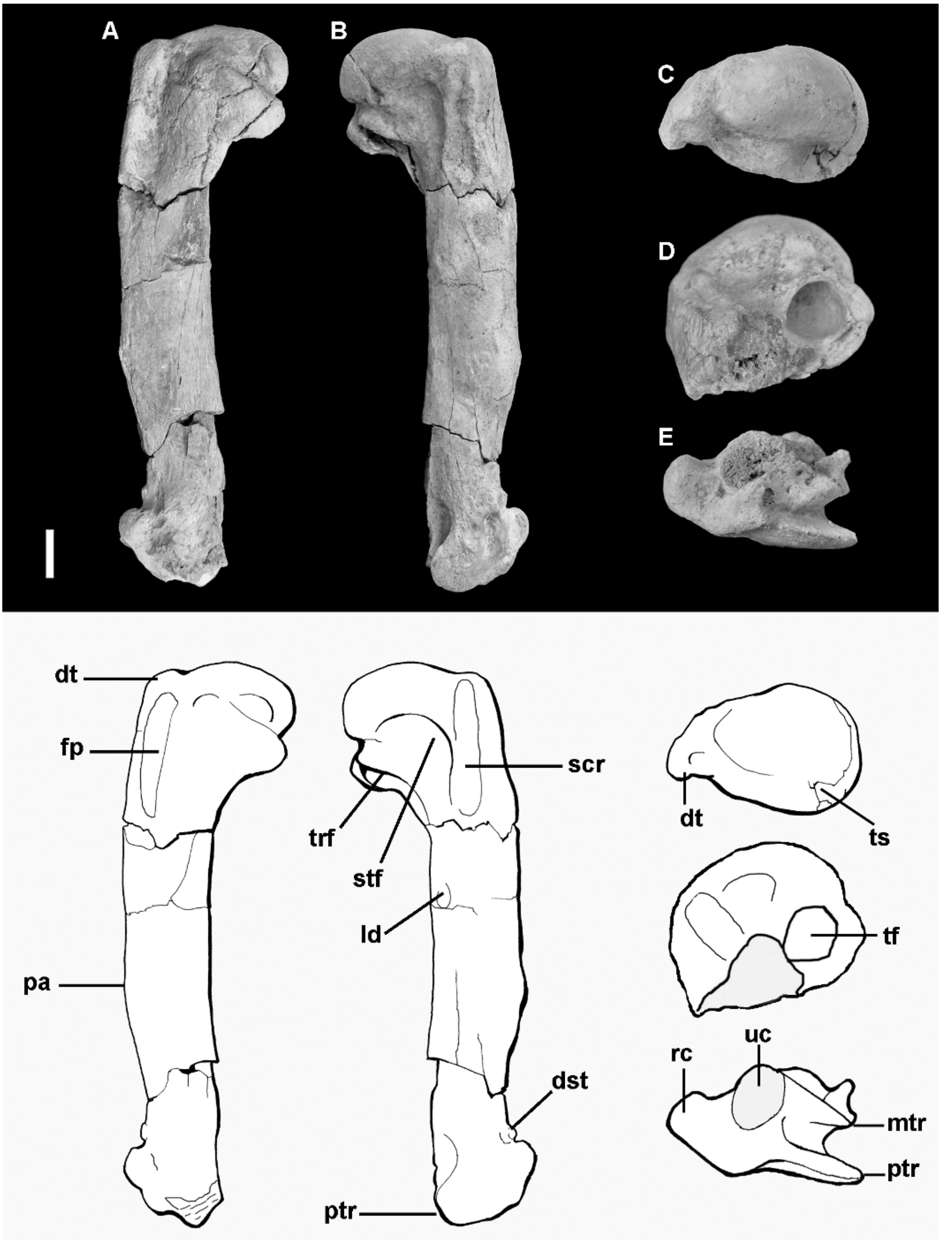

Fig. 5. Right humerus of MUSM 889 in (**A**) cranial, (**B**) cadual, (**C**) proximal, and (**E**) distal views. Head of left humerus (**D**) in oblique distal view. The remainder of the shaft is missing from the left humerus. Scale bar = 1 cm. See appendix 5 for abbreviations.

TABLE 1

Comparative dimensions of penguin humeri

Because the distal edges of the trochlear ridges are often damaged in fossil specimens, length was measured from the head to the distal edge of the ulnar condyle. For extant species, only wild specimens were sampled. All other measurements were taken with digital calipers and rounded to the nearest 0.1 mm. Depth was measured from the anterior to posterior margin and width from the dorsal to ventral margin.

Taxon	Specimen	Total Length	Width Index (midshaft width/ length)	Thickness Index (midshaft depth/ length)	Flatness Index (midshaft width/ midshaft depth)
Anthropodyptes gilli	AMNH 7609 (cast of holotype)	157.6	0.19	0.08	2.36
Archaeospheniscus lowei	OM GL407	125.3	0.19	0.08	2.29
Burnside "*Palaeeudyptes*"	OM GL435	152.1	0.20	0.09	2.21
Duntroon "*Palaeeudyptes*"	OM GL427	164.9	0.19	0.08	2.55
Duntroon "*Palaeeudyptes*"	OM GL432	161.6	0.20	0.08	2.59
Icadyptes salasi	MUSM 897	164.0	0.22	0.10	2.14
Pachydyptes ponderosus	MNZS 1450	172.5	0.26	0.11	2.33
cf. "*Palaeeudyptes*" Australian specimen	AMNH 7201 (cast of SAM P7158)	151.7	0.17	0.08	2.02
Palaeeudyptes gunnari	UCMP 321826	135.9	0.17	0.08	2.17
Palaeeudyptes klekowskii	UCMP 321023	156.2	0.17	0.09	1.99
Palaeospheniscus patagonicus	AMNH 3340	70.3	0.23	0.10	2.51
Paraptenodytes antarcticus	AMNH 3338	106.4	0.17	0.08	2.06
Paraptenodytes robustus	OU 2251	88.1	0.22	0.09	2.30
Perudyptes devriesi	MUSM 889	113.8	0.16	0.08	1.93
Platydyptes amiesi	OM GL434	108.4	0.26	0.11	2.48
Tereingaornis moisleyi	CM zfa-11	59.7	0.19	0.08	2.43
Waimanu tuatahi	OU 12651	107.1	0.12	0.07	1.81
Aptenodytes forsteri	$n = 12$	125.1 ± 4.1	0.20	0.08	2.39
Eudyptes chrysolophus	$n = 3$	63.3 ± 2.3	0.22	0.09	2.45
Eudyptula minor	$n = 5$	45.2 ± 1.8	0.17	0.08	2.26
Megadyptes antipodes	$n = 2$	73.9 ± 1.0	0.20	0.08	2.40
Pygoscelis adeliae	$n = 9$	68.0 ± 2.4	0.21	0.08	2.59
Spheniscus magellanicus	$n = 7$	69.2 ± 3.8	0.18	0.08	2.40

cidae. Although the ulnar condyle is incomplete in MUSM 889, it is clear that the shelf is very close in width to the condyle. In other fossil penguins possessing this morphology, a corresponding flat surface on the proximal ulna articulates with the shelf and would have limited movement at the joint between the humerus and ulna during the downstroke part of the wingbeat cycle (Ksepka et al., 2006). The angle between the shaft and condyles (i.e., the angle between a line tangent to the distal condyles of the humerus and the long axis of the shaft) would have been low (<45°), but the exact measurement cannot be obtained because of damage to the ulnar condyle.

In all extant and extinct penguin taxa except for *Waimanu*, three trochlear ridges (=trochlear processes of Marples [1952], Ksepka et al. [2006], and Acosta Hospitaleche et al. [2007]; processlike crests of Göhlich [2007]) contribute to the formation of two deeply grooved trochleae for the tendons of m. humerotricipitalis and m. scapulotricipitalis at the distal end of the humerus. In *Waimanu tuatahi*, the sulcus for m. scapulotricipitalis is deep, but it is not bounded by distinct trochlear ridges (Slack et al., 2006). The anterior trochlear ridge is broken in *Perudyptes devriesi*, so it is uncertain whether a complete trochlea bounded the tendon of m. humerotricipitalis. However, the middle and posterior trochlear ridges are preserved and contribute to the formation of a trochlea for the tendon of m. scapulotricipitalis. The posterior trochlear ridge differs from that of all other penguins in its large size and rounded distal border. Additionally, the posterior trochlear ridge extends distal to the middle trochlear ridge, while the opposite is true in all other penguins preserving these ridges.

CARPOMETACARPUS: The carpometacarpus (fig. 6) is less dorsoventrally compressed than in extant penguins. This feature is especially noticeable at the anterior border, which has a blunt rounded shape rather than forming a sharp edge. In part, the sharp edge in extant penguins is related to the fusion of phalanx I-1 to the anterior border of metacarpal II (Pycraft, 1907; Ksepka et al., 2008). The rounded anterior border of metacarpal II suggests a free alular phalanx was retained into adulthood in *Perudyptes devriesi*, as inferred for several basal penguin taxa (see discussion in Ksepka et al., 2008). The pisiform process is developed as a low ridge, whereas this process is further reduced to a barely perceptible scar in more crownward penguins. In volant birds, the pisiform process acts as a pulley for the tendon of m. flexor digitorum profundus. Living penguins lack a discernable pisiform process and also possess a completely tendinous m. flexor digitorum profundus (Schreiweis, 1982). As noted by Clarke et al. (2007), the morphology of the pisiform process in *Perudyptes devriesi* is consistent with retention of a functional m. flexor digitorum profundus and a thus a less rigid distal wing. Metacarpal II is strongly bowed anteriorly and extends slightly distal to metacarpal III. Metacarpals II and III are of near equal length in *Waimanu tuatahi*, *Pachydyptes ponderosus*, and *Icadyptes salasi*, but metacarpal III is distinctly longer in more crownward sphenisciform taxa. Metacarpal II presents a subtriangular wedge-shaped articular surface for the first phalanx in *Perudyptes devriesi*. Its shape is unlike the oval surface of living penguins and represents a plesiomorphic feature based on outgroup morphology. The distal articular surface for phalanx III-1 is also subtriangular.

PELVIS: Part of the pelvis is preserved, with the proximal end of the left femur contacting the acetabulum, but out of natural articulation (fig. 7). The sutures between the synsacrum and ilium remain open, as in other penguins with the exception of extant *Pygoscelis*, in which these elements are partially or fully fused (Clarke et al., 2003). The dorsal surface of the synsacral crest is strongly thickened. The dorsal iliac crests approach the synsacral crest more closely than in extant penguins, but this difference may be an artifact of crushing. The relative width of the synsacrum posterior to the acetabulum is comparable to that in extant penguins. Unfortunately, the precise number of vertebrae incorporated into the synsacrum cannot be determined.

FEMUR: The right femur (fig. 8) lacks only the distal end, while the left femur preserves the head and a portion of the shaft. The trochanteric crest is very weakly proximally projected, and the articular surface for the antitrochanter is slightly convex. In these features, the proximal femur is more similar to an albatross (*Diomedea*) than to extant penguins. Penguin femora typically have a more concave profile between the head and trochanteric crest in posterior view. The femoral shaft of *Perudyptes devriesi* is nearly straight in cranial view. A straight femur characterizes most Sphenisciformes, although Walsh and Suárez (2006) reported a strongly curved femoral shaft in the crown fossil *Pygoscelis grandis* and extant *Pygoscelis papua*, *Eudyptula minor*, and "*Eudyptes crestatus*" (=*Eudyptes chrysocome*). At the intersection of the medial and lateral supracondylar crests, a large tubercle is present.

TIBIOTARSUS: Two portions of the tibiotarsus are preserved: the proximal end of the left element and the distal end of the right element (fig. 8). The degree of proximal projection of cnemial crests is not observable due to damage and encrusting matrix. The fibular crest arises more proximally than in extant penguins, as in an unnamed penguin from Tierra del Fuego (CADIC P 21: Clarke et al., 2003) and *Paraptenodytes antarcticus*. Damage to the shaft precludes estimation of cross-sectional shape. The supratendinal bridge is proximodistally narrow. The distal tibiotarsus is distinct in the extremely weak anterior projection of the lateral condyle. In all other penguins we examined, the lateral condyle projects relatively farther anteriorly, giving the condyle a subcircular shape in medial view. In Gaviiformes and Procellariiformes the lateral condyle projects even

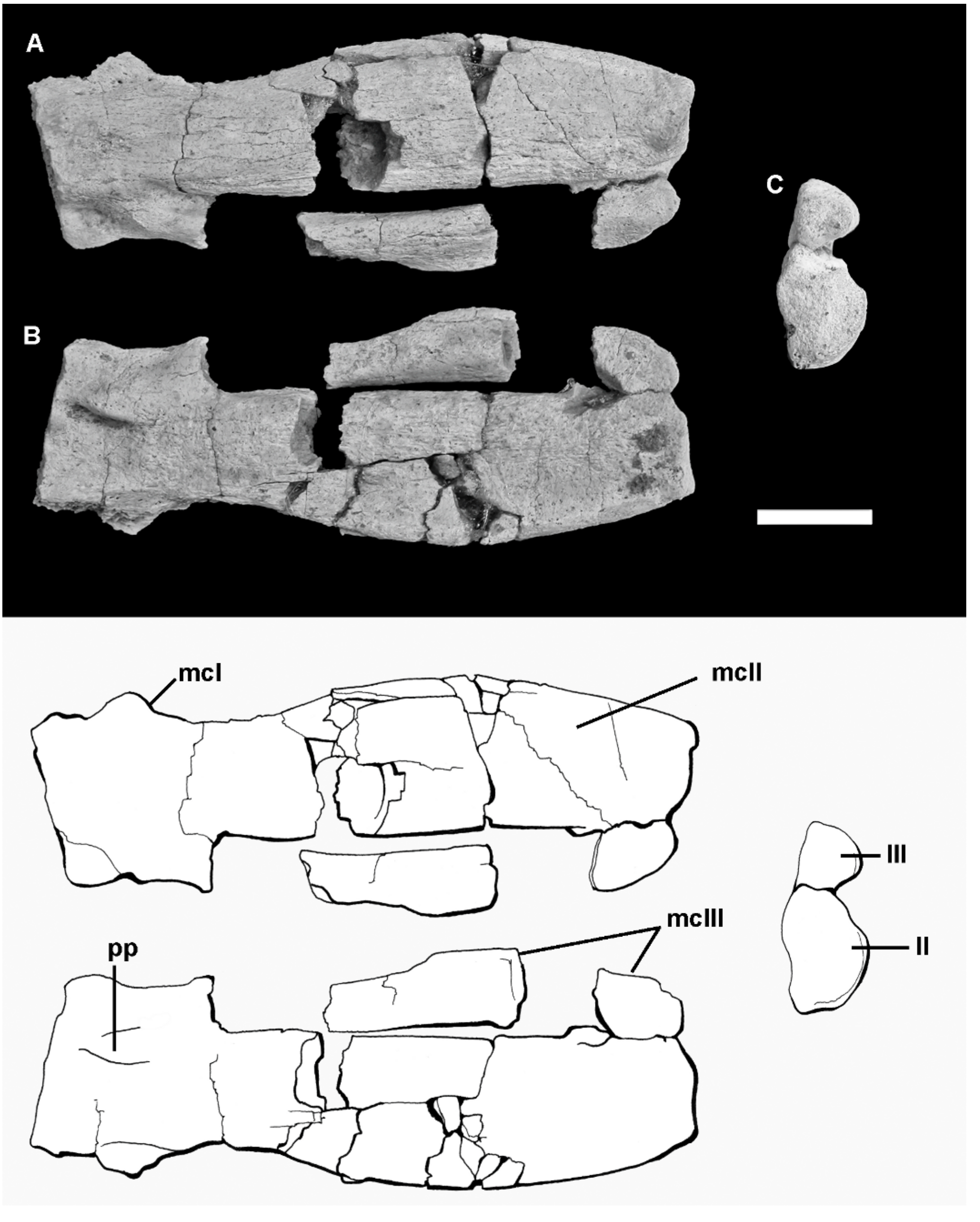

Fig. 6. Right carpometacarpus of MUSM 889 in (**A**) dorsal view, (**B**) ventral view, and (**C**) distal view. Scale bar = 1cm. See appendix 5 for abbreviations.

farther anteriorly, giving the condyle an elliptical shape in lateral view (Acosta Hospitaleche, 2004).

TARSOMETATARSUS: The left tarsometatarsus is intact distally, but it lacks the proximal end (fig. 9). This element is very stout, as is typical for penguins, although exact proportions cannot be determined due to incompleteness. Metatarsal II is deflected medially at its distal end, while metatarsal IV

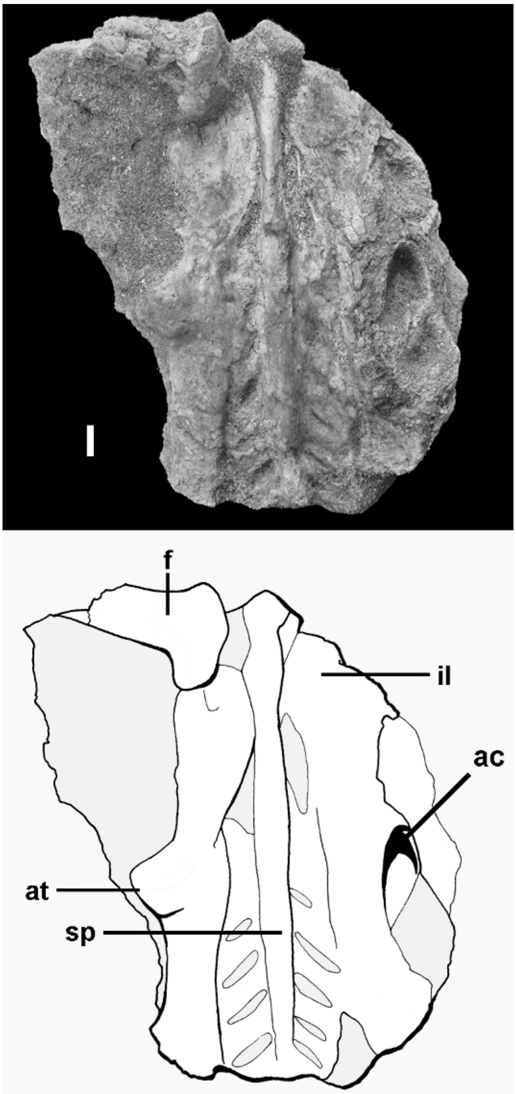

Fig. 7. Pelvis and proximal portion of left femur of MUSM 889 in dorsal view. Scale bar = 1 cm. See appendix 5 for abbreviations.

is straight throughout its length. The degree of concavity of the medial border of metatarsal II is similar to that in *Palaeeudyptes klekowskii* (Myrcha et al., 2002: fig. 7). Previously, we considered the medial proximal vascular foramen to be absent in the *Perudyptes devriesi* holotype (Clarke et al., 2007). However, based on the further comparisons with undescribed materials from the Paleogene of Peru (MUSM 1432), we now consider the presence or absence of this foramen to be uncertain, as it appears possible that the foramen could have been located proximal to the preserved margin of the tarsometatarsus. The medial intermetatarsal sulcus is extremely shallow, a primitive feature for penguins. Metatarsal IV is detached from metatarsal III as a matter of preservation, but the borders indicate that the lateral intermetatarsal sulcus was deep as in all other penguins. Intact borders of the metatarsals also indicate the absence of a distal vascular foramen. Trochlea IV is similar in shape to that in extant penguins, although the lateral flange is slightly more pronounced in *Perudyptes devriesi*.

PHYLOGENETIC ANALYSIS

Primary Analysis

In order to evaluate the phylogenetic placement of *Perudyptes devriesi* and recently discovered fossil taxa such as *Madrynornis mirandus*, *Pygoscelis grandis*, and *Spheniscus muizoni*, we employed a large combined morphological and molecular dataset for Sphenisciformes. Earlier versions of this dataset were formulated and utilized by Giannini and Bertelli (2004), Bertelli and Giannini (2005), Bertelli et al. (2006), Ksepka et al. (2006), Clarke et al. (2007), and, most recently, by Ksepka (2007). In the present study, we modified Ksepka's (2007) version of this matrix, including 25 morphological characters and 11 fossil taxa added since the most recent published version of the matrix (Clarke et al., 2007). In addition to increasing taxonomic sampling, we were also able to incorporate additional codings for *Palaeospheniscus biloculata* based on new material reported by Acosta Hospitaleche et al. (2007) and for *Palaeospheniscus patagonicus* based on new material reported by Acosta Hospitaleche et al. (2008). The current dataset contains 219 morphological characters and >6000 bp of sequence data. Fossil specimens examined are presented in appendix 1, GenBank accession numbers for sequences are presented in appendix 2, morphological character definitions are presented in appendix 3, and the morphological matrix is presented in appendix 4.

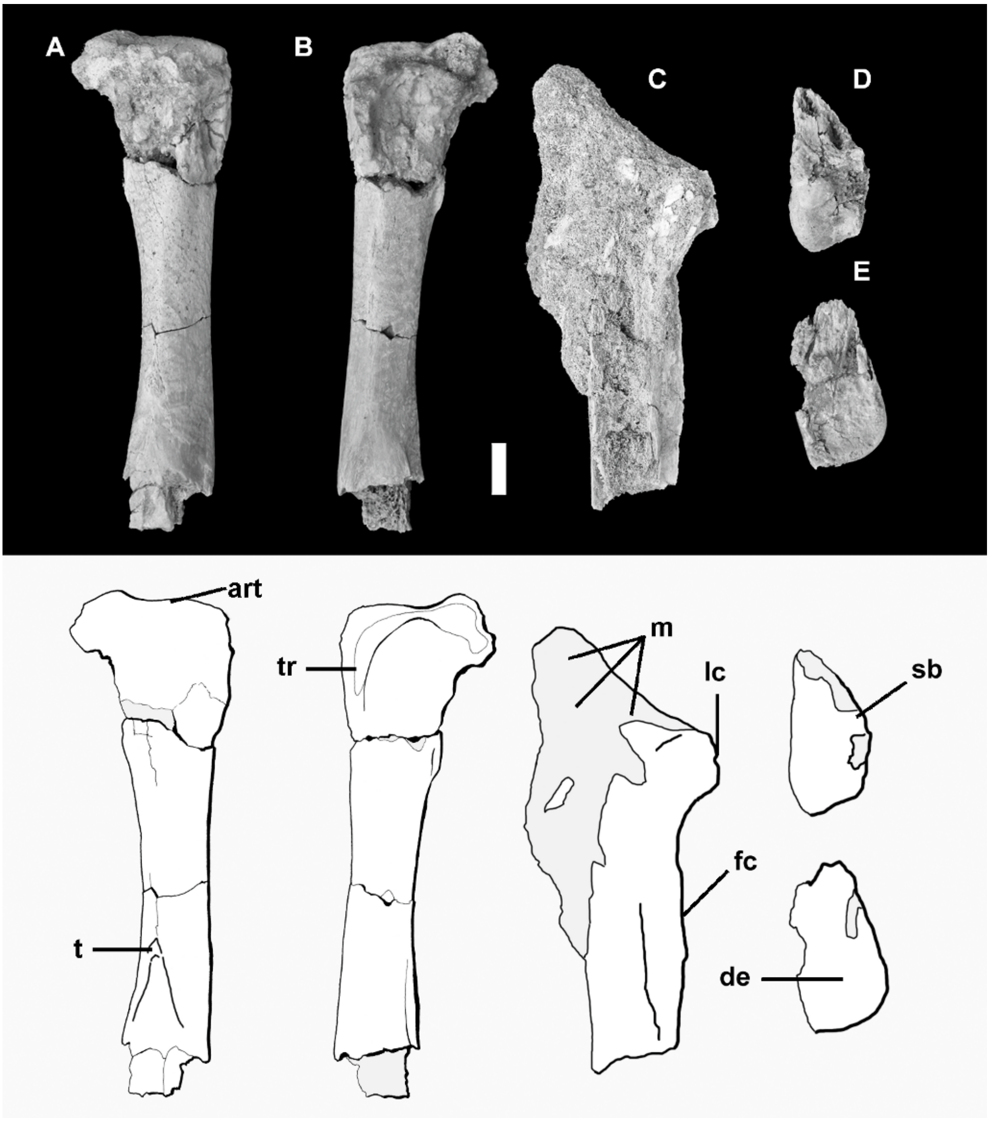

Fig. 8. Right femur of MUSM 889 in (**A**) caudal view and (**B**) cranial view, proximal left tibiotarsus in (**C**) cranial view, and distal right tibiotarsus in (**D**) cranial view and (**E**) lateral view. Scale bar = 1 cm. See appendix 5 for abbreviations.

Outgroups

Recent studies of avian higher level phylogeny have generally supported a sister group relationship between Sphenisciformes and Procellariiformes (McKitrick, 1991; van Tuinen et al., 2000; Livezey and Zusi, 2006, 2007; Hackett et al., 2008), Gaviiformes (Mayr and Clarke, 2003), or a clade uniting Procellariiformes + Gaviiformes (Sibley and Ahlquist, 1990; Cooper and Penny, 1997) (see also summary hypothesis and discussion of Cracraft et al., 2004). Groth and Barrowclough (1999) recovered a Sphenisciformes-Gaviiformes clade, but they did not include representatives of Procellariiformes in their analysis. A few authors have recovered a sister group relationship between Sphenisciformes and a clade uniting Gaviiformes and Podicipediformes (Cracraft, 1985, 1988;

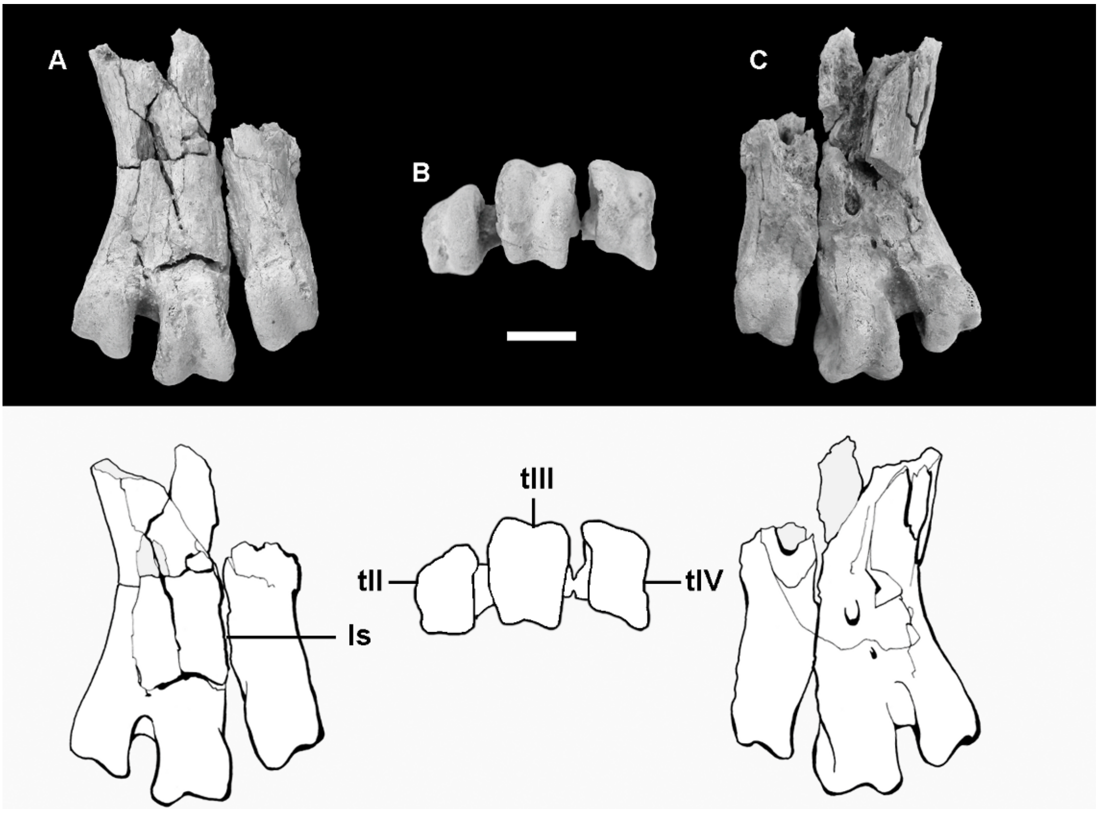

Fig. 9. Left tarsometatarsus MUSM 889 in (**A**) dorsal view, (**B**) distal view, and (**C**) plantar view. Note that because metatarsal IV is broken, the orientations of the trochleae in distal view are approximated. Scale bar = 1 cm. See appendix 5 for abbreviations.

Mayr and Clarke, 2003; Bourdon et al., 2005), although clustering of Gaviiformes and Podicipediformes has typically been attributed to convergence in these two foot-propelled diving lineages (e.g., Storer, 1971; Mayr and Clarke, 2003). Strong molecular evidence (van Tuinen et al., 2000; Chubb, 2004; Ericson et al., 2006; Hackett et al., 2008), as well as some morphological data (Mayr, 2004; Manegold, 2006), suggests that Podicipediformes are the sister taxon of Phoenicopteriformes, and that these two taxa are distantly related to Gaviiformes and Sphenisciformes.

Two alternative hypotheses regarding the higher level relationships of Sphenisciformes have recently been proposed. One hypothesis posits that Sphenisciformes are closely related to core Pelecaniformes (Fain and Houde, 2004; Mayr, 2005, 2007). This hypothesis was supported by sequence data from the beta-fibrinogen gene (Fain and Houde, 2004), although it should be noted that when additional genes are considered alongside beta-fibrinogen, Sphenisciformes are either placed in an unresolved position (Ericson et al., 2006) or united with Procellariiformes (Hackett et al., 2008). Morphological data have been presented for a sister group relationship between Sphenisciformes and the extinct flightless diving clade Plotopteridae, and for the placement of this clade within Pelecaniformes (Mayr, 2005, 2007), although some workers instead attribute similarities between penguins and plotopterids to convergence (e.g., Olson and Hasegawa, 1979, 1996). Mayr (2005) conducted a phylogenetic analysis resulting in a Sphenisciformes-Plotopteridae clade, nested within a larger clade including most traditional members of Pelecaniformes. Data from the basal penguin *Waimanu*, unpublished at the time of Mayr's (2005) analysis, change the distribution of some characters presented to support these proposed relationships (Ksepka, 2007; Mayr, 2007), and one morphological analysis of higher level avian relationships including data from *Waimanu* resulted in a sister group relationship between Sphenisciformes and Gaviiformes + Podicipediformes to the exclusion of representative Pelecaniformes (Slack et al., 2006). Unfortunately, the cranial anatomy of Plotopteridae remains essentially unknown, precluding further exploration of the Sphenisciformes-Plotopteridae hypothesis.

A second alternative hypothesis links Sphenisciformes and Ciconiiformes (Slack et al., 2003, 2006; Harrison et al., 2004; Watanabe et al., 2006). Thus far, this hypothesis has been supported exclusively by mitochondrial sequence data, and no morphological evidence has not been put forward to support a Sphenisciformes-Ciconiiformes clade.

Interestingly, several recent large-scale analyses of avian phylogeny support a general framework in which Sphenisciformes are part of a large seabird clade including Procellariiformes, Gaviiformes, Pelecaniformes, and Ciconiiformes (Ericson et al., 2006; Livezey and Zusi, 2006, 2007; Hackett et al., 2008), indicating that each alternate hypothesis may be supported by underlying synapomorphies of this larger clade. The balance of available evidence suggests Sphenisciformes and Procellariiformes are sister taxa, while Gaviiformes, Pelecaniformes, and Ciconiiformes represent more distal outgroups to penguins. In the present study we selected two species of Gaviiformes and 13 species of Procellariiformes as outgroups. Trees were rooted to *Gavia immer*.

Ingroup Taxonomic Sampling

We included 19 extant penguin taxa in our ingroup, reflecting ongoing refinement of penguin species limits. Recently, Banks et al. (2006) presented molecular evidence supporting species status for three taxa formerly considered subspecies of *Eudyptes chrysocome*: *Eudyptes chrysocome* (Southern Rockhopper Penguin), *Eudyptes moseleyi* (Northern Rockhopper Penguin), and *Eudyptes filholi* (Eastern Rockhopper Penguin). This conclusion is also supported by morphological differences and the allopatric distribution of the three species (Banks et al., 2006). In past studies (Giannini and Bertelli, 2005; Bertelli and Giannini, 2006; Ksepka et al., 2006; Clarke et al., 2007), *Eudyptes chrysocome chrysocome* and *Eudyptes chrysocome moseleyi* were coded as separate operational taxonomic units in recognition of these morphological differences. Here, we treat all three of the newly recognized rockhopper species as separate terminals.

We included 33 extinct penguin species as well as multiple specimens exhibiting distinct and novel combinations of characters (Ksepka, 2007). Two important sets of specimens originally referred to *Palaeeudyptes antarcticus* (Marples, 1952), but which differ significantly from one another and cannot be assigned to that species (see Simpson, 1971b; Fordyce and Jones, 1990; Fordyce, 1991; Ando, 2007; Ksepka, 2007), were included as two distinct terminals named for their localities: Burnside "*Palaeeudyptes*" (OM GL435) and Duntroon "*Palaeeudyptes*" (OM GL427, OM GL432). We also included a giant penguin tarsometatarsus (UCMP 321023) preserving synapomorphies of *Anthropornis* but differing strongly in proportions from *Anthropornis nordenskjoeldi* and *Anthropornis grandis* (Ksepka, 2007) as a separate terminal. Following Ksepka (2007), we excluded multiple fossil taxa that are taxonomic equivalents of more well-known species included in our matrix. The exclusion of taxonomic equivalents can improve resolution in consensus trees without changing the relationships of the remaining taxa (Wilkinson, 1995). A few fragmentary taxa are not taxonomic equivalents because they include infrequently recovered elements (e.g., *Palaeeudyptes marplesi*, which is known from a few incomplete limb elements but includes the rarely preserved patella). However, these taxa were excluded, as simultaneous inclusion of all such taxa has been demonstrated to result in a complete lack of resolution in the strict consensus of resultant trees (Ksepka, 2007). Instead, these incomplete specimens were evaluated using synapomorphies identified in the primary analysis (see below).

Treatment of Problematic Fossils

Isolated specimens can create difficulties for both taxonomy and phylogenetic analysis. The first fossil penguin species to be named was based on a single broken tarsometatarsus (Huxley, 1859), and the taxonomic difficulties associated with fragmentary holotypes and disassociated specimens have remained a constant thread in discussions of penguin evolution (e.g., Simpson, 1971b; Fordyce, 1991; Ksepka, 2007). Deciding how to treat isolated fossils is particularly difficult when multiple taxa are present at a locality. Erecting new taxa from single, nonoverlapping elements in cases where comparisons to previously named taxa cannot be made is poor taxonomic practice, and it can obscure understanding of radiation and extinction by artificial taxonomic inflation of species diversity. On the other hand, to make referrals without evidence from associated specimens risks the creation of chimeric taxa, which may confound phylogenetic analysis. We comment on the taxonomic issues surrounding two recently proposed species based on isolated elements below.

Challenges posed by isolated fossils must be addressed in dealing with penguin fossils from the Eocene La Meseta Formation of Seymour Island (Antarctic Peninsula). For largely historical reasons, the taxonomy of fossil penguins from the La Meseta Formation has been based primarily on the tarsometatarsus (Wiman, 1905a, 1905b; Marples, 1953; Myrcha et al., 1990, 2002). Although penguin fossils are abundant particularly in the upper levels of the La Meseta Formation, articulated specimens remain extremely rare, and no specimens including a tarsometatarsus and additional elements identifiable to a single individual are known. Davis and Briggs (1998) examined 1233 USNM penguin specimens from the La Meseta and found all to be completely disarticulated and 90% to be broken. Jadwiszczak (2006a: 7) indicated the IB/P/B collections include "more than a thousand almost exclusively isolated bones." Tambussi et al. (2006) noted that of >2000 Antarctic penguin elements curated in the MLP collections, only one partial skeleton is articulated. This presumably refers to the single incomplete specimen of *Palaeeudyptes gunnari* described by Accosta Hospitaleche and Reguero (in press). Aside from this specimen, we are aware of only three articulated penguin specimens from Seymour Island, all of which are highly incomplete and none of which preserves the tarsometatarsus (see Ksepka and Bertelli, 2006). Thus, it currently remains impossible to directly identify non-tarsometatarsus elements from the La Meseta to the species level by association (except for the case of *Palaeeudyptes gunnari*).

Five distinct small penguin humerus morphotypes have been described from the La Meseta Formation: type A1, type A2, type B (sensu Jadwiszczak, 2006a; see Discussion below), a *Tonniornis mesetaensis* type, and a *Tonniornis minimum* type. These humerus morphotypes probably represent isolated humeri belonging to six previously named species known only from the tarsometatarsus: *Delphinornis arctowskii*, *Delphinornis gracilis*, *Delphinornis larseni*, *Delphinornis wimani*, *Marambiornis exilis*, *Mesetaornis polaris*. Given the lack of associated material to guide referral of isolated elements to named taxa, however, it is not possible to assign the five humerus morphotypes to previously named species with certainty. In order to provide a rigorous consideration of the character data from these fossils, we conducted a series of 14 iterative analyses alternatively combining codings from these humerus morphotypes with those from the six named species based on tarsometatarsi and also including the humeri as separate terminals (see Additional Analyses). A detailed discussion of taxonomic issues surrounding the La Meseta material is presented below.

Tonniornis mesetaensis and *Tonniornis minimum* are comparatively recently named species from the La Meseta Formation (Tambussi et al., 2006). The holotype specimen of each species is a single isolated humerus, and these species were diagnosed solely on features of the humerus. These diagnoses do not allow *Tonniornis mesetaen-*

sis and *Tonniornis minimum* to be differentiated from six previously named, similarly sized taxa known from tarsometatarsi: *Delphinornis arctowskii*, *Delphinornis gracilis*, *Delphinornis larseni*, *Delphinornis wimani*, *Marambiornis exilis*, and *Mesetaornis polaris*. These six taxa and the two *Tonniornis* holotypes are known from the same unit of the La Meseta Formation (Telm VII of Sadler, 1988; Submeseta Allomember of Marennsi et al., 1998).

Humeri (i.e., elements directly comparable to the *Tonniornis* holotypes) have only been formally referred to one of the nine tarsometatarsus-based species. Nine isolated humeri were referred to *Delphinornis larseni* (Tambussi et al., 2006). Referral of these humeri to *Delphinornis larseni* is unfortunately not based on associated specimens. The humeri assigned to *Delphinornis* were differentiated as "conspicuously smaller and more slender than those of *Tonniornis*" (Tambussi et al., 2006: 155). However, the difference in length between the holotype of *Tonniornis minimum* and the only complete specimen referred to *Delphinornis larseni* is <0.5 mm (93.6 versus 93.2 mm: table 1 of Tambussi et al., 2006).

Tambussi et al. (2006) noted that the *Tonniornis* holotype humeri differ from humeri assigned to *Delphinornis*, *Mesetaornis*, and *Marambiornis* in the unpublished Master's thesis of Kandefer (1994). However, the referrals of Kandefer (1994) were also not based on articulated or associated specimens (Jadwiszczak, personal commun.) and were made before *Mesetaornis* and *Marambiornis* were formally named (Myrcha, 2002). Jadwiszczak (2006a) examined the same material studied by Kandefer (1994) and noted that genus and species referrals could not be reliably made. He therefore classified these humeri into three morphotypes (types A1, A2, and B) and concluded that "there is no justification for erecting new taxa based solely on bones other than tarsometatarsi" from the La Meseta Formation given our present state of knowledge (Jadwiszczak 2006b: 296). The A1, A2, and B humerus types differ from one another by discrete features, and all three also differ from the *Tonniornis* holotype humeri in possessing a weakly bipartite tricipital fossa (this fossa is single in the *Tonniornis* humeri).

Because none of the five small humerus morphotypes can be firmly associated with a species named from the tarsometatarsus, it is not possible to determine whether the humeri used to erect the *Tonniornis* species belong to previously named taxa or do in fact represent distinct species, or to determine which species the type A1, A2, or B humeri might represent. Further hindering attempts at species referrals for these isolated humeri, intraspecific size variation (as well as interspecific variation) in the relative lengths of the forelimb and hindlimb elements are significant in penguins. For example, tarsometatarsus length ranges from 34% to 53% of humerus length in extant penguins (Ksepka, personal obs.). This makes matching humeri to tarsometatarsi based on length alone risky at best. Firm referrals await associated specimens as well as further quantification of variation in the La Meseta taxa.

Molecular Data

The molecular dataset utilizes sequences from the nuclear gene RAG-1 (recombination-activating gene 1) and the mitochondrial genes 12S, 16S, COI (cytochrome oxidase I) and cytochrome *b*, sampled for extant penguins and some outgroup taxa by Baker et al. (2006). Additionally, because we recognize *Eudyptes chrysocome*, *Eudyptes moseleyi*, and *Eudyptes filholi* as distinct species, we included sequences for these taxa provided by Banks et al. (2006). For outgroup taxa unsampled by Baker et al. (2006), we collected available sequences from GenBank (accession numbers and authorship of all sequences are provided in appendix 2). This molecular dataset is largely the same as that employed by Ksepka et al. (2006) and Clarke et al. (2007). For a few outgroup taxa, recently published data were added (e.g., COI sequences for *Oceanites oceanicus* from Kerr et al., 2007). Sequences for each gene were aligned separately in ClustalX (Thompson et al., 1997), adjusted manually in MacClade (Maddison and Maddison, 1992), and then concatenated.

Search Strategy

Searches were conducted in TNT (Goloboff et al., 2008) and consisted of 10,000 random taxon addition replicates with tree bisection-reconnection branch swapping, saving 10 trees per replicate. All characters were equally weighted and branches with a minimum length of 0 were collapsed. Support values were calculated in PAUP*4.0b10 (Swofford, 2003). Bremer support was calculated using a decay index file constructed in MacClade and executed in PAUP*4.0b10, with the same search strategy as the primary analysis applied.

Additional Analyses: Testing New Hypotheses Regarding the Crown Penguin Radiation

One major debate in penguin evolution revolves around the timing of the crown radiation (see additional discussion in Recommended Calibration Points for Divergence Estimation). Molecular studies have placed the basal divergence in crown Spheniscidae in the Eocene (Baker et al., 2006), whereas the late appearance of crown penguins in the fossil record suggests this divergence occurred more recently, probably during the Miocene (Ksepka et al., 2006; Clarke et al., 2007). Recently, Jadwiszczak (2006b) proposed that some species of the small penguin taxa *Delphinornis*, *Marambiornis*, and *Mesetaornis* from the Eocene La Meseta Formation of Seymour Island (Antarctic Peninsula) could represent the last common ancestor of extant Spheniscidae. This hypothesis is intriguing, particularly because the age of these fossil taxa would be consistent with the molecular dating studies and biogeographic reconstructions of Baker et al. (2006), which estimate that the basal divergence within crown Spheniscidae occurred ~40 million years ago in Antarctica. We conducted additional iterative phylogenetic analyses designed to test this hypothesis as outlined below.

Jadwiszczak (2006b: 298) specifically hypothesized that "small penguins from the Eocene of Antarctica (*Delphinornis*, *Marambiornis*, and *Mesetaornis*) are promising candidates for ancestors of extant Sphenisciformes." Jadwiszczak (2006b) considered these taxa to be possible candidates for the ancestor of Spheniscidae because their estimated body size range falls within that of living penguins, whereas he ruled out the "giant" La Meseta Formation taxa as extremely specialized lineages representing evolutionary dead ends (Jadwiszczak, 2001, 2003). Jadwiszczak (2006b) gave special mention to *Delphinornis arctowskii* because this species possesses a tarsometatarsus similar in proportions to extant penguins (see Myrcha et al., 2002), and he presented characters in support of his hypothesis, including the derived coalescence of the intermediate hypotarsal crests of the tarsometatarsus (primitively separated by a groove).

Jadwiszczak's (2006b) hypothesis was also based partially on observations from isolated small penguin humeri from the La Meseta Formation (humerus morphotypes A1, A2, and B). These humeri preserve a bipartite tricipital fossa, a feature that is is present in crown Spheniscidae, but also some stem taxa (i.e., *Palaeospheniscus*, *Eretiscus*, *Dege*, *Marplesornis*). Although the character data in these isolated humeri are important, it is not yet possible to assign these humeri to any particular species because all of the plausible candidate species (*Delphinornis arctowskii*, *Delphinornis gracilis*, *Delphinornis larseni*, *Delphinornis wimani*, *Marambiornis exilis*, and *Mesetaornis polaris*) are known only from tarsometatarsi (see Treatment of Problematic Fossils above). We therefore designed a set of iterative analyses exploring different ways of incorporating character codings from these humeri into the phylogenetic dataset.

Jadwiszczak's (2006a) humerus morphotypes A1, A2, and B are differentiable, but they are taxonomic equivalents when evaluated for the character matrix used here. We therefore selected the most complete humerus preserving the morphologies central to Jadwiszczak's (2006b) hypothesis (IB/P/B-0382, a type B specimen) for evaluation. In a series of six analyses, codings from this representative humerus were iteratively combined with those from the holotype and referred tarsometatarsi of six La Meseta species (i.e., *Delphinornis arctowskii*, *Delphinornis gracilis*, *Delphinornis larseni*, *Delphinornis wimani*, *Marambiornis exilis*, and *Mesetaornis polaris*). In one additional analysis, IB/P/B-0382 was scored as a separate terminal to model the possibility that the type A1, A2, and B humeri belong to distinct taxa that are as yet unknown from other elements.

As discussed above, we think that it is highly likely that the holotype humeri of *Tonniornis mesetaensis* and *Tonniornis minimum* belong to previously named species known from the tarsometatarsus (i.e., some species of *Delphinornis*, *Marambiornis*, and/or *Mesetaornis*). Unfortunately, we were able to assess only line drawings and descriptions (Tambussi et al 2006) of the *Tonniornis mesetaensis* and *Tonniornis minimum* holotypes for this study. These species share identical codings for our matrix. In another series of six analyses, representative codings from the holotype of *Tonniornis mesetaensis* (MLP 93-X-1-145) were iteratively combined with those from the holotype and referred tarsometatarsi of *Delphinornis arctowskii*, *Delphinornis gracilis*, *Delphinornis larseni*, *Delphinornis wimani*, *Marambiornis exilis*, and *Mesetaornis polaris* to create new terminals for each species. Finally, we conducted one analysis including *Tonniornis mesetaensis* and *Tonniornis minimum* as separate operational taxonomic units to test the possibility that they represent distinct taxa.

All 14 permutations of the data outlined above were evaluated using the same matrix, outgroups, and search strategies as the primary analysis.

RESULTS

Primary Analysis

The primary analysis resulted in 420 most parsimonious trees (MPTs) of 4492 steps. In the strict consensus of these trees (fig. 11), monophyletic Sphenisciformes and Procellariiformes are recovered. Outgroup relationships are the same as those reported by Clarke et al. (2007: see supplemental data) and agree with Ksepka (2007) except for greater resolution within Diomedeidae. Although the matrix was not designed specifically to consider fine-scale relationships within Procellariiformes, it is worth noting that two of the four traditional families within Procellariiformes are supported as monophyletic: Diomedeidae (albatrosses) and Hydrobatidae (storm petrels). Monophyly of Pelecanoididae (diving petrels) was not tested, as only a single species (*Pelecanoides urinatrix*) from this group was included. However, the monophyly of this monogeneric family of highly apomorphic diving birds has never been questioned. Procellariidae (shearwaters, fulmars, giant petrels, and allies) as traditionally defined is rendered nonmonophyletic because *Pachyptila* is recovered as the sister taxon of Pelecanoididae, and other traditional members of Procellariidae (*Procellaria*, *Pterodroma*, *Puffinus*, *Daption*, and *Macronectes*) are unresolved with respect to this clade. This finding in particular deserves further scrutiny, and increased sequence representation within Procellariiformes is desirable to confirm or refute the relationships recovered here.

Relationships within Sphenisciformes are well resolved. Support values are low for most branches, but this is not unexpected given the large proportion of missing data for many fossil taxa. *Perudyptes devriesi* is recovered as a relatively basal member of Sphenisciformes. Placement of this species and other taxa shared in common between the current analysis and that of Clarke et al. (2007) are the same, with the exception that the positions of *Icadyptes salasi*, *Pachydyptes ponderosus*, and Burnside "*Palaeeudyptes*" are less resolved in the strict consensus cladogram. These three taxa form a polytomy with *Palaeeudyptes gunnari*, *Palaeeudyptes klekowskii*, and more crownward penguins in the present result, whereas they were placed one node closer to the crown clade than *Palaeeudyptes gunnari* and *Palaeeudyptes klekowskii* in the results of Clarke et al. (2007). No codings were changed for these taxa, so this difference may stem from the addition of new taxa and characters, more complete codings for several fossil taxa (reflecting newly described specimens), and a single modified coding for *Perudyptes devriesi* (coding for character 200 changed from 2 to ?; see description of tarsometatarsus above). Given the congruence with the topology of Clarke et al. (2007), we concentrate discussion on the placements of newly sampled taxa.

TABLE 2

Most exclusive placement of incomplete fossils supported by synapomorphies identified in the primary phylogenetic analysis

Numbers in placement column refer to the clades labeled in figure 21. When interpreting table 2, it is important to bear in mind that the placements presented are the most exclusive that can be justified by preserved synapomorphies, not estimates of precise phylogenetic position. Region abbreviations: AF, Africa; AP, Antarctic Peninsula; AU, Australia; NZ, New Zealand; SA, South America.

Taxon	Region	Age	Most Exclusive Placement Supported by Synapomorphies	Character States Supporting Most Exclusive Placement	Character States Supporting Exclusion from Crown Clade
Stem fossils					
Crossvallia unienwillia	AP	Late Paleocene	Clade 1	143: 1, 144: 1, 163: 0	150: 0, 155: 0, 163: 0, 193: 0
CADIC P21[a]	SA	Late middle Eocene	Clade 1	189: 0	190: 1, 193: 0
IB/P/B-0541c[b]	AN	Late Eocene	Clade 2	199: 1	196: 0
Palaeeudyptes marplesi	NZ	Late Eocene	Clade 4	201: 2	196: 1, 197: 0
Korora oliveri	NZ	Late Oligocene	Clade 4	201: 2	197: 0
Palaeeudyptes antarcticus (holotype only)	NZ	Uncertain, probably Oligocene	Clade 4	201: 2	196: 1, 197: 0
MNZS 1449 (Seal Rock, Woodpecker Bay "*Palaeeudyptes*")	NZ	Late Oligocene? (see Simpson, 1972a)	Clade 5	151: 2	145: 0, 146: 0. 148: 1, 150: 0, 153: 0
"*Tonniornis minimum*" (MLP 93-I-6-3)	AP	Late Eocene	Clade 5	151: 2	150: 0, 155: 0, 163: 0
"*Tonniornis mesetaensis*" (MLP 93-X-1-145)	AP	Late Eocene	Clade 5	151: 2	150: 0, 155: 0, 163: 0
SAMA P14157 ("*Pachydyptes simpsoni*"/Australian "*Anthropornis*")	AU	Late Eocene	Clade 7	173: 1	140: 0, 141: 0, 153: 0
SAMA P7158 (Australian "*Palaeeudyptes*")	AU	Late Eocene	Clade 8	163: 1	145: 0, 148: 1, 150: 0, 155: 0, 164: 0
Arthrodytes andrewsi	SA	Late Oligocene	Clade 8	155: 1, 163: 1	140: 0, 141: 0, 145: 0, 146: 0, 148: 1, 150: 0, 153: 1
Paraptenodytes brodkorbi	SA	Late Oligocene	Clade 8	163: 1	145: 0
Anthropodyptes gilli	AU	Early Miocene? (see Gill, 1959; Jenkins, 1974)	Clade 8	155: 1, 163: 1	150: 0, 153: 0, 164: 0
"*Paraptenodytes*" *robustus*	SA	Early Miocene	Clade 9	146: 1	145: 0, 150: 0; 164: 0
Platydyptes amiesi	NZ	Late Oligocene	Clade 9	148: 2	145: 0, 146: 0, 150: 0, 153: 1, 164: 0, 165: 1
Pseudaptenodytes macraei	AU	Late Miocene	Clade 11	150: 1[c]	158: 1

TABLE 2
(Continued)

Taxon	Region	Age	Most Exclusive Placement Supported by Synapomorphies	Character States Supporting Most Exclusive Placement	Character States Supporting Exclusion from Crown Clade
Status undetermined					
(NMV P2669) (“*Pseudaptenodytes minor*”)	AU	Late Miocene	Clade 11	150: 1[c]	None preserved
SAM Q1882 (“*Palaeospheniscus huxleyorum*”)	AF	Probably early Pliocene (see Olson, 1983)	Clade 11	145: 1, 150: 1, 165: 0	None preserved
Spheniscus chilensis	SA	Late Pliocene	Clade 11	141: 1, 145: 1, 147: 1, 150: 1, 167: 2	None preserved
Aptenodytes ridgeni	NZ	Probably middle-late Miocene	Clade 12	188: 1	None preserved
Nucleornis insolitus	AF	Probably early Pliocene (see Olson, 1983)	Clade 12	197: 2	None preserved
Pygoscelis tyreei	NZ	Probably middle-late Miocene	Clade 12	164: 1	None preserved
Crown fossils					
Pygoscelis calderensis	SA	Uncertain, middle Miocene- Pliocene	Clade 13	82: 0, 83: 1	None preserved
Inguza predemersus	AF	Probably early Pliocene (see Olson, 1983)	Clade 13	153: 2	None preserved
Tereingaornis moisleyi	NZ	Middle Pliocene	Clade 13	153: 2, 164: 1	None preserved
“*Tasidyptes hunteri*”	AU	Holocene	Clade 14	126: 1	None preserved

[a]This specimen is a partial pelvis and hindlimb from Tierra del Fuego, Argentina (Clarke et al. 2003).

[b]This specimen (a partial tarsometatarsus) is differentiable from other La Meseta Formation penguin species and may represent a distinct species, but it has not yet been named due to incompleteness (Jadwiszczak, 2008).

[c]Although a bifurcated tricipital fossa (150: 1) is optimized as an unambiguous synapomorphy of clade 11 in the primary analysis, homoplasy may occur (see Discussion). In the cases of *Pseudaptenodytes macraei* and NMV P2669, character state 155: 1 supports placing these taxa to clade 8 should bifurcation of the tricipital fossa be removed from consideration.

The analysis supports the monophyly of *Delphinornis*, here proposed to also include the taxon "*Archaeospheniscus*" *wimani* (see Taxonomic Implications below). *Delphinornis wimani* is nested within a clade of small Eocene Antarctic penguins, including *Delphinornis larseni* and the newly included *Delphinornis arctowskii* and *Delphinornis gracilis* in our result. *Delphinornis wimani* shares no close relationships with any species of *Archaeospheniscus* in out results, although another newly added small penguin, *Duntroonornis parvus* from the Oligocene of New Zealand, is placed in a polytomy with *Archaeospheniscus lowei*, *Archaeospheniscus lopdelli*, and a clade of more crownward penguins.

The rather poorly known African fossil *Dege hendeyi* (represented only by the humerus and tarsometatarsus) is placed just outside of Spheniscidae, a relationship that merits further evaluation should more material become available for study in the future. At present, only a single plesiomorphic character state (153: 1), moderate separation of the m. supracoracoideus and m. latissimus dorsi insertion scars on the humerus, supports exclusion of *Dege hendeyi* from the crown clade. Thus, we view the phylogenetic position of this taxon as tentative. It is noteworthy that if *Dege hendeyi* does in fact represent a stem member of Sphenisciformes, a minimum of two invasions of Africa by penguins would be supported (one by the lineage leading to *Dege hendeyi* and a second by the extant *Spheniscus demersus* lineage). The status of the poorly known African fossils *Inguza predemersus*, *Nucleornis insolitus*, and "*Palaeospheniscus*" *huxleyorum* is summarized in table 2 below. Olson (1983) considered these four species valid, but probably congeneric. The phylogenetic positions of these taxa cannot be resolved sufficiently to provide additional insight into African penguin taxonomy or biogeography at present. Only a single penguin species, *Spheniscus demersus* (Jackass Penguin), occurs in coastal South Africa today. Despite early uncertainty in the precise age of the four fossil species mentioned above, all are now known to occur in the early Pliocene, supporting a significantly higher level of penguin diversity in Pliocene Africa than in the present day (Dingle, 1983; Olson, 1983).

Relationships among the three extant Rockhopper Penguin groups recently recognized as species agree with those reported by Banks et al. (2006) in that the Northern Rockhopper, *Eudyptes moseleyi*, is sister taxon to a clade uniting the Southern Rockhopper, *Eudyptes chrysocome*, and Eastern Rockhopper, *Eudyptes filholi*. The implications of this topology were discussed by Banks et al. (2006). More detailed comments on critical sectors of the tree are presented below.

Identifying Extinct Parts of the Crown Penguin Radiation: Congruence and Conflict with Previous Studies

Our analysis supports placement within the extant penguin radiation for three recently described fossil penguins: *Spheniscus muizoni* (Göhlich, 2007), *Madrynornis mirandus* (Acosta Hospitaleche et al., 2007), and *Pygoscelis grandis* (Walsh and Suárez, 2006). *Spheniscus muizoni* has not been previously included in a phylogenetic analysis, although Göhlich (2007) listed characters supporting the assignment of this fossil to the genus *Spheniscus*. This assignment is corroborated here, although the relationships of *Spheniscus muizoni* relative to other extinct species of *Spheniscus* (i.e., *Spheniscus urbinai*, *Spheniscus megaramphus*, and *Spheniscus chilensis*) remain unresolved. The estimated age for this taxon (~11–13 Ma; Göhlich, 2007) makes it the oldest confirmed record of crown penguins (see further discussion below). *Spheniscus chilensis*, *Spheniscus urbinai*, and *Spheniscus megaramphus* are also recovered as members of the *Spheniscus* clade, although all are younger than *Spheniscus muizoni*.

Madrynornis mirandus, one of the most complete fossil penguins yet discovered, was previously identified as the sister taxon of extant *Eudyptes* by Acosta Hospitaleche et al. (2007, 2008). However, these authors reported a significantly different phylogeny (fig. 12) than that recovered in the present study. Because those results supported inclusion of the early Miocene taxon *Palaeospheniscus* in the crown clade and the nonmonophyly of the extant genus *Pygoscelis*, they are directly relevant to our discussion of fossil calibration points and taxonomy. Specifically, if this

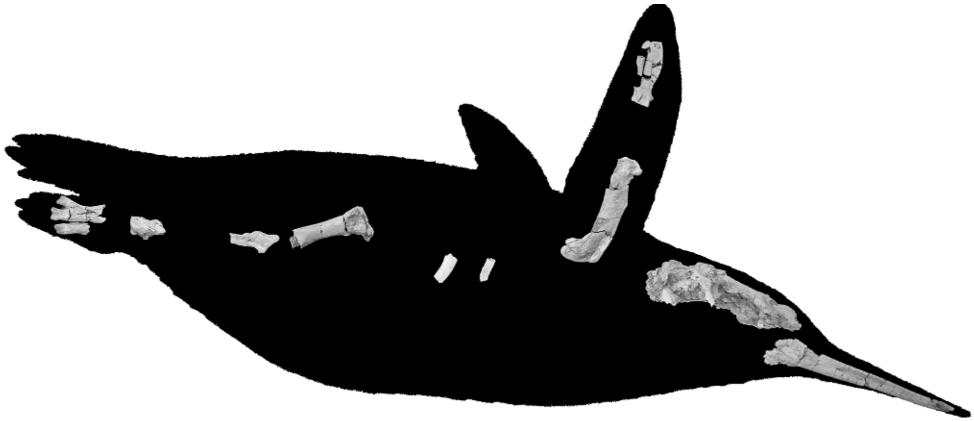

Fig. 10. Reconstruction of *Perudyptes devriesi* diving, with preserved elements of the holotype indicated (left humerus, pelvis and left femur not shown). Silhouette by Kristin Lamm.

alternative topology is correct, *Palaeospheniscus* (Gaiman Formation: early Miocene–earliest middle Miocene; Flynn and Swisher, 1995; Palazzesi et al., 2006) would represent the oldest crown spheniscid fossil.

Some differences between our results and those of Acosta Hospitaleche et al. (2007, 2008) can be accounted for by the effect of the different preferred rooting for crown penguins when molecular data are included (discussed by Bertelli and Giannini, 2005). However, reexamination of the character evidence suggests that three major differences are driven by character sampling issues and erroneous scorings. These include the placement of *Megadyptes* as sister taxon to a clade uniting *Pygoscelis*, *Aptenodytes*, and *Palaeospheniscus* (versus as sister taxon to *Eudyptes* + *Madrynornis* in the present study), the paraphyly of extant *Pygoscelis* (versus monophyly in the present study), and the placement of *Palaeospheniscus* in Spheniscidae (versus as a stem sphenisciform in the present study).

Exclusion of >100 osteological and soft tissue characters from previous studies that could not be scored in sampled fossil taxa (*Paraptenodytes*, *Palaeospheniscus*, and *Madrynornis*) from the analyses of Acosta Hospitaleche et al. (2007,2008) may account for some differences in topology. Rather than improving accuracy or resolution, exclusion of characters with missing data is likely to reduce accuracy (e.g., Wiens, 1998). Bertelli et al. (2006) showed that in the case of penguins, excluding particular classes of characters (e.g., integumentary, osteological, molecular) resulted in lower resolution and the failure to recover clades that are well supported by both the full morphological dataset and the combined dataset. Exclusion of synapomorphies grouping *Megadyptes* and *Eudyptes* (e.g., shelf of bone bounding the salt gland fossa, yellow crown feathers) and supporting the monophyly of extant *Pygoscelis* (e.g., fusion of the synsacrum and ilium) appears to account for the failure to recover these clades. We consider the monophyly of all extant *Pygoscelis* species and the monophyly of the clade uniting *Megadyptes* and *Eudyptes* to the exclusion of all other extant penguins to be well supported based on the strong molecular support for these clades reported by Baker et al. (2006), morphological support reported by others (Giannini and Bertelli, 2004; Bertelli and Giannini, 2005; Walsh and Suárez, 2006), and the results of the analyses presented in this paper.

Palaeospheniscus is represented by three species that occur in the Miocene of South America. In the present study, we found all *Palaeospheniscus* species to form a clade that also includes *Eretiscus tonnii*, placed outside of crown Spheniscidae (fig. 10). In contrast, Acosta Hospitaleche et al. (2007, 2008) placed *Palaeospheniscus* within the crown clade, as sister taxon to extant *Aptenodytes*. Although Acosta Hospitaleche et al. (2008) commented that Bertelli et al. (2006) pro-

Fig. 11. Strict consensus of 420 most parsimonious trees of 4492 steps fom the primary analysis. Bremer support values are indicated above branches. Support values reflect the low proportion of codable informative cells for several fossil taxa and the high proportion of missing data in all fossil taxa (all 6000+ molecular characters are missing data for all fossils). For a more complete understanding of support within extant clades, see Bertelli and Giannini (2005) and Baker et al. (2006).

posed the same set of relationships, Bertelli et al. (2006) did not include *Palaeospheniscus* in their analyses or mention this taxon in their discussion.

Plesiomorphic character states for two unambiguous synapomorphies of the crown clade support exclusion of *Palaeospheniscus* from Spheniscidae: m. latissimus dorsi and m. supracoracoideus insertion scars on the humerus separated by a moderate gap (character state 153: 1) and ulnar condyle of humerus rounded and projected (character state 164: 0). In crown Spheniscidae, the m. latissimus dorsi and m. supracoracoideus insertion scars are nearly confluent (character state 153: 2) and the ulnar condyle is flattened (character state 164: 1). Additionally, *Palaeospheniscus* possesses a shallow sulcus between metatarsals III and IV (character state 197: 1), whereas a deep sulcus (character state 197: 2) is optimized as a synapomorphy of the clade uniting *Dege hendeyi*, *Marplesornis novaezealandiae*, and Spheniscidae (reversed in *Pygoscelis*).

The incorporation of 12 vertebrae into the synsacrum of *Palaeospheniscus bergi* (see Simpson, 1946) may also represent a primitive feature given that the most basal known penguin, *Waimanu manneringi*, possesses 11 synsacral vertebrae (Slack et al., 2006) and extant penguins typically possess 13 synsacral vertebrae. We observed 14 synsacral vertebrae in *Pygoscelis papua* and some exemplars of *Eudyptes robustus*, and 12 synsacral vertebrae in *Eudyptula minor* (these totals are optimized as apomorphic increases/decreases on our strict consensus tree). Thus, there appears to be a trend toward an increase in number of synsacral vertebrae in penguins. Unfortunately, complete synsacra remain unknown for almost all fossil taxa, and synsacral vertebral count varies significantly amongst outgroup taxa, precluding a full understanding of the phylogenetic distribution of this character.

Several characters proposed to support placing *Palaeospheniscus* in the crown clade (Acosta Hospitaleche et al., 2007) were scored differently in our analysis or omitted as uninformative. Absence of the medial proximal vascular foramen of the tarsometatarsus (character state 40: 1 of Acosta Hospitaleche et al., 2007) was proposed as an unambiguous synapomorphy of *Pygoscelis*, *Palaeospheniscus*, and *Aptenodytes*. However, this foramen is actually present in all species of *Pygoscelis* and *Aptenodytes* (character 200 of this study; see also Watson, 1883: plate VII; Bertelli and Giannini, 2005: fig. 27; Walsh and Suárez, 2006: fig. 2). Additionally, this foramen is present in all other crown taxa. Therefore, its absence in *Palaeospheniscus* does not support the proposed placement of this fossil taxon. Lateral proximal vascular foramen of the tarsometatarsus "present in posterior view" (character state 41: 1 of Acosta Hospitaleche et al., 2007) was proposed as a synapomorphy of *Megadyptes*, *Pygoscelis*, *Aptenodytes*, and *Palaeospheniscus*. However, the lateral proximal vascular foramen is present and visible in posterior (plantar) view in *Palaeospheniscus*, all penguin taxa included in the analysis of Acosta Hospitaleche et al. (2007), and all outgroup taxa (see Bertelli and Giannini, 2005: fig. 27; Ksepka et al., 2006: fig. 15), rendering it uninformative for the sampled taxa. Given these observations and the characters discussed above, we consider the stem position for *Palaeospheniscus* recovered here to be the more strongly supported hypothesis.

Pygoscelis grandis was placed in the crown clade in the results of our analysis. However, because this fossil is placed in a polytomy including extant *Pygoscelis* and a large clade of non-*Pygoscelis* taxa, the monophyly of *Pygoscelis grandis* plus extant *Pygoscelis* species could not be confirmed. In their original description of *Pygoscelis grandis*, Walsh and Suárez (2006) found this species to be the sister taxon of a clade uniting the three extant *Pygoscelis* species (fig. 13). This topology is present in a subset of the most parsimonious trees recovered in the present study. Two alternative placements of *Pygoscelis grandis* were also found to be equally parsimonious: sister taxon to the clade uniting *Spheniscus*, *Eudyptula*, *Megadyptes*, *Madrynornis*, and *Eudyptes* or sister taxon to a more inclusive clade uniting those taxa and extant *Pygoscelis*. Recovery of these alternative arrangements may be the result of differences in the morphological character sets between our study and that of Walsh and Suárez (2006), changing character optimizations due to the inclusion of stem penguin

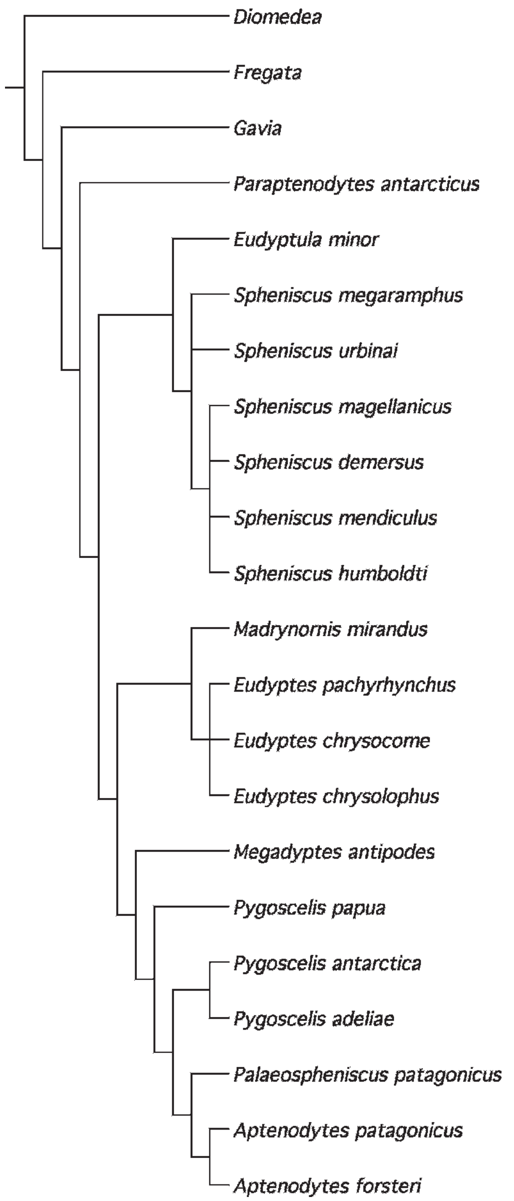

Fig. 12. Single most parsimonious tree from analysis of 44 morphological characters by Acosta Hospitaleche et al. (2007, 2008).

fossils in our analysis, or the influence of molecular data on crown penguin relationships. The results of the present analysis indicate that *Pygoscelis grandis* possesses an interesting combination of character states, and suggest that future finds, particularly of cranial material, may yield better insight into its affinities. *Pygoscelis grandis* lacks partial or complete fusion of the ilia to synsacrum (character states 180: 1–2), a synapomorphy shared by all extant *Pygoscelis* species. Hence, if *Pygoscelis grandis* is part of a clade including the extant *Pygoscelis* species, it almost certainly represents a divergence basal to any extant member of the *Pygoscelis* lineage, as hypothesized by Walsh and Suárez (2006).

Evaluating Potential "Direct Ancestors" of Spheniscidae from the Eocene

In the results of the primary analysis, the small Eocene Antarctic taxa *Delphinornis*, *Mesetaornis*, and *Marambiornis* were placed well outside the crown clade. However, because these taxa are known with certainty only from one bone (the tarsometatarsus), support for their placement is necessarily weak. Iterative analyses (details in Additional Analyses above) explore the effects of adding data from isolated humeri that may belong to these taxa. This allows investigation of Jadwiszczak's (2006b) hypothesis that these penguins represent ancestors of the Spheniscidae by evaluating their placement relative to the crown. These iterative analyses also provide a test of the different possible species assignments for the *Tonniornis* humeri (see Treatment of Problematic Fossils above).

Analysis of the permutation of the dataset adding the type B humerus (IB/P/B-0382) morphotype codings to the *Delphinornis arctowskii* terminal resulted in an increase in the number and length of most parsimonious trees recovered (2642 MPTs, 4494 steps). The strict consensus tree (fig. 14) is congruent with, but less resolved than, the tree obtained from the primary analysis. All taxa placed intermediate between *Waimanu* and clade 8 (see fig. 21), including the modified *Delphinornis arctowskii* terminal, are collapsed into a polytomy. Analyses adding codings from the type B humerus to the terminals for the other three species of *Delphinornis* resulted in strict consensus trees identical to the strict consensus tree recovered in the *Delphinornis arctowskii* permutation, although the number of MPTs varied somewhat among the *Delphinornis gracilis* (1920 MPTs, 4494 steps),

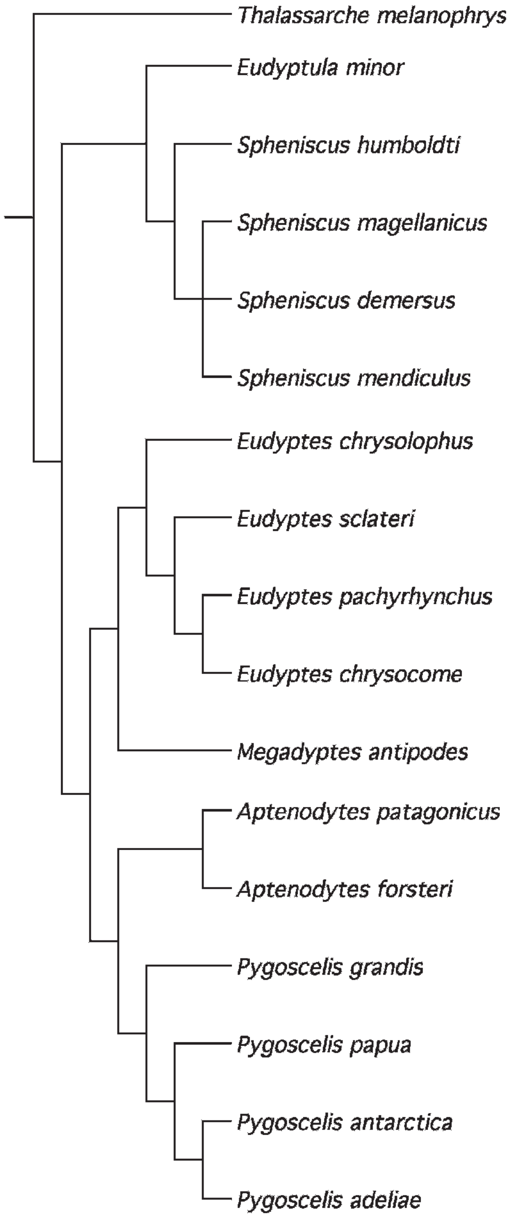

Fig. 13. Strict consensus cladogram from analysis of 37 morphological characters by Walsh and Suárez (2006), designed to test the relationships of *Pygoscelis grandis*.

Delphinornis larseni (2170 MPTs, 4494 steps), and *Delphinornis wimani* (2832 trees, 4494 steps) results.

Analysis of the permutation of the dataset adding the type B humerus codings to the *Marambiornis exilis* terminal resulted in 1503 MPTs of 4494 steps. The strict consensus tree (fig. 15) differs from those from the *Delphinornis* permutations in supporting one branch (that uniting Duntroon *Palaeeudyptes* + clade 8) that was recovered in the primary analysis, but collapsed in the *Delphinornis* permutations. Analysis of the permutation by adding B humerus codings to the *Mesetaornis polaris* terminal also resulted in 1503 MPTs of 4494 steps (*Marambiornis exilis* and *Mesetaornis polaris* share identical sets of character codings).

When the type B humerus (IB/P/B-0382) is treated as a separate terminal, 480 MPTs of 4494 steps are recovered. In the strict consensus tree (fig. 16), the type B humerus terminal does not cluster with *Delphinornis*, *Mesetaornis*, or *Marambiornis*, but is instead recovered as part of clade 6 (see fig. 21). The strict consensus is otherwise similar to that from the primary analysis, with the exception that the branch uniting Duntroon *Palaeeudyptes* + clade 8 is collapsed. As mentioned above, the type A1 and type A2 humerus morphotypes of Jadwiszczak (2006a) are taxonomic equivalents (sensu Wilkinson, 1995) to the type B humerus terminal when coded into our matrix from preserved material.

Analysis of the permutation of the dataset adding codings from the *Tonniornis mesetaensis* holotype humerus (MLP 93-X-1-145) to the *Delphinornis gracilis* terminal also resulted in an increase in the number and length of most parsimonious trees recovered (1920 MPTs, 4493 steps) relative to the primary analysis. In the strict consensus of these trees (fig. 17), all four *Delphinornis* terminals shifted to a slightly more crownward position. These terminals form a polytomy with *Pachydyptes ponderosus*, *Icadyptes salasi*, *Palaeeudyptes gunnari*, *Palaeeudyptes klekowskii*, Duntroon "*Palaeeudyptes*," Burnside "*Palaeeudyptes*," and clade 8 (see fig. 21). Additionally, the branch supporting a more crownward position for *Perudyptes devriesi* than *Mesetaornis polaris* and *Marambiornis exilis* collapses. For the permutation adding codings from the *Tonniornis mesetaensis* humerus to the *Delphinornis larseni* terminal, the strict consensus tree (2090 MPTs, 4493 steps) is identical in

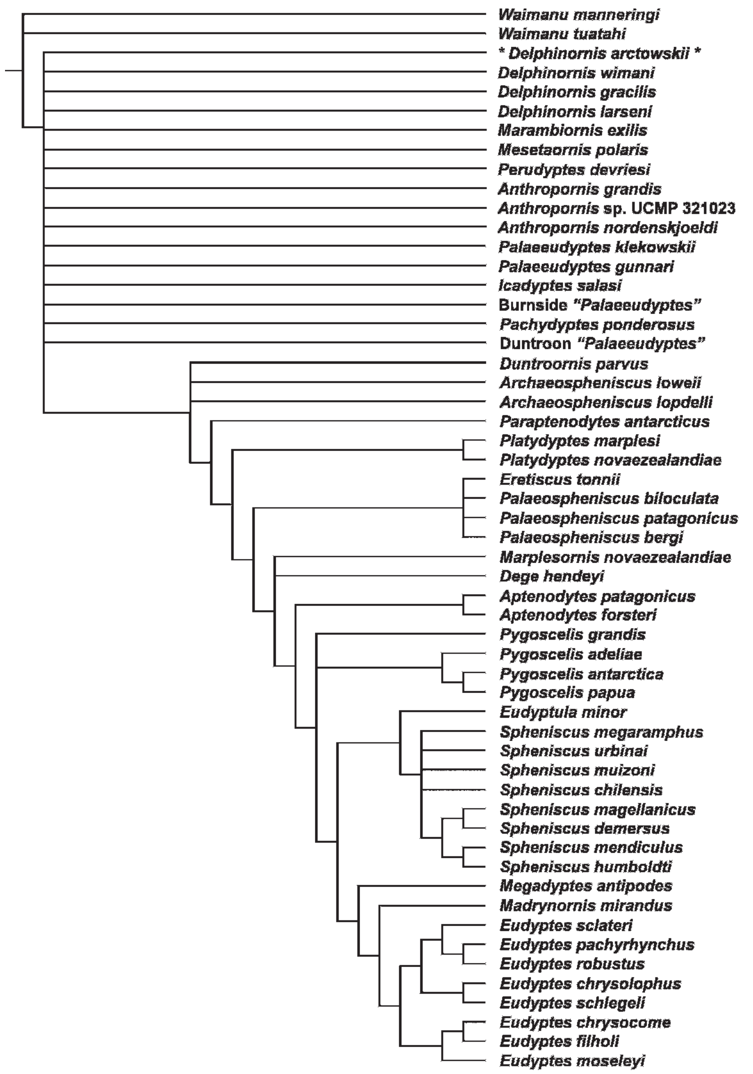

Fig. 14. Results of iterative analyses testing the effect of assigning character codings from isolated elements to species terminals. Strict consensus of 2642 MPTs of 4494 steps from the analysis applying codings from IB/P/B-0382 (type B humerus) to the *Delphinornis arctowskii* terminal. An identical strict consensus topology, with some variation in number of MPTs, resulted from the permutations adding the type B humerus codings to the *Delphinornis gracilis* (1920 MPTs, 4494 steps), *Delphinornis larseni* (2170 MPTs, 4494 steps), and *Delphinornis wimani* (2832 trees, 4494 steps) terminals.

topology to that from the *Delphinornis gracilis* permutation.

Permutations adding codings from the *Tonniornis mesetaensis* holotype humerus (MLP 93-X-1-145) to the *Delphinornis arctowskii* terminal resulted in 3090 MPTs of 4493 steps. The strict consensus of these trees (fig. 18) is less resolved than the permutations for the other *Delphinornis* species. All taxa placed intermediate between *Waimanu* and clade 8 in the primary analysis are collapsed into a polytomy, with the exception that the monophyly of *Anthropornis* is supported. For the permutations adding codings from the *Tonniornis mesetaensis* humerus to the *Delphinornis wimani* terminal, the strict consensus tree (2850 MPTs, 4493 steps) is identical in topology

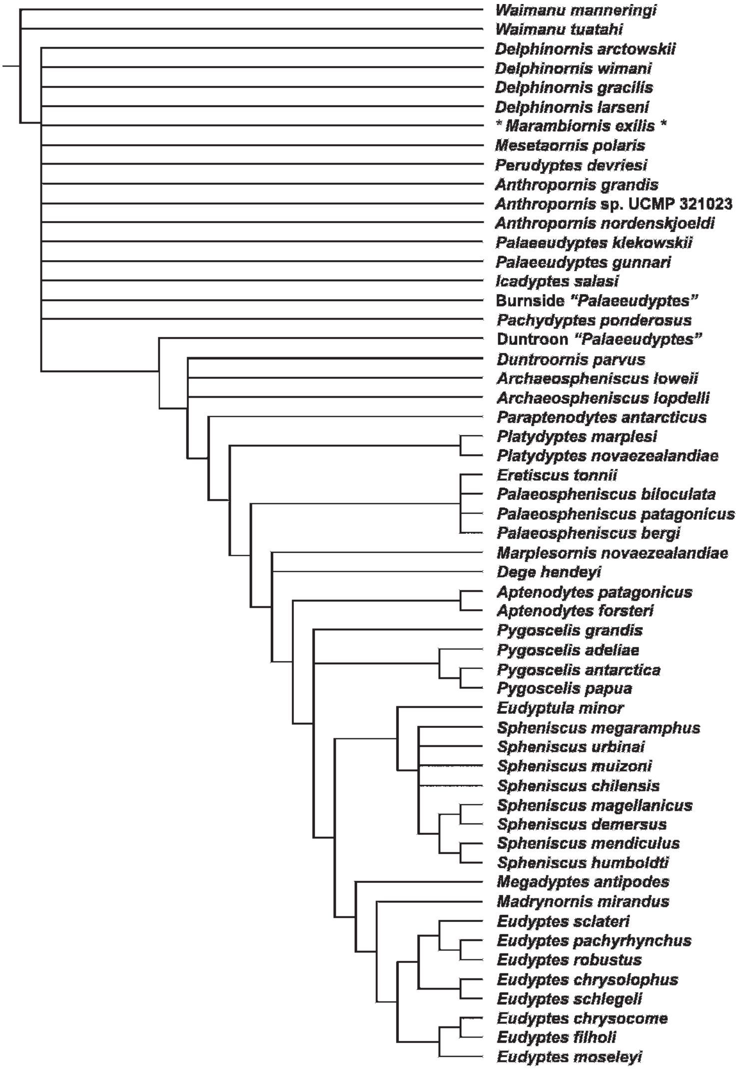

Fig. 15. Results of iterative analyses testing the effect of assigning character codings from isolated elements to species terminals. Strict consensus of 1503 MPTs of 4494 steps from the analysis applying codings from IB/P/B-0382 (type B humerus) to the *Marambiornis exilis* terminal. An identical strict consensus topology resulted from the permutations adding the type B humerus codings to the *Mesetaornis polaris* terminal.

to that from the *Delphinornis gracilis* permutation.

Permutations adding codings from the *Tonniornis mesetaensis* humerus to the *Mesetaornis polaris* terminal resulted in 930 MPTs of 4493 steps. In the strict consensus tree (fig. 19), all taxa placed intermediate between *Delphinornis* and clade 7 in the primary analysis are collapsed into a polytomy, with the exception that the monophyly of *Anthropornis* is supported. Results were identical for the *Marambiornis exilis* permutation.

Finally, the analyses including the holotypes of *Tonniornis mesetaensis* and *Tonniornis minimum* as operational taxonomic units result in 1400 most parsimonious trees of 4492 steps, placing both fossils in a large

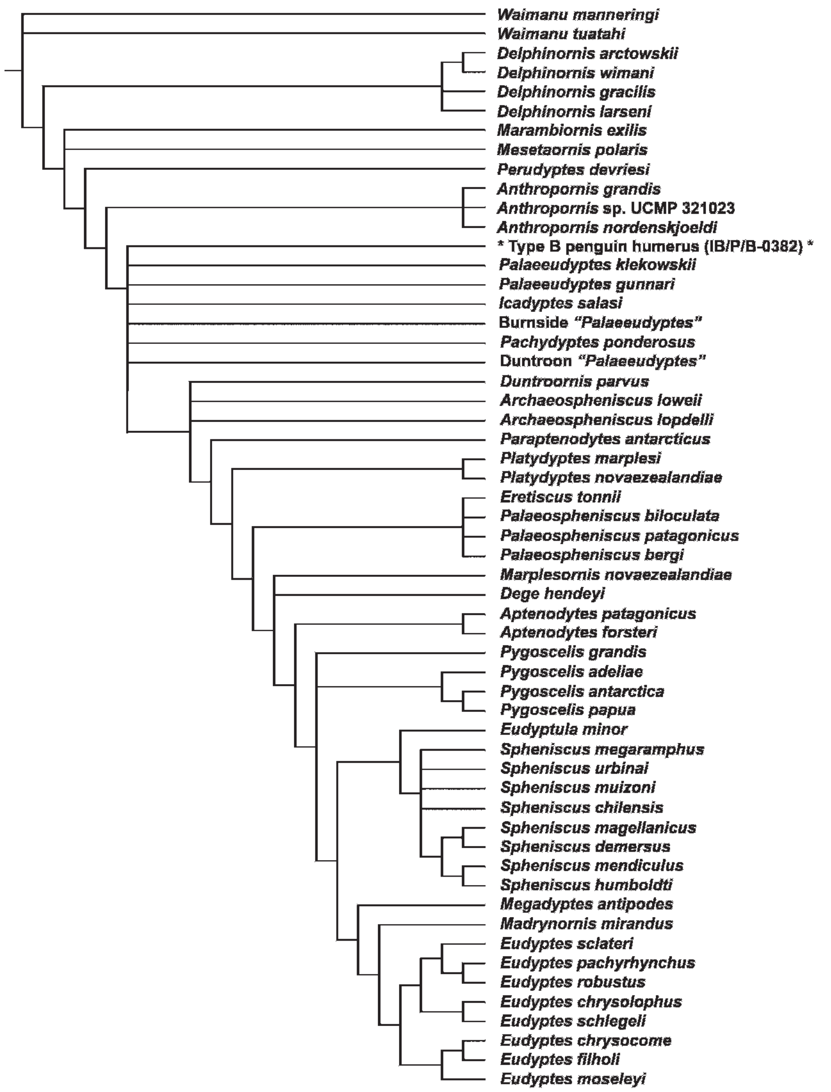

Fig. 16. Strict consensus of 480 MPTs of 4494 steps from the analysis including the type B humerus (IB/P/B-0382) as a separate terminal.

polytomy with other members of clade 6 in the strict consensus tree (fig. 20).

The failure of the small humeri to cluster with any of the La Meseta penguin taxa founded on tarsometatarsi could result from two phenomena. Either (1) all described humeri from the La Meseta Formation represent taxa that are unrelated to *Delphinornis*, *Mesetaornis*, and *Marambiornis*, or (2) homoplasy is present, resulting in different placements for isolated humeri and isolated tarsometatarsi belonging to the same species. The first case would require that humeri of *Delphinornis*, *Mesetaornis*, and *Marambiornis* remain either unpreserved or undiscovered, which we consider unlikely given the large collections of tarsometatarsi from these taxa (e.g., Wiman, 1905a, 1905b; Simpson, 1971c; Myrcha et al., 2002). We consider it more likely that the effect of homoplastic characters, combined with the scarcity of informative characters codable from single elements, accounts for this situation. Given the presence of six small- to medium-sized penguin species based on

Fig. 17. Results of iterative analyses testing the effect of assigning character codings from isolated elements to species terminals. Strict consensus of 1920 MPTs of 4493 steps from the analysis applying codings from the *Tonniornis mesetaensis* holotype humerus to the *Delphinornis gracilis* terminal. In the results of the permutation for *Delphinornis larseni* (6390 trees of 4493 steps), the same strict consensus tree was recovered.

tarsometatarsi, the five differentiable small- to medium-sized humerus types (A1, A2, B, *Tonniornis mesetaensis*, and *Tonniornis minimum*) are most conservatively accounted for as representatives of these species.

Despite difficulties stemming from taxonomic uncertainties, some important conclusions can be drawn. Critically, all coding strategies resulted in *Delphinornis*, *Mesetaornis*, and *Marambiornis*, as well as IB/P/B-0382 and the *Tonniornis* humeri when treated as separate terminals, being placed several nodes basal to the crown clade. Our analyses suggest that regardless of what taxonomic status one affords these isolated specimens, all of the Eocene La Meseta fossil penguins are comparatively distantly related to the crown clade. The placement of *Delphinornis*, *Mesetaornis*, and *Marambiornis* near the base of the sphenisciform

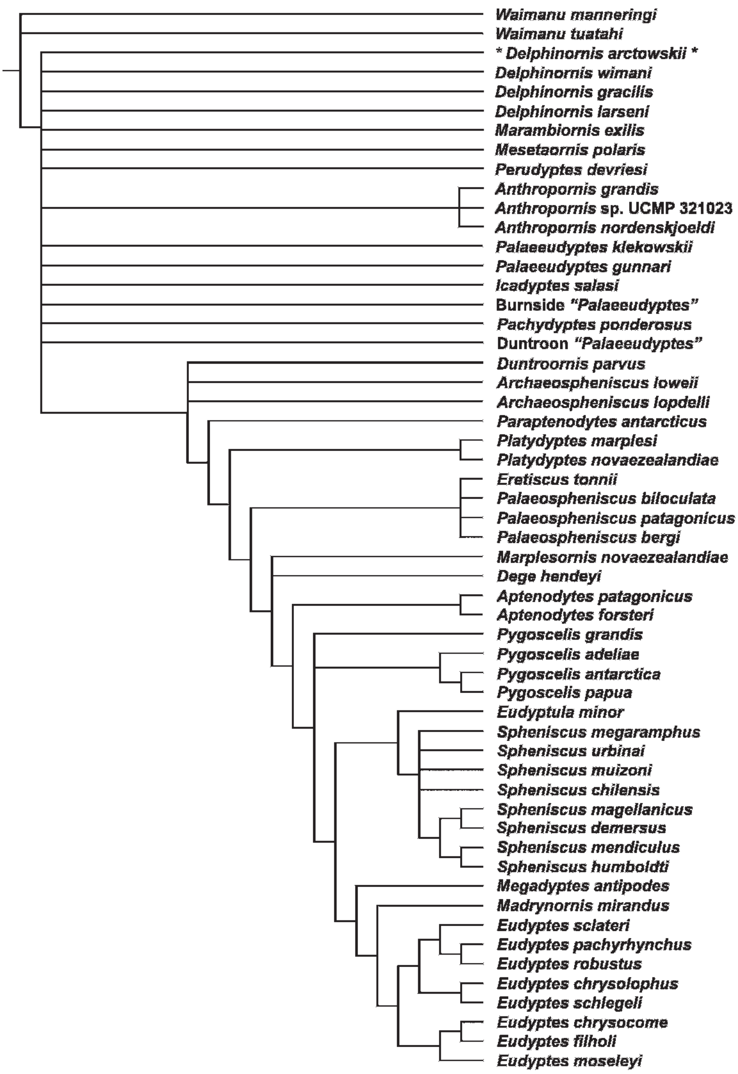

Fig. 18. Results of iterative analyses testing the effect of assigning character codings from isolated elements to species terminals. Strict consensus of 3090 MPTs of 4493 steps from the analysis applying codings from the *Tonniornis mesetaensis* holotype humerus to the *Delphinornis arctowskii* terminal. In the results of the permutation for *Delphinornis wimani* (2850 trees of 4493 steps), the same strict consensus tree was recovered.

tree in the primary analysis, despite relying on sparse morphological data, is the most parsimonious solution that relies only on definitively assignable elements and further agrees well with stratigraphic distribution. This placement is unambiguously supported by the primitive absence of a sulcus between metatarsals II and III (character state 197: 0) and primitive presence of a distal vascular foramen (character state 201: 0) for all species, and additionally by the primitively less shortened tarsometatarsus (character 194: 1) for *Delphinornis gracilis*, *Delphinornis larseni*, *Marambiornis exilis*, and *Mesetaornis polaris*. Bifurcation of the tricipital fossa of the humerus is most parsimoniously interpreted as homoplasy in the taxa represented by the type A1, A2, and B humeri and clade 11 (*Palaeospheniscus*, *Eretiscus*, *Dege*, *Marplesornis*, and Sphenis-

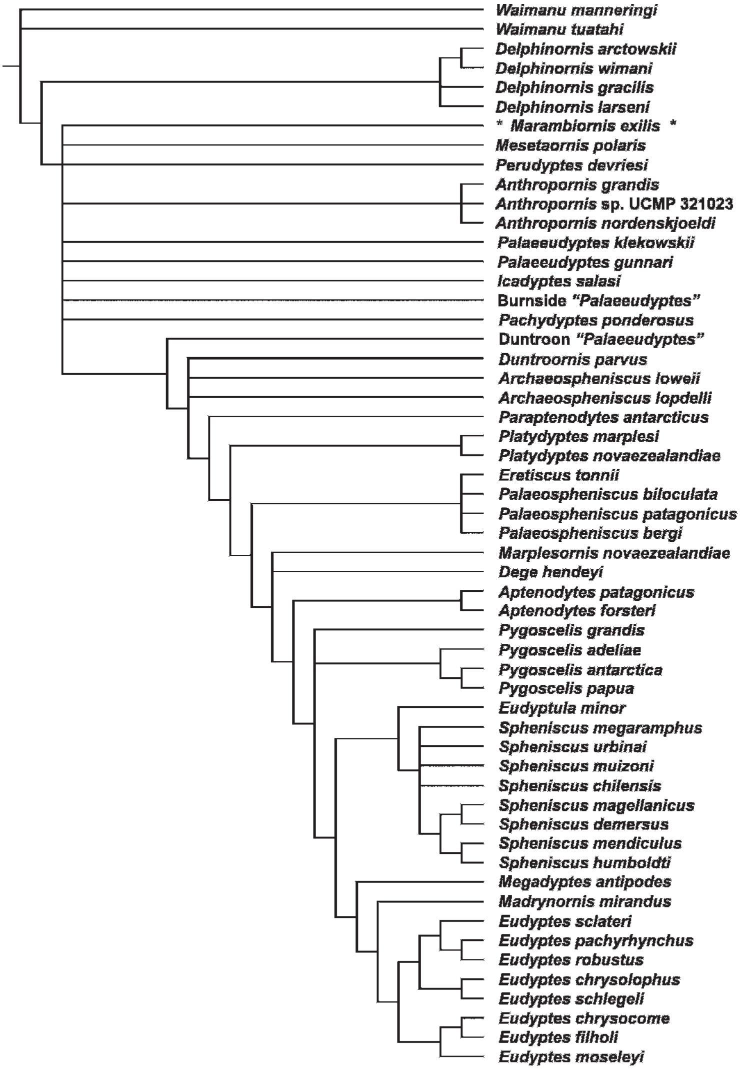

Fig. 19. Results of iterative analyses testing the effect of assigning character codings from isolated elements to species terminals. Strict consensus of 930 MPTs of 4493 steps from the analysis applying codings from the *Tonniornis mesetaensis* holotype humerus to the *Mesetaornis polaris* terminal. An identical strict consensus topology resulted from the permutations adding the *Tonniornis mesetaensis* humerus codings to the *Mesetaornis polaris* terminal.

cidae), regardless of whether the type A1, A2, and B humeri are considered to belong to *Delphinornis*, *Mesetaornis*, or *Marambiornis* or are considered to represent distinct taxa.

The situation addressed here underscores the challenges of working with isolated remains, a problem that has historically hindered studies of penguin evolution (discussed by Fordyce and Jones, 1990) but is increasingly being alleviated by discoveries and descriptions of more complete specimens (e.g., Slack et al., 2006; Clarke et al., 2007; Ando, 2007; Acosta Hospitaleche et al., 2007, 2008). Results from the iterative evaluations of isolated elements reveal potential instability in the placement of *Delphinornis*, *Mesetaornis*, and *Marambiornis* and suggest that

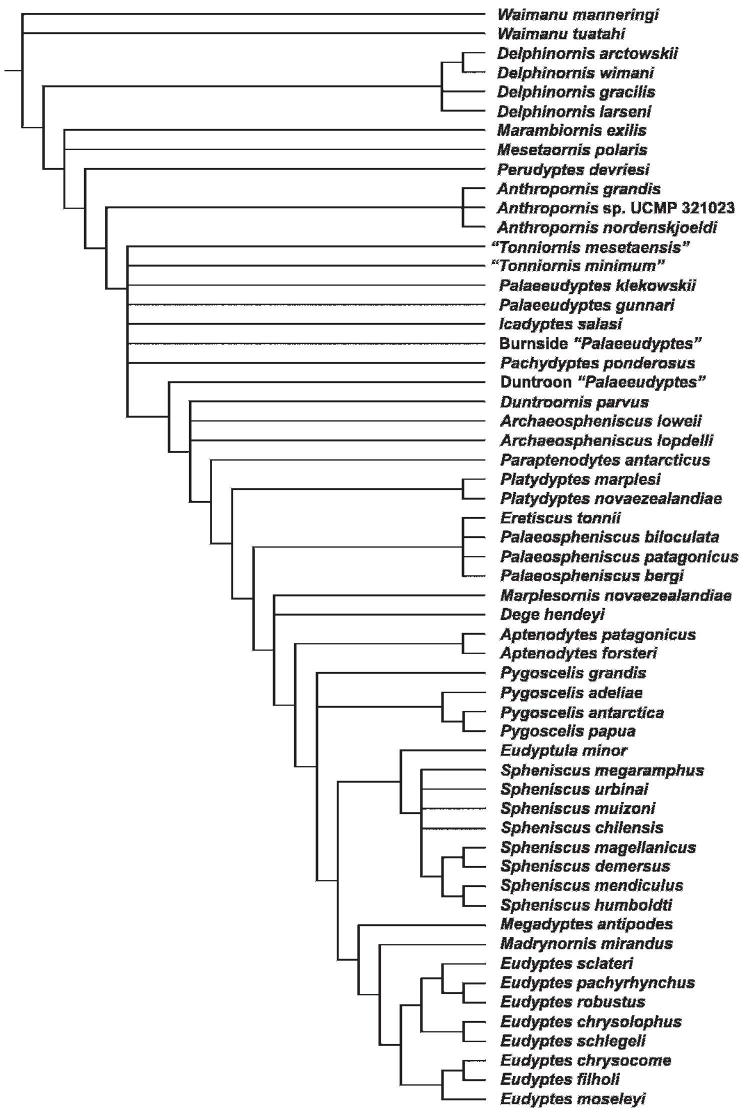

Fig. 20. Strict consensus of 1400 MPTs of 4492 steps from the analysis including the *Tonniornis mesetaensis* and *Tonniornis minimum* holotype humeri as separate terminals.

caution in both taxonomic and phylogenetic interpretations of the La Meseta penguins is needed until articulated materials become available to resolve these issues. Specifically, we note that because the inclusion of data from exemplar humeri results in widened array of equally most parsimonious positions for *Delphinornis*, *Mesetaornis*, and *Marambiornis*, these taxa should be regarded as poorly phylogenetically constrained pending discovery of more complete remains.

A New Consideration of Fragmentary Fossils: Implications for the Timing of Penguin Evolution

Although incompleteness may preclude full resolution of the phylogenetic position of many fragmentary penguin fossils, the relationships of these fossils are relevant to understanding the timing of the radiation of Sphenisciformes. We evaluated the phylogenetic position of all valid named fossil taxa and several unnamed but important specimens that were not included in the primary analysis by identifying synapomorphies in the strict consensus tree from the primary analysis. Specimens were placed to the most exclusive level supported by the distribution of observable synapomorphies. We also evaluated whether these fossils retained character states optimized as plesiomorphies that support exclusion from the crown clade. In cases where the monophyly of a set of specimens assigned to a species was in question, we considered specimens individually. For example, we evaluated several fossils (e.g., the "Seal Rock *Palaeeudyptes*" specimen) originally assigned to *Palaeeudyptes antarcticus*, but no longer considered referable to that taxon (Simpson, 1971b), at the specimen level.

Of 27 poorly known taxa and isolated fossils evaluated, 17 were found to represent stem lineage Sphenisciformes based on the presence of plesiomorphic character states, 4 were found to represent crown Spheniscidae based on synapomorphies, and 6 preserved insufficient character evidence to determine crown/stem status (table 2).

Additional data from more fragmentary penguin fossils considered here are also consistent with a recent radiation of the crown clade. All of the 14 pre-Miocene fossils evaluated can be excluded from Spheniscidae, as they possess plesiomorphic character states unknown in crown taxa. However, one of these fossils contributes stratigraphic data relevant to deeper divergences (reflected in the dotted line in fig. 21). SAMA P14157, a partial wing from the late Eocene of Australia (formerly referred to *Pachydyptes* or *Anthropornis*, see Taxonomic Implications below), is supported as a member of clade 7 by one synapomorphy of that clade (character state 173: 1, extension of metacarpal III markedly distal to metacarpal II). All members of clade 7 identified in the primary analysis are Oligocene or younger in age. Therefore, SAMA P14157 extends the known range of clade 7 by several million years.

Six fossils cannot be included in, or excluded from, Spheniscidae based on preserved character states. However, none of these fossils can be demonstrated to be older than *Spheniscus muizoni*. Therefore, even if future discoveries were to identify one or more of them as representing Spheniscidae, it would not extend the stratigraphic range of the crown clade. Among these six fossils are the holotypes of two New Zealand taxa (*Aptenodytes ridgeni* and *Pygoscelis tyreei*). Both of these specimens were both collected from eroded blocks found loose on a beach, and they are thus poorly constrained in age. A range of ages spanning from middle Miocene to early Pleistocene have been considered plausible for these fossils (Simpson, 1972b). Most recently Feldmann and Keyes (1992) noted that a middle-late Miocene age for these fossils was most likely, although not certain. *Aptenodytes* and *Pygoscelis* are today restricted to higher latitudes, and so if correctly identified to these clades, the fossil species would extend the geographic ranges of these taxa (Simpson, 1972b). *Aptenodytes ridgeni* may belong within *Aptenodytes* given overall resemblance (Simpson, 1972b), but we cannot identify any unambiguous synapomorphies of extant *Aptenodytes* in the partial hindlimb holotype. Likewise, whether *Pygoscelis tyreei* forms a clade with extant *Pygoscelis* cannot be confirmed or refuted given the available material. Simpson (1972b: 159) also considered the affinities of these two species to be "not absolutely certain."

Four fragmentary fossils are positively supported as members of crown Spheniscidae (clade 13) based on synapomorphies. All of these taxa are Miocene or younger in age. Two of these taxa, *Inguza predemersus* and *Tereingaornis moisleyi*, were originally considered to represent new species of the extant genus *Spheniscus* (Simpson, 1971c; see discussion in Scarlett, 1983). Relationships of *Inguza predemersus* cannot currently be resolved relative to other crown penguin taxa, due to the paucity of known material. *Tereingaornis moisleyi* lacks one unambiguous synapomorphy of *Spheniscus* (character state 162: 1, posterior trochlear ridge of humerus fails to extend beyond the ventral margin of the humeral shaft). This taxon further has a distinctly shaped humeral shaft with a prominently curved ventral margin, supporting its separation from *Spheniscus* and also differentiating it from other extant

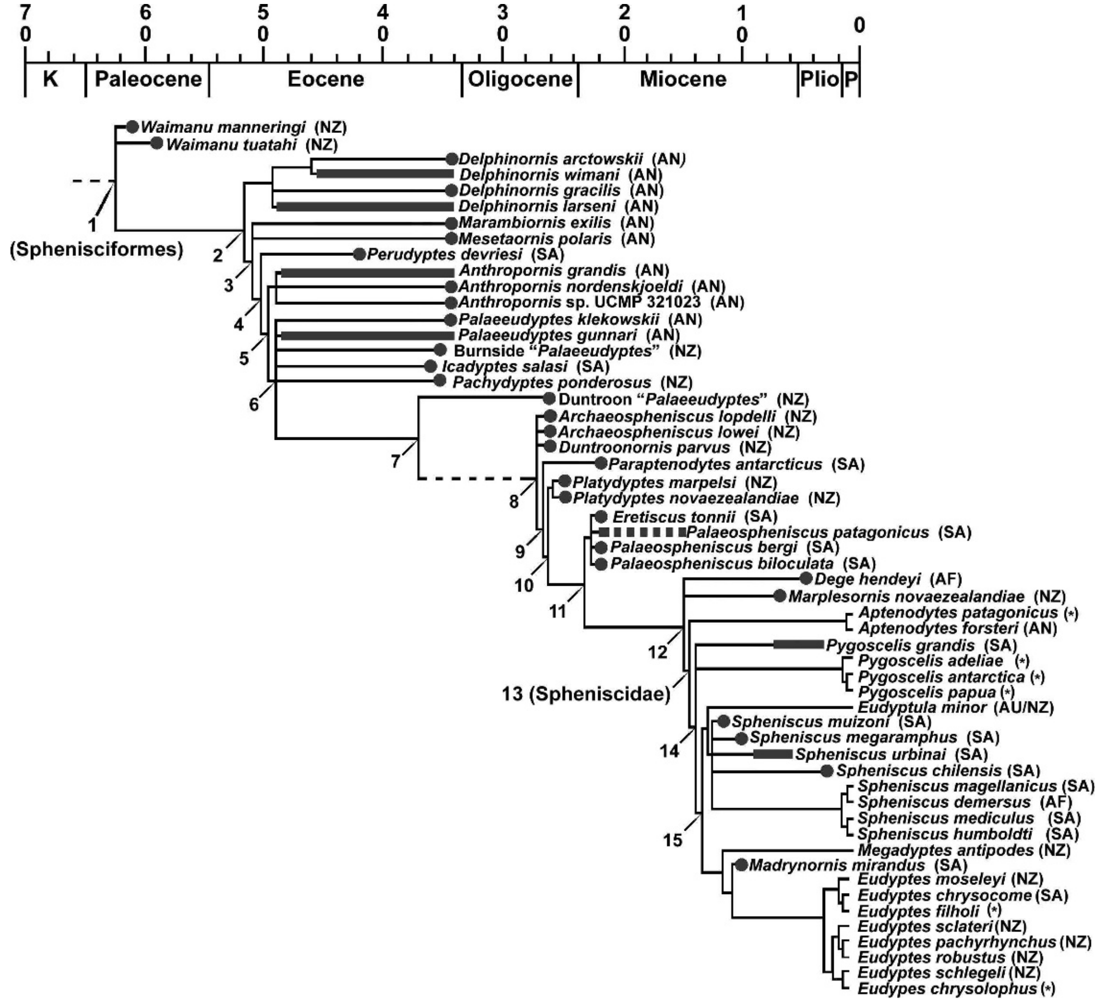

Fig. 21. Phylogeny of Sphenisciformes calibrated to the stratigraphic record. Ghost lineages (Norell, 1992) are minimized. Dotted lines extending the range of clade 7 are based on identification of fragmentary fossils of late Eocene age to this clade. We utilize age ranges for *Spheniscus urbinai* and *Spheniscus megaramphus* provided by Stucchi (2007). Most penguins from the La Meseta Formation occur in Telm 7 (34.2–36.1 Ma), but a few species have been reported from lower units (see Myrcha et al., 2002; Jadwiszczak, 2006a), accounting for the extended ranges of *Delphinornis larseni*, *Anthropornis grandis*, and *Palaeeudyptes gunnari*. A specimen from the Chilcatay Formation (see fig. 1) referred to *Palaeospheniscus* sp. by Acosta Hospitaleche and Stucchi (2005) is provisionally referred to *Palaeospheniscus patagonicus* (Ksepka, 2007), accounting for the longer range of this taxon. For taxa that are poorly constrained in age, the midpoint of possible ages is used (e.g., *Marplesornis* is placed at the late Miocene). Geographical locality for fossil taxa and breeding range of extant taxa are provided in parentheses following taxa names. Asterisks indicate taxa with extensive breeding ranges including oceanic islands (see Bertelli and Giannini [2005] for more data on these species). Abbreviations: AF, Africa; AN, Antarctica; AU, Australia; NZ, New Zealand and surrounding islands; SA, South America.

penguin genera. The third fossil assigned here to Spheniscidae, *Pygoscelis calderensis*, is known from three partial skulls. These skulls preserve weakly developed temporal fossa (character state 83: 1) and a shelf of bone bounding the lateral margin of the salt gland fossa (character state 81: 1) (Acosta Hospitaleche et al., 2006). These morphologies are observed in combination only in extant *Pygoscelis*. However, given the current optimizations of these character states in the strict consensus tree, their presence in *Pygoscelis calderensis* would also be consistent with placement of *Pygoscelis calderensis* as the sister taxon to clade 14 or sister taxon to clade 15. Thus, the monophyly of *Pygoscelis calderensis* plus extant *Pygoscelis* cannot be supported or refuted given current data.

The last of the four extinct taxa identified to the crown clade is the late Holocene (760 ± 60 ybp) subfossil taxon *Tasidyptes hunteri* (van Tets and O'Conner, 1983). Whether *Tasidyptes hunteri* represents a diagnosable species remains debatable (Fordyce and Jones, 1990) due to the incomplete nature of the fossil and the tenuous link between holotype and referred specimens. Some of the hypodigm elements are indistinguishable from corresponding elements of extant *Eudyptes*, and it is possible that these represent a vagrant individual of *Eudyptes* sp. (Ksepka, 2007). Given the young age of *Tasidyptes hunteri* and successful recovery of sequence data from bones of *Megadyptes waitaha* dated to 600–1500 ybp (Boessenkool et al., 2009), recovery of sequence data may be one possible avenue to firmly resolving the status of this taxon.

Pre-cladistic assessments of penguin relationships (e.g., Simpson, 1946; Marples, 1952, 1962) implied that pre-Miocene fossil taxa were not closely related to extant penguins. All such taxa were placed in subfamilies separate from extant penguins. The present study confirms Simpson's (1946) hypothesis that the fossil taxa known at the time he created his classification scheme are indeed not part of the crown penguin radiation. However, it should be noted that the original subfamily classification of fossil Sphenisciformes (Simpson, 1946), although still occasionally employed, was discarded by Simpson (1971b) himself when he concluded that these subfamilies did not reflect evolutionary relationships. Phylogenetic analyses support Simpson's (1971b) decision. Of the four extinct subfamilies originally proposed, only Palaeospheniscinae has been supported as monophyletic, while Palaeeudyptinae, Anthropornithinae, and Paraptenodytinae are polyphyletic (Ksepka et al., 2006; Ksepka, 2007).

Taxonomic Implications

The results of the primary analysis support several taxonomic revisions and also highlight some taxonomically problematic areas.

Delphinornis: We identify one unambiguous synapomorphy of the *Delphinornis* clade: intermediate hypotarsal crests coalesced (character state 196: 1; see also additional differential diagnosis in Myrcha et al., 2002). All recognized species of *Delphinornis* are small Eocene Antarctic penguins. "*Archaeospheniscus*" *wimani* is nested within the *Delphinornis* clade (also including *Delphinornis larseni*, *Delphinornis arctowskii*, and *Delphinornis gracilis*). This species was originally named *Notodyptes wimani* by Marples (1953) and subsequently referred to *Archaeospheniscus* by Simpson (1971a). However, the species shows no close relationship to *Archaeospheniscus lowei* (the type species of *Archaeospheniscus*, known only from the late Oligocene of New Zealand) in our results. *Notodyptes* (Marples, 1953) is here recognized as a junior synonym of *Delphinornis* (Wiman, 1905), creating the new combination *Delphinornis wimani*.

Australian "*Anthropornis*": SAMA P14157, comprising a coracoid, several damaged wing bones, and a vertebra from the late Eocene Blanche Point Formation of Australia, was originally designated the holotype of the species *Pachydyptes simpsoni* (Jenkins, 1974). Jenkins (1985) later considered these remains to represent an Australian occurrence of *Anthropornis nordenskjoeldi* (otherwise known only from the Eocene of Antarctica). However, placement of this specimen to clade 8 (table 2, fig. 21) indicates that SAMA P14157 occupies a more crownward position than both *Pachydyptes* and *Anthropornis*. This placement is supported by projection of metacarpal III significantly beyond the distal end of metacarpal II (character state 173: 1). This character has a consistency index of 1.0, and the primitive state (173: 0) is retained in *Pachydyptes ponderosus*. The condition in *Anthropornis nordenskjoeldi* remains unknown. An isolated carpometacarpus tentatively referred to

Anthropornis nordenskjoeldi by Simpson (1971a) retains the plesiomorphic state, but this specimen was not considered for purposes of character coding in our study given the tenuous nature of the referral. Given the limited comparisons possible and lack of recognizable apomorphies, we recommend that SAMA P14157 be considered Sphenisciformes incerta sedis for the present.

PALAEEUDYPTES: *Palaeeudyptes antarcticus*, the first named fossil penguin species (Huxley, 1859), is currently known with certainty only from a partial tarsometatarsus. It is clear that all specimens previously referred to the species *Palaeeudyptes antarcticus* or to the taxon *Palaeeudyptes* do not form a clade. In our primary analysis, the New Zealand Duntroon "*Palaeeudyptes*" specimens are placed closer to the crown clade than to the New Zealand Burnside "*Palaeeudyptes*" specimens and the Antarctic taxa *Palaeeudyptes klekowskii* and *Palaeeudyptes gunnari*. Additionally, an Australian humerus (SAMA P7158) considered *Palaeeudyptes* cf. *antarcticus* by Simpson (1957) is supported as one node closer to the crown clade than Duntroon "*Palaeeudyptes*" by synapomorphy. Clearly, *Palaeeudyptes* has become a wastebasket taxon in dire need of revision.

Pending a taxonomic revision and publication of new material, it is not yet possible to determine which species, if any, form a clade with the poorly known holotype species *Palaeeudyptes antarcticus*. More complete specimens referable to *Palaeeudyptes antarcticus* and other taxa previously placed in *Palaeeudyptes* are currently under study (see Fordyce and Jones, 1990; Fordyce, 1991; Ando, 2007). It is hoped that publication of this new material will soon resolve the relationships of these specimens, allow a taxonomic revision, and obviate the need for informal names such as "Duntroon *Palaeeudyptes*."

RECOMMENDED CALIBRATION POINTS FOR DIVERGENCE ESTIMATION

Phylogenetic analysis confirms two internal calibration points for molecular sequence-based divergence estimation projects targeting Spheniscidae. *Spheniscus muizoni* provides a minimum estimate for the *Spheniscus-Eudyptula* split. The age of the deposits at the Cerro la Bruja locality where the *Spheniscus muizoni* holotype was collected (Göhlich, 2007) is proposed to be latest middle Miocene or earliest late Miocene (11–13 Ma) based on biostratigraphy (Muizon, 1988; Dunbar et al., 1990). Unfortunately, radiometric dates are unavailable from the relevent deposits and the estimated age range can not yet be rigorously constrained. More precise dates are unavailable at present, so ideally stratigraphic uncertainty should be considered when applying this calibration point.

Madrynornis mirandus provides a minimum estimate for the age of the *Eudyptes-Megadyptes* split. The single known specimen, comprising most of a skeleton, was collected from the "Entrerriense" sequence of the Puerto Madryn Formation (Acosta Hospitaleche et al., 2007). This sequence was deposited at $\sim$10.0 $\pm$ 0.3 Ma based on $^{87}Sr/^{86}Sr$ dates obtained from fossil mollusks (Scasso et al., 2001).

The oldest specimens of *Pygoscelis grandis* were collected from the Bonebed Member of the Bahía Inglesa Formation $\sim$7 m below an ash layer dated to 7.6 $\pm$ 1.3 Ma (Walsh and Suárez, 2006). Given the unresolved placement of *Pygoscelis grandis* in our analysis, we do not recommend it as a calibration point for the divergence of *Pygoscelis* from other penguin lineages. Indeed, even if the phylogenetic placement of *Pygoscelis grandis* was fully resolved, the young age of this fossil precludes its use as a calibration point. Older fossils of *Spheniscus muizoni* and *Madrynornis mirandus* both calibrate more nested divergences, and they thereby provide an older minimum date for divergence of the *Pygoscelis* clade.

Waimanu manneringi remains the oldest stem record of Sphenisciformes and provides a calibration for the Procellariiformes-Sphenisciformes divergence at 60.5–61.6 Ma (Slack et al., 2006). This calibration of course represents a minimum, and the true age of this divergence may well be significantly older given the patchy distribution of fossil Sphenisciformes and lack of fossil Procellariiformes in the Paleocene.

Molecular divergence estimates have placed the basal divergence within crown Spheniscidae in the Eocene ($\sim$40 Ma: Baker et al., 2006), which would require a dramatically different picture of penguin evolution than presented in this contribution. One possible explanation for the conflict between the fossil record and the molecular divergence estimates is that Paleogene fossils of Spheniscidae remain unsampled. Another potential explanation is that such fossils have been collected, but not yet recognized as belonging to crown penguins. Reevaluation of fragmentary remains using synapomorphies in the present study indicates that the apparent absence of crown clade fossils in the Paleogene is most likely not an artifact of a failure to properly identify less complete specimens. While the fossil record of many avian groups remains patchy, Sphenisciformes have one of the more complete records due to their marine habitat and dense bone structure. Clarke et al. (2007) calculated that to account for an Eocene origination of Spheniscidae, the fossil record of penguins would have to be 172%–205% more incomplete as measured in lengths of ghost lineages (Norell, 1992) than inferred from cladogram topology and stratigraphy alone (range results from taking into account different possible resolutions of polytomies). Such a large amount of inferred missing record seems unlikely, given the reasonably continuous global Cenozoic record of penguins and the strong fit of phylogeny to stratigraphy exhibited by penguins (Clarke et al., 2007; Ksepka, 2007) (fig. 21).

Alternatively, problematic aspects of divergence dating methods potentially contribute to overestimation of the age of Spheniscidae. The ~40 Ma estimates for the origin of the penguin crown clade were obtained using two externally derived calibration points: a 104 Ma estimate for the Galloanserae-Neoaves divergence and a 90 Ma estimate for the Galliformes-Anseriformes divergence (Baker et al., 2006). However, these calibration points are not based on avian fossils, but instead they represent extrapolations derived from a primary reptile-mammal calibration point based on the fossil record and a secondary primate-rodent calibration point (itself extrapolated from the primary reptile-mammal calibration) (van Tuinen and Hedges, 2001). Secondary calibrations have been widely criticized for methodological inconsistencies that may lead to erroneous estimates and artificially narrow envelopes of uncertainty (e.g., Shaul and Graur, 2002; Graur and Martin, 2004). However, these challenges can be overcome with new fossil data that sidestep the problems of secondary calibration points.

The true age of Spheniscidae most likely lies somewhere in between the extremes of the Eocene estimate obtained from divergence dating and the first appearance of the crown clade in the fossil record in the middle-late Miocene. Primary calibration points from stratigraphically and phylogenetically constrained fossils have been advocated as the most appropriate sources of calibrations for divergence studies (e.g., Reisz and Müller, 2004; Müller and Reisz, 2005). Two such well-corroborated fossil calibration points (*Spheniscus muizoni* and *Madrynornis mirandus*) have now been identified for future divergence dating studies targeting Sphenisciformes. Such primary internal calibrations may help reduce discordance between the fossil record and molecular estimations.

DISCUSSION

Expanded phylogenetic analysis confirms the position of *Perudyptes devriesi*, facilitates a better understanding of some of the less complete records of Sphenisciformes, clarifies several taxonomic issues, and contributes to the debate surrounding the age of the penguin crown clade. When this phylogenetic framework is combined with temporal data from fragmentary fossils, an improved understanding of broad patterns in penguin evolution emerges.

Sphenisciformes first appear in the fossil record in the early Paleocene, shortly after the K-T boundary, although Pansphenisciformes most likely diverged from their extant sister taxon in the Cretaceous (Slack et al., 2006). The oldest described penguin, *Waimanu manneringi*, is clearly flightless (Slack et al., 2006). Specimens of volant Pansphenisciformes are as yet unknown from the fossil record, but they are inferred to have existed in the earliest Paleocene or the Cretaceous. Insight into the crucial evolutionary interval between the divergence of Pansphenisciformes from its sister taxon and the loss of aerial flight must await new discoveries.

Although late Paleocene–middle Eocene sampling of the penguin record is poor, phylogeny reveals that significant radiation took place during this interval: at minimum, clades 2–6 diverged by the early Eocene (fig. 21). Furthermore, *Perudyptes devriesi* and other fossils indicate that penguins attained a wide geographical distribution prior to the late Eocene (Tambussi et al; 2005; Clarke et al., 2003; Clarke et al., 2007). Stem penguin diversity peaks in the late Eocene (fig. 21, table 2), by which time these birds are taxonomically diverse, geographically widespread, and abundant at many localities (e.g., Marples, 1952; Myrcha et al., 2002). Currently, 15 diagnosable species are recognized from late Eocene deposits, a total approaching modern global species-level diversity (19 species). This count is sure to increase as distinct fossils (e.g., Burnside "*Palaeeudyptes*") are formally named and better specimens resolve the taxonomic status of unique fragmentary fossils (e.g., Jadwiszczak, 2008). When sampling is taken into account, it seems likely that Eocene penguin diversity was much higher than today. Given that most extant penguin species breed primarily or exclusively on small oceanic islands, and that pre-Pleistocene fossils from such islands are essentially unknown, a substantial proportion of extinct diversity is likely unsampled. Indeed, in the case of previously emergent islands that have since subsided, such diversity may be unrecoverable.

A naive reading of figure 21 suggests an abrupt extinction at the end of the Eocene and a subsequent radiation in the late Oligocene. However, extinction and artifact cannot be distinguished based on currently available data. Most late Eocene penguin species are from the La Meseta Formation of Seymour Island, which extends only to the latest Eocene before ending at an unconformity below the contact with the overlying latest Pliocene-Pleistocene Weddell Formation (Marenssi et al., 1998; Dutton et al., 2002; Gadzicki et al., 2004; MacPhee, 2005). Shallow marine strata from the Eocene-Pliocene of Antarctica have not been extensively sampled due to inaccessibility. Thus, any number of the La Meseta penguin species may have survived into the Oligocene or later. Likewise, while late Eocene penguins are well known from New Zealand (Marples, 1952; Fordyce and Jones, 1990) and are also reported from South America (Clarke et al., 2007), fossiliferous early Oligocene marine deposits are so far rare in both regions. Thus, survivorship across the Eocene-Oligocene boundary for penguin taxa cannot yet be adequately addressed.

The early Oligocene represents another poorly known interval in the sphenisciform fossil record (Fordyce and Jones, 1990; Ando, 2007). At present, no formally named penguin species is documented with certainty to this interval, with the possible exception of *Palaeeudyptes antarcticus*. The precise age of the partial tarsometatarsus holotype, collected at Kakanui, New Zealand, is uncertain but may be from the late Eocene or early Oligocene (see Simpson, 1971b; Fordyce and Jones, 1990). Published remains are otherwise limited to a few associated bones and impressions from the Glen Massey Sandstone of the North Island of New Zealand (Grant-Mackie and Simpson, 1973). Penguin fossils of possible early Oligocene age occur in the Ototara Limestone of New Zealand, which spans the Eocene-Oligocene boundary. *Pachydyptes ponderosus* can be placed stratigraphically to late Eocene (Runungan Stage) beds of the Ototara Limestone (Marples, 1952). However, several penguin fossils of uncertain taxonomic affinities were collected from unknown horizons within the Ototara Limestone (Hector, 1871; Marples, 1952), and thus the possibility that these fossils represent early Oligocene occurrences cannot be entirely ruled out. Regardless of whether these fossils are taken into consideration, early Oligocene penguins remain rare. A scarcity of early Oligocene fossils has also been commented on in other marine clades such as cetaceans (e.g., Fordyce, 2003; Uhen and Pyenson, 2007). The paucity of records from this interval may thus be an artifact of the limited amount of exposed shallow marine units available for this interval (Uhen and Pyenson, 2007). Exposures of early Oligocene shallow marine deposits are more rare than exposures of late Eocene and late Oligocene deposits, probably due to global eustatic sea level fall and erosion (Fordyce, 2003).

Following the poorly sampled early Oligocene interval, a second diverse fossil penguin fauna is recorded from the late Oligocene (fig. 21, table 2). Interestingly, all well-known late Oligocene Sphenisciformes are placed closer to Spheniscidae than taxa from the late Eocene fauna (recall that fragmentary taxa in table 2 have simply been assigned to the most exclusive clade supported by synapomorphy). This pattern is consistent with complete replacement of the Eocene penguin fauna by an Oligocene fauna of more crownward stem taxa, although again the timing of this placement is poorly constrained.

In many respects, the late Eocene and late Oligocene stem penguin faunas are similar. Both include "giant" penguins and, as far as can be determined from the scarce fossil record of sphenisciform cranial remains, both faunas are composed largely or entirely of taxa with elongate, narrow beaks (Slack et al., 2006; Clarke et al., 2007; Ksepka et al., 2008). These morphologies have been interpreted as consistent with a diet focused on large prey items such as fish and squid (Olson, 1985; Myrcha et al., 1990), as opposed to one focusing on planktonic crustaceans (seen in many living penguins). Survival of giant penguins into the early Miocene rules out abrupt Eocene/Oligocene cooling (Baker et al., 2006) as an explanation for their extinction (Clarke et al., 2007). Alternative explanations such as competition with marine mammals have yet to be rigorously tested. Warheit and Lindberg (1988) presented evidence for interference competition between pinnipeds and seabirds in recent communities and hypothesized that the trend in reduced body size between Paleogene and Neogene penguin faunas could be related to breeding site competition with pinnipeds. Intriguingly, isotope evidence suggests that historical decimation of pinniped and cetacean populations in the Southern Ocean by humans allowed Adélie penguins to exploit surplus krill (Emslie and Patterson, 2007), providing evidence of competition with other marine clades influencing penguin feeding ecology. These examples emphasize that different factors, including direct predation, competition for food resources, and competition for breeding space, should all be considered in testing for competition between penguins and aquatic mammals.

The penguin fossil record is more continuous across the Oligocene-Miocene transition than the Eocene-Oligocene transition, although sampling in the Miocene interval is largely restricted to the rich record in South America. Giant penguins appear to have died out by, or during, the Miocene. In South American, the latest surviving giant taxon is *Arthrodytes andrewsi* from the late Oligocene San Julian Formation (Parras et al., 2008), while in New Zealand the giant Duntroon "*Palaeeudyptes*" and the very large *Archaeospheniscus lopdelli* are known from the late Oligocene. Putatively, the youngest record of a giant penguin is the rarely mentioned *Anthropodyptes gilli* from Australia (Gill; 1959; Simpson, 1959), known only from a single humerus (see measurements in table 1). Based on foraminifera from the type locality, *Anthropodyptes gilli* appears to be from the lower Miocene (Jenkins, 1974). The only other Neogene taxon exceeding the extant Emperor Penguin in body size is *Aptenodytes ridgeni*, estimated to be 10% larger than *Aptenodytes forsteri* based on the holotype hindlimb (Simpson, 1972b). This taxon is poorly constrained stratigraphically because the single known specimen was collected from a loose concretion at the Motunau (South Island, New Zealand) locality (Simpson, 1972b). Simpson (1972b) considered this penguin-bearing concretion to be derived from the Greta Siltstone and noted the plausible age range was rather broad (middle Miocene to early Pleistocene), although he considered a late Pliocene age to be most probable. More recently, Feldmann and Keyes (1992) concluded a middle-late Miocene age to be most likely for the Greta Siltstone, but because index fossils have not been reported, this age remains poorly constrained (discussed in Feldmann et al., 2006).

Spheniscidae first appear in the fossil record in the middle/late Miocene (Göhlich, 2007), consistent with a recent radiation of crown penguins replacing more basally divergent taxa early in the Neogene (Ksepka et al., 2006). Most major divergences in Spheniscidae occurred by the late Miocene (fig. 21). Although members of extant subclades of Spheniscidae are recognized in the fossil record, no individual species has a deep stratigraphic range. The oldest specimens assignable to extant species are bones of *Megadyptes antipodes* and bones and eggs of *Eudyptula minor* from deposits at Cape Wanbrow, New Zealand, dated to 110,000–130,000 ybp (Worthy and Grant-Mackie, 2003). *Pygoscelis adeliae* has the perhaps the most extensive record of any extant species in terms of material, with subfossil bones, feathers, and eggshell from multiple localities in Antarctica providing insight into colonization patterns extending as far back as 45,000 ybp (e.g., Lambert et al., 2002; Ritchie et al., 2004; Emslie and Patterson, 2007; Emslie et al., 2007). Younger material has been assigned to other extant species, including *Pygoscelis papua* (4500 ybp; King George Island; del Valle et al., 2002), *Eudyptes schlegeli* (~6000 ybp; Macquarie Island; McEvey and Vestjens, 1973), *Aptenodytes patagonicus* (~4000 ybp; Macquarie Island; McEvey and Vestjens, 1973), *Eudyptes pachyrhynchus* (30,000–70,000 ybp; New Zealand; Worthy and Grant-Mackie, 2003; <2000 ybp; New Zealand; Worthy, 1997), *Megadyptes antipodes* (<2000 ybp; New Zealand; Worthy, 1997) and *Eudyptula minor* (690–830 ybp; Tasmania; van Tets and O'Conner, 1983).

Notably, the Neogene penguin fauna is characterized by smaller bodied penguins, most known or inferred from phylogeny to possess a relatively short-beaked skull more similar to extant penguins (extant *Aptenodytes* is one exception) than to Eocene and Oligocene taxa. Undescribed material of the Oligocene taxon *Platydyptes* preserves an elongate, narrow beak (referenced in Slack et al., 2006), and a recently reported partial beak of the Miocene taxon *Palaeospheniscus patagonicus* resembles those of modern short-beaked penguins (Acosta Hospitaleche et al., 2008). Current evidence is thus consistent with the first acquisition of a short-beaked skull type occurring by the Miocene in clade 11, close to the origination of Spheniscidae. Additional cranial features related to diet, such as the reduced temporal musculature and deeper beak shape characterizing extant penguins that specialize on planktonic prey (Zusi, 1975), are restricted to the crown clade (Ksepka et al., 2006). Thus, a shift in feeding ecology may be an important factor in the success of Spheniscidae. Potential drivers of this shift remain untested, but two intriguing possibilities include the development of the biomass-rich "fertile crescent" of the Southern Ocean created by the circumpolar current in the early Neogene (Kooyman, 2002) and competition with marine mammals (Simpson, 1976; Olson, 1985; Warheit and Lindberg, 1988).

ACKNOWLEDGMENTS

Part of this work on the penguin fossil record was completed in fulfillment of the dissertation requirements of the Columbia University–American Museum of Natural History joint graduate program in paleontology (D.T.K.). Mark Norell, Paul Olsen, and Jin Meng are acknowledged for extensive support and guidance. We thank Tom DeVries for providing important geological background on the type locality, and Mario Urbina, Marcelo Stucchi, Rodolfo Salas, Alí Altamirano, Niels Valencia, Dan Omura, Julia Tejada, Walter Aguirre, and Eusebio Díaz of the Museo de Historia Natural, Universidad Nacional Mayor de San Marcos, Leonard Brand of Loma Linda University, and Cesar Aguirre for invaluable contributions to fieldwork and logistics. R. Ewan Fordyce and Tatsuro Ando (OU), Sue Heath and Cody Fraser (OM), Alan Tennyson (MNZS), Paul Scofield and Norton Hiller (CM), Joel Cracraft, Paul Sweet, and Peter Capainolo (AMNH), Mark Florence and Storrs Olson (USNM), and Pat Holroyd (UCMP) kindly provided access to material, and Jun Liu (IVPP) provided photographs of SAM specimens. Discussions with Marcelo Stucchi and Tatsuro Ando helped improve the content of this paper. We thank Kristin Lamm for the skillful line drawings and the silhouette reconstructions, as well as for helpful comments on this manuscript. Research is funded by NFS DEB-0949899 (D.T.K.) and DEB-0949897 (J.A.C.), and grants from the National Geographic Society Expeditions Council and National Science Foundation Office of International Science and Engineering (J.A.C). Support from the Frank M. Chapman Memorial Fund, Doris O. and Samuel P. Welles Fund, and AMNH Division of Paleontology to D.T.K during dissertation research is gratefully acknowledged.

REFERENCES

Acosta Hospitaleche, C. 2004. Los pinguinos (Aves, Sphenisciformes) fosiles de Argentina. Sistematica, biogeografia y evolution. Ph.D. dissertation, Universidad Nacional de La Plata.

Acosta Hospitaleche, C. 2005. Systematic revision of *Arthrodytes* Ameghino, 1905 (Aves, Spheniscidae) and its assignment to the Paraptenodytinae. Neues Jahrbuch für Geologie und Paläontologie - Abhandlungen 7: 404–414.

Acosta Hospitaleche, C. 2007. Revísion sistemática de *Palaeospheniscus biloculata* (Simpson) nov. comb. (Aves, Spheniscidae) de la Formación Gaiman (Mioceno Temprano), Chubut, Argentina. Ameghiniana 44: 417–426.

Acosta Hospitaleche, C., and J. Canto. 2005. Primer registro de cráneos asignados a *Palaeospheniscus* (Aves, Spheniscidae) procedentes de la Formación Bahía Inglesa (Mioceno Medío-Tardio), Chile. Revista Chilena de Historia Natural 78: 219–231.

Acosta Hospitaleche, C., L. Castro, C. Tambussi, and R.A. Scasso. 2008. *Palaeospheniscus patagonicus* (Aves, Sphenisciformes): new discoveries from the early Miocene of Argentina. Journal of Paleontology 82: 565–575.

Acosta Hospitaleche, C., M. Chávez, and O. Fritis. 2006. Pingüinos fósiles (*Pygoscelis calderensis* nov. sp.) en la Formación Bahía Inglesa (Mioceno Medio-Plioceno), Chile. Revista Geológica de Chile 33: 327–338.

Acosta Hospitaleche, C., and M. Reguero. In press. First articulated skeleton of Palaeeudyptes gunnari *from the late Eocene of Isla Marambio (Seymour Island), Antarctica* Antarctic Science.

Acosta Hospitaleche, C., and M. Stucchi. 2005. Nuevos restos terciarios de Spheniscidae (Aves, Sphenisciformes) procedentes de la costa del Perú. Revista Española de Paleontología 20: 1–5.

Acosta Hospitaleche, C., C. Tambussi, and M. Cozzuol. 2004. *Eretiscus tonnii* (Simpson) (Aves, Sphenisciformes): materiales adicionales, status taxonómico y distribución geográfica. Revista del Museo Argentino de Ciencias Naturales 6: 233–237.

Acosta Hospitaleche, C., C. Tambussi, M. Donato, and M. Cozzuol. 2007. A new Miocene penguin from Patagonia and its phylogenetic relationships. Acta Palaeontologica Polonica 52: 299–314.

Ameghino, F. 1905. Enumeración de los impennes fosiles de Patagonia y de la Isla Seymour. Anales del Museum Nacional de Buenos Aires (36) 6: 97–167.

Ando, T. 2007. New Zealand fossil penguins: origin, pattern, and process. Ph.D. dissertation, University of Otago.

Baker, A.J., S.L. Pereira, O.P. Haddrath, and K.-A. Edge. 2006. Multiple gene evidence for expansion of extant penguins out of Antarctica due to global cooling. Proceedings of the Royal Society Series B 217: 11–17.

Banks, J., A. van Buren, Y. Cherel, and J.B. Whitfield. 2006. Genetic evidence for three species of rockhopper penguins, *Eudyptes chrysocome*. Polar Biology 30: 61–67.

Baumel, J.J., and L.M. Witmer. 1993. Osteologia. *In* J.J. Baumel, A.S. King, J.E. Breazile, H.E. Evans, and J.C. Vanden Berge (editors), Handbook of avian anatomy: nomina anatomica avium: 45–132. Cambridge: Nuttall Ornithology Club.

Bertelli, S., and N.P. Giannini. 2005. A phylogeny of extant penguins (Aves: Sphenisciformes) combining morphology and mitochondrial sequences. Cladistics 21: 209–239.

Bertelli, S., N.P. Giannini, and D.T. Ksepka. 2006. Redescription and phylogenetic position of the early Miocene penguin *Paraptenodytes antarcticus* from Patagonia. American Museum Novitates 3525: 1–36.

Boessenkool, S., et al. 2009. Relict or colonizer? Extinction and range expansion of penguins in southern New Zealand. Proceedings of the Royal Society Series B 276: 815–821.

Bourdon, E., B. Bouya, and M. Iarochene. 2005. Earliest African neornithine bird: a new species of Prophaethontidae (Aves) from the Paleocene of Morocco. Journal of Vertebrate Paleontology 25: 157–170.

Chubb, A.L. 2004. New nuclear evidence for the oldest divergences among neognath birds: phylogenetic utility of ZENK (I). Molecular Phylogenetics and Evolution 30: 140–151.

Clarke, J.A., et al. 2007. Paleogene equatorial penguins challenge the proposed relationship between biogeography, diversity, and Cenozoic climate change. Proceedings of the National Academy of Sciences 104: 11545–11550.

Clarke, J.A., E.B. Olivero, and P. Puerta. 2003. Description of the earliest fossil penguin from South America and first Paleogene vertebrate locality of Tierra del Fuego, Argentina. American Museum Novitates 3423: 1–18.

Cooper, A., and D. Penny. 1997. Mass survival of birds across the Cretaceous-Tertiary boundary: molecular evidence. Science 275: 1109–1113.

Cooper, R.A. 2004. The New Zealand geological timescale. Lower Hutt, New Zealand: Institute of Geological and Nuclear Sciences Monograph 22.

Cracraft, J. 1985. Monophyly and phylogenetic relationships of the Pelecaniformes: a numerical cladistic analysis. Auk 102: 834–853.

Cracraft, J. 1988. The major clades of birds. *In* M.J. Benton (editor), The phylogeny and classification of the tetrapods. Vol. 1. Amphibians, reptiles, birds: 339–361. Oxford: Systematics Association.

Cracraft, J., et al. 2004. Phylogenetic relationships among modern birds (Neornithes): towards an avian tree of life. *In* J. Cracraft and M.J. Donoghue (editors), Assembling the tree of life: 468–489. New York: Oxford Press.

Davis, P.G., and D.E.G. Briggs. 1998. The impact of decay and disarticulation on the preservation of fossil birds. Palaios 13: 3–13.

del Valle, R.A., D. Montalti, and M. Inbar. 2002. Mid-Holocene macrofossil-bearing raised marine beaches at Potter Peninsula, King George Island, South Shetland Islands. Antarctic Science 14: 263–269.

DeVries, T.J. 1998. Oligocene deposition and Cenozoic sequence boundaries in the Pisco Basin (Peru). Journal of South American Earth Sciences 11: 217–231.

DeVries, T.J. 2007. Cenozoic Turritellidae (Gastropoda) from southern Peru. Journal of Paleontology 81: 331–351.

DeVries, T.J., Y. Narváez, A. Sanfilippo, N. Malumian, and P. Tapia. 2006. New microfossil evidence for a late Eocene age of the Otuma Formation (southern Peru). *In* Extended Abstracts, 13 Congreso Peruana de Geología: 615–618. Lima: Sociedad Geológica del Perú.

Dingle, R.V., W.G. Siesser, and A.R. Newton. 1983. Mesozoic and Tertiary geology of Southern Africa. Rotterdam: Balkema.

Dunbar, R.B., R.C. Marty, and P.A. Baker. 1990. Cenozoic marine sedimentation in the Sechura and Pisco basins, Peru. Palaeogeography Palaeoclimatology Palaeoecology 77: 235–261.

Dutton, A.L., K.C. Lohmann, and W.J. Zinmeister. 2002. Stable isotope and minor element proxies for Eocene climate of Seymour Island, Antarctica. Paleoceanography 17: 1016–1029.

Elliot, D.H., and T.A. Trautman. 1982. Lower Tertiary strata on Seymour Island, Antarctic Peninsula. *In* C. Craddock (editor), Antarctic geoscience: 287–297. Madison: University of Wisconsin Press.

Emslie, S.D., L. Coats, and K. Licht. 2007. A 45,000 yr record of Adélie penguins and climate change in the Ross Sea, Antarctica. Geology 35: 61–64.

Emslie, S.D., and C. Guerra Correa. 2003. A new species of penguin (Spheniscidae: *Spheniscus*) and other birds from the late Pliocene of Chile. Proceedings of the Biological Society of Washington 116: 308–316.

Emslie, S.D., and W.P. Patterson. 2007. Abrupt recent shift in δC and δN values in Adélie penguin eggshell in Antarctica. Proceedings of the National Academy of Sciences 104: 11666–11669.

Emslie, S.D., and E.J. Woehler. 2005. A 9000-year record of Adélie penguin occupation and diet in the Windmill Islands, East Antarctica. Antarctic Science 17: 57–66.

Ericson, P.G.P., et al. 2006. Diversification of Neoaves: integration of molecular sequence data and fossils. Biology Letters 4: 543–547.

Esperante, R., L. Brand, K.E. Nick, O. Poma, and M. Urbina. 2008. Exceptional occurrence of fossil baleen in shallow marine sediments of the Neogene Pisco Formation, Southern Peru. Palaeogeography Palaeoclimatology Palaeoecology 257: 344–360.

Fain, M.G., and P. Houde. 2004. Parallel radiations in the primary clades of birds. Evolution 58: 2558–2573.

Feldmann, R.M., and I.W. Keyes. 1992. Systematic and stratigraphic review with catalogue and locality index of the Mesozoic and Cenozoic decapod Crustacea of New Zealand. New Zealand Geological Survey Record 45: 1–73.

Feldmann, R.M., C.E. Schweitzer, and D. McLauchlan. 2006. Additions to the records for decapod Crustacea from Motunau and Glenafric Beaches, North Canterbury, New Zealand. New Zealand Journal of Geology and Geophysics 49: 417–427.

Flynn, J.J., and C.C. Swisher, III. 1995. Cenozoic South American Land Mammal Ages: correlation to global geochronologies. *In* W.A. Berggren, D.V. Kent, M.-P. Aubry, and J. Hardenbol (editors), Geochronology, time scales and global stratigraphic correlation (SEPM Special Publication 54): 317–333. Tulsa, OK: Society for Sedimentary Geology.

Fordyce, R.E. 1991. A new look at the fossil vertebrate record of New Zealand. *In* P. Vickers-Rich, J.M. Monaghan, R.F. Baird, and T.H. Rich (editors), Vertebrate palaeontology of Australasia: 1191–1316. Melbourne: Pioneer Design Studio and Monash University.

Fordyce, R.E. 2003. Cetacean evolution and Eocene-Oligocene oceans revisited. *In* D.R. Prothero, L.C. Ivany, and E.A. Nesbitt (editors), From greenhouse to icehouse: the marine Eocene-Oligocene transition: 154–170. New York: Columbia University Press.

Fordyce, R.E., and C.M. Jones. 1990. Penguin history and new fossil material from New Zealand. *In* L.S. Davis and J.T. Darby (editors), Penguin biology: 419–446. San Diego, CA: Academic Press.

Gadzdzicki, A., A. Tatur, U. Hara, and R.A. del Valle. 2004. The Weddell Sea formation: post Late-Pliocene terrestrial glacial deposits on Seymour Island, Antarctic Peninsula. Polish Polar Research 25: 189–204.

Gauthier, J. 1986. Saurischian monophyly and the origin of birds. Memoirs of the California Academy of Sciences 8: 185–197.

Giannini, N.P., and S. Bertelli. 2004. Phylogeny of extant penguins based on integumentary and breeding characters. Auk 121: 422–434.

Gill, E.D. 1959. Provenance of a fossil penguin from western Victoria. Proceedings of the Royal Society of Victoria 71: 121–123.

Göhlich, U.B. 2007. The oldest fossil record of the extant penguin genus *Spheniscus* – a new species from the Miocene of Peru. Acta Paleontologica Polonica 52: 285–298.

Goloboff, P.A., J.S. Farris, and K.C. Nixon. 2008. TNT, a free program for phylogenetic analysis. Cladistics 24: 1–13.

Grant-Mackie, J.A., and G.G. Simpson. 1973. Tertiary penguins from the North Island of New Zealand. Journal of the Royal Society of New Zealand 3: 441–452.

Graur, D., and D. Martin. 2004. Reading the entrails of chickens: molecular timescales of evolution and the illusion of precision. Trends in Genetics 20: 80–86.

Groth, J.G., and G.F. Barrowclough. 1999. Basal divergences in birds and the phylogenetic utility of the nuclear RAG-1 gene. Molecular Phylogenetics and Evolution 12: 115–123.

Hackett, S.J., et al. 2008. A phylogenomic study of birds reveals their evolutionary history. Science 320: 1763–1768.

Harrison, G.L., et al. 2004. Four new avian mitochondrial genomes help get to basic evolutionary questions in the Late Cretaceous. Molecular Biology and Evolution 21: 974–983.

Hartley, A.J., G. Chong, J. Houston, and A.E. Mather. 2005. 150 million years of climactic stability: evidence from the Atacama Desert, northern Chile. Journal of the Geological Society (London) Special Paper 162: 421–424.

Hebert, P.D.N., M.Y. Stoeckle, T.S. Zemlak, and C.M. Francis. 2004. Identification of birds through DNA barcodes. PLoS Biology 2: e312.

Huxley, T.H. 1859. On a fossil bird and a cetacean from New Zealand. Quarterly Journal of the Geological Society of London 15: 670–677.

Jadwiszczak, P. 2001. Body size of Eocene Antarctic penguins. Polish Polar Research 22: 147–158.

Jadwiszczak, P. 2003. The early evolution of Antarctic penguins *In* A.H.L. Huiskes, et al. 2003. Antarctic biology in a global context: 148–151. Leiden: Bachhuys.

Jadwiszczak, P. 2006a. Eocene penguins of Seymour Island, Antarctica: taxonomy. Polish Polar Research 27: 3–62.

Jadwiszczak, P. 2006b. Eocene penguins of Seymour Island, Antarctica: the earliest record, taxonomic problems and some evolutionary considerations. Polish Polar Research 27: 287–302.

Jadwiszczak, P. 2008. An intriguing penguin bone from the late Eocene of Seymour Island, Antarctic Peninsula. Antarctic Science 20: 589–590.

Jenkins, R.J.F. 1974. A new giant penguin from the Eocene of Australia. Palaeontology 17: 291–310.

Jenkins, R.J.F. 1985. *Anthropornis nordenskjoeldi* Wiman, 1905: Nordenskjoeld's giant penguin. *In* P.V. Rich and G.F. van Tets (editors), Kadimakara, extinct vertebrates of Australia: 183–187. Victoria: Pioneer Design Studio.

Jesinkey, C., R.D. Forsythe, C. Mpodozis, and J. Davidson. 1987. Concordant late Paleozoic paleomagnetizations from the Atacama Desert: implications for tectonic models of the Chilean Andes. Earth and Planetary Science Letters 85: 461–472.

Jouventin, P., P.M. Nolan, J. Ornborg, and F.S. Dobson. 2005. Ultraviolet beak spots in King and Emperor penguins. Condor 107: 144–150.

Kandefer, H.M. 1994. Róznorodnosc fauny pingwinów kopalnych antarktycznej Wyspy Seymour w oparciu o analize humeri z kolekcji Instytutu Biologii Filii Uniwersytetu Warszawskiego w Bialymstoku. Dissertation, Warszawski University.

Keller, G., et al. 1997. The Cretaceous/Tertiary boundary event in Ecuador: reduced biotic effects due to eastern boundary current setting. Marine Micropaleontology 31: 97–133.

Kerr, K.C.R., et al. 2007. Comprehensive DNA barcode coverage of North American birds. Molecular Ecology Notes 7: 535–543.

Kooyman, G.L. 2002. Evolutionary and ecological aspects of some Antarctic and sub-Antarctic penguin distributions. Oecologia 130: 485–495.

Ksepka, D.T. 2007. Phylogeny, histology and functional morphology of fossil penguins (Aves:

Sphenisciformes). Ph.D. dissertation, Columbia University.

Ksepka, D.T., and S. Bertelli. 2006. Fossil penguin (Aves: Sphenisciformes) cranial material from the Eocene of Seymour Island (Antarctica). Historical Biology 18: 389–395.

Ksepka, D.T., S. Bertelli, and N.P. Giannini. 2006. The phylogeny of the living and fossil Sphenisciformes (penguins). Cladistics 22: 412–441.

Ksepka, D.T., J.A. Clarke, T.J. DeVries, and M. Urbina. 2008. Osteology of *Icadyptes salasi*, a giant penguin from the Eocene of Peru. Journal of Anatomy 213: 131–147.

Lambert, D.M., et al. 2002. Rates of evolution in ancient DNA from Adélie penguins. Science 295: 2270–2273.

Lambert, O., G. Bianucci, and C. de Muizon. A new stem-sperm whale (Cetacea, Odontoceti, Physeteroidea) from the Latest Miocene of Peru. Comptes Rendus Palevol 7: 361–369.

Livezey, B.C. 1989. Morphometric patterns in recent and fossil penguins (Aves, Sphenisciformes). Journal of the Zoological Society of London 219: 269–307.

Livezey, B.C., and R.L. Zusi. 2006. Higher-order phylogenetics of modern birds (Theropoda, Aves: Neornithes) based on comparative anatomy. I. Methods and characters. Bulletin of the Carnegie Museum of Natural History 37: 1–544.

Livezey, B.C., and R.L. Zusi. 2007. Higher-order phylogeny of modern birds (Theropoda, Aves: Neornithes) based on comparative anatomy. II. Analysis and discussion. Zoological Journal of the Linnean Society 149: 1–95.

MacPhee, R.D.E. 2005. 'First' appearances in the Cenozoic land-mammal record of the Greater Antilles: significance and comparison with South American and Antarctic records. Journal of Biogeography 32: 551–564.

Maddison, W.P., and D.R. Maddison. 1992. MacClade: analysis of phylogeny and character evolution, Version 4.08. Sunderland, MA: Sinauer Associates.

Manegold, A. 2006. Two additional synapomorphies of grebes Podicipedidae and flamingos Phoenicopteridae. Acta Ornithologica 41: 79–82.

Marenssi, S.A., S.N. Santillana, and C.A. Rinaldi. 1998. Stratigraphy of the La Meseta Formation (Eocene), Marambio (Seymour) Island, Antarctica. *In* S. Casadío (editor), Paleógeno de América del Sur y de la Península Antarctica. Asociacón Paleontológica Argentia Publicación Especial 5: 137–146.

Marples, B.J. 1952. Early Tertiary penguins of New Zealand. New Zealand Geological Survey Paleontological Bulletin 20: 1–66.

Marples, B.J. 1953. Fossil penguins from the mid-Tertiary of Seymour Island. Falkland Islands Dependencies Survey Scientific Reports 5: 1–15.

Marples, B.J. 1960. A fossil penguin from the Late Tertiary of North Canterbury. Records of the Canterbury Museum 7: 185–195.

Marples, B.J. 1962. Observations on the history of penguins. *In* G.W. Leeper (editor), The evolution of living organisms: 408–416. London: Cambridge University Press.

Marples, B.J., and C.A. Fleming. 1963. A fossil penguin bone from Kawhia, New Zealand. New Zealand Journal of Geology and Geophysics 6: 189–192.

Mayr, G. 2004. Morphological evidence for sister group relationship between flamingos (Aves: Phoenicopteridae) and grebes (Podicipedididae). Zoological Journal of the Linnean Society 140: 157–169.

Mayr, G. 2005. Tertiary plotopterids (Aves, Plotopteridae) and a novel hypothesis on the phylogenetic relationships of penguins (Spheniscidae). Journal of Zoological Systematics and Evolutionary Research 43: 61–71.

Mayr, G. 2007. The contribution of fossils to the reconstruction of the higher-level phylogeny of birds. Species, Phylogeny and Evolution 1: 58–64.

Mayr, G., and J. Clarke. 2003. The deep divergences of neornithine birds: a phylogenetic analysis of morphological characters. Cladistics 19: 527–553.

McEvey, A.R., and W.J.M. Vestjens. 1973. Fossil penguin bones from Macquarie Island, Southern Ocean. Proceedings of the Royal Society of Victoria 86: 151–174.

McKitrick, M.C. 1991. Phylogenetic analysis of avian hindlimb musculature. Miscellaneous Publications University of Michigan Museum of Zoology 179: 1–85.

Muizon, C. de. 1981. Les vertébrés fossiles de la formation Pisco (Pérou). Première partie: deux nouveaux Monachinae (Phocidae: Mammalia) du Pliocène inférieur de Sud-Sacaco. Travaux de l'Institut Français d'Études Andines 22: 1–160.

Muizon, C. de. 1984. Les vertébrés fossiles de la formation Pisco, Pérou. Deuxième partie: les Odontocètes (Cetacea, Mammalia) du Pliocène inférieur de Sud-Sacaco. Travaux de l'Institut Français d'Études Andines 27: 1–888.

Muizon, C. de. 1988. Les vertébrés fossiles de la formation Pisco, Pérou. Troisième partie: les Odontocètes (Cetacea, Mammalia) du Miocène. Travaux de l'Institut Français d'Études Andines 42: 1–244.

Muizon, C. de. 1993. Walrus-like feeding adaptation in a new cetacean from the Pliocene of Peru. Nature 365: 745–748.

Muizon, C. de., and T.J. Devries. 1985. Geology and paleontology of late Cenozoic marine deposits in the Sacaco area (Peru). International Journal of Earth Sciences 74: 547–563.

Muizon, C. de., G. McDonald, R. Salas, and M. Urbina. 2003. A new early species of the aquatic sloth *Thalassocnus* (Mammalia, Xenarthra) from the late Miocene of Peru. Journal of Vertebrate Paleontology 23: 886–894.

Muizon, C. de., G. McDonald, R. Salas, and M. Urbina. 2004. The evolution of feeding adaptations of the aquatic sloth *Thalassocnus*. Journal of Vertebrate Paleontology 24: 401–413.

Müller, J., and R.R. Reisz. 2005. Four well-constrained calibration points from the vertebrate fossil record for molecular clock estimates. BioEssays 27: 1069–1075.

Myrcha, A., et al. 2002. Taxonomic revision of Eocene Antarctic penguins based on tarsometatarsal morphology. Polish Polar Research 23: 5–46.

Myrcha, A., A. Tatur, and R. del Valle. 1990. A new species of fossil penguin from Seymour Island, West Antarctica. Alcheringa 14: 195–205.

Norell, M.A. 1992. The effect of phylogeny on temporal diversity and evolutionary tempo. *In* M.J. Novacek and Q.D. Wheeler (editors), Extinction and phylogeny: 89–118. New York: Columbia University Press.

Nunn, G.B., J. Cooper, P. Jouventin, C.J.R. Robertson, and C.G. Robertson. 1996. Evolutionary relationships among extant albatrosses (Procellariiformes: Diomedeidae) established from complete cytochrome b gene sequences. Auk 113: 784–801.

Nunn, G.B., and S.E. Stanley. 1998. Body size effects and rates of cytochrome b evolution in tube-nosed seabirds. Molecular Biology and Evolution 15: 1360–1371.

O'Hara, R.J. 1989. Systematics and the study of natural history, with an estimate of the phylogeny of penguins (Aves: Spheniscidae). Ph.D. dissertation, Harvard University.

Olson, S.L. 1983. Fossil seabirds and changing marine environments in the Late Tertiary of South Africa. South African Journal of Science 79: 399–402.

Olson, S.L. 1985. The fossil record of birds. *In* D.S. Framer, J.R. King, and K.C. Parkes (editors), Avian biology: 79–238. New York: Academic Press.

Olson, S.L., and Y. Hasegawa. 1979. Fossil counterparts of giant penguins from the North Pacific. Science 330: 51–57.

Olson, S.L., and Y. Hasegawa. 1996. A new genus and two new species of gigantic Plotopteridae from Japan (Aves: Plotopteridae). Journal of Vertebrate Paleontology 16: 742–751.

Palazzesi, L., V. Barreda, and R.A. Scasso. 2006. Early Miocene spore and pollen record of the Gaiman Formation (northeastern Patagonia, Argentina): correlations and paleoenvironment implications. *In* Abstracts 4th Congreso Latinoamericano de Sedimentología and 11th Reunion Argentina de Sedimentología: 11. San Carlos de Bariloche.

Parras, A., et al. 2008. Correlation of marine beds based on Sr- and Ar-date determinations and faunal affinities across the Paleogene/Neogene boundary in southern Patagonia, Argentina. Journal of South American Earth Sciences 26: 204–216.

Paterson, A.M., G.P. Wallis, and R.D. Gray. 1995. Penguins, petrels, and parsimony: does cladistic analysis of behavior reflect seabird phylogeny? Evolution 49: 974–989.

Pycraft, W.P. 1907. On some points in the anatomy of the emperor and adelie penguins. British National Antarctic Expedition (1901–1904) Report 2: 1–21.

Reisz, R.R., and J. Müller. 2004. Molecular timescales and the fossil record: a paleontological perspective. Trends in Genetics 20: 569–597.

Rinaldi, C.A., A. Massabie, J. Morelli, H.L. Rosenman, and R. del Valle. 1978. Geologia de la isla Vicecomodoro Marambio. Contribuciones del Instituto Antártico Argentino 217: 5–43.

Ritchie, P.A., C.D. Millar, G.C. Gibb, C. Baroni, and D.M. Lambert. 2004. Ancient DNA enables timing of the Pleistocene origin and Holocene expansion of two Adélie penguin lineages in Antarctica. Molecular Biology and Evolution 21: 240–248.

Rivera, R. 1957. Muluscos fósiles de la Formación Parcas, departmento de Ica. Boletín de la Sociedad Geológica del Perú 32: 165–220.

Scarlett, R.J. 1983. *Tereingaornis moisleyi* – a new Pliocene penguin. New Zealand Journal of Geology and Geophysics 26: 419–428.

Scasso, R.A., J.M. McArthur, C.J. del Río, S. Martínez, and M.F. Thirlwall. 2001. 87Sr/86Sr Late Miocene age of fossil molluscs in the 'Entrerriense' of the Valdés Peninsula (Chubut, Argentina). Journal of South American Earth Sciences 14: 319–329.

Schreiweis, D.O. 1982. A comparative study of the appendicular musculature of penguins (Aves: Sphenisciformes). Smithsonian Contributions to Zoology 341: 1–46.

Shaul, S., and D. Graur. 2002. Playing chicken (*Gallus gallus*): methodological inconsistencies of molecular divergence date estimates due to secondary calibrations. Gene 300: 59–61.

Sibley, C.G., and J.E. Ahlquist. 1990. Phylogeny and classification of birds: a study in molecular evolution. New Haven, CT: Yale University Press.

Simpson, G.G. 1946. Fossil penguins. Bulletin of the American Museum of Natural History 87(1): 1–99.

Simpson, G.G. 1957. Australian fossil penguins, with remarks on penguin evolution and distribution. Records of the South Australian Museum 13: 51–70.

Simpson, G.G. 1959. A new fossil penguin from Australia. Proceedings of the Royal Society of Victoria 71: 113–119.

Simpson, G.G. 1965. New record of a fossil penguin in Australia. Proceedings of the Royal Society of Victoria 79: 91–93.

Simpson, G.G. 1970. Miocene penguins from Victoria, Australia, and Chubut, Argentina. Memoirs of the National Museum of Victoria 31: 17–24.

Simpson, G.G. 1971a. Review of fossil penguins from Seymour Island. Proceedings of the Royal Society of London B Biological Sciences 178: 357–387.

Simpson, G.G. 1971b. A review of the pre-Pliocene penguins of New Zealand. Bulletin of the American Museum of Natural History 144(5): 321–378.

Simpson, G.G. 1971c. Fossil penguin from the Late Cenozoic of South Africa. Science 171: 1144–1145.

Simpson, G.G. 1972a. Conspectus of Patagonian fossil penguins. American Museum Novitates 2488: 1–37.

Simpson, G.G. 1972b. Pliocene penguins from North Canterbury. Records of the Canterbury Museum 9: 159–182.

Simpson, G.G. 1973. Tertiary penguins (Sphenisciformes, Spheniscidae) from Ysterplaats, Cape Town, South Africa. South African Journal of Science 69: 342–344.

Simpson, G.G. 1975. Notes on variation in penguins and on fossil penguins from the Pliocene of Langebaanweg, Cape Province, South Africa. Annals of the South African Museum 69: 59–72.

Simpson, G.G. 1976. Penguins: past and present, here and there. New Haven, CT: Yale University Press.

Simpson, G.G. 1979a. Tertiary penguins from the Duinefontein site, Cape Province, South Africa. Annals of the South African Museum 79: 1–17.

Simpson, G.G. 1979b. A new genus of Late Tertiary penguin from Langebaanweg, South Africa. Annals of the South African Museum 78: 1–9.

Simpson, G.G. 1981. Notes on some fossil penguins, including a new genus from Patagonia. Ameghiniana 18: 266–272.

Slack, K.E., A. Janke, D. Penny, and U. Amason. 2003. Two new avian mitochondrial genomes (penguin and goose) and a summary of bird and reptile mitochondrial features. Gene 302: 43–52.

Slack, K.E., et al. 2006. Early penguin fossils, plus mitochondrial genomes, calibrate avian evolution. Molecular Biology and Evolution 23: 1144–1155.

Somoza, R., and A. Tomlinson. 2002. Paleomagnetism in the Precordillera of northern Chile (22°30′S): implications for the history of tectonic rotations in the Central Andes. Earth and Planetary Science Letters 194: 369–381.

Stanley, S.E., and R.G. Harrison. 1999. Cytochrome b evolution in birds and mammals: an evaluation of the avian constraint hypothesis. Molecular Biology and Evolution 16: 1575–1585.

Storer, R.W. 1971. Adaptive radiation of birds. *In* D.S. Farmer and J.R. King (editors), Avian biology, Vol. 1: 149–188. New York: Academic Press.

Stucchi, M. 2002. Una nueva especie de *Spheniscus* (Aves: Spheniscidae) de la Formación Pisco, Perú. Boletín de la Sociedad Geológica del Perú 94: 17–24.

Stucchi, M. 2003. Los Piqueros (Aves: Sulidae) de la Formación Pisco. Boletín de la Sociedad Geológica del Perú 95: 75–91.

Stucchi, M. 2007. Los pingüinos de la Formación Pisco (Neógeno), Perú. *In* E. Díaz-Martínez and I. Rábano (editors), 4th European Meeting on the Palaeontology and Stratigraphy of Latin America Cuadernos del Museo Geominero 8: 367–373. Madrid: Instituto Geológico y Minero de España.

Stucchi, M., and S.D. Emslie. 2005. A new condor (Ciconiiformes, Vulturidae) from the late Miocene/early Pliocene Pisco formation, Peru. Condor 107: 107–113.

Stucchi, M., and M. Urbina. 2004. *Ramphastosula* (Aves, Sulidae): a new genus from the Pisco formation, Peru. Journal of Vertebrate Paleontology 24: 974–978.

Stucchi, M., M. Urbina, and A. Giraldo. 2003. Una nueva specie de Spheniscidae del Mioceno Tardío de la Formacíon Pisco, Perú. Bulletin de l'Institut Français d'Études Andines 32: 361–375.

Swofford, D.L. 2003. PAUP*. Phylogenetic analysis using parsimony (* and other methods). Version 4. Sunderland, MA: Sinauer Associates.

Tambussi, C.P., C.I. Acosta Hospitaleche, M.A. Reguero, and S.A. Marenssi. 2006. Late Eocene penguins from West Antarctica: systematics and biostratigraphy. Geological Society of London Special Publications 258: 145–161.

Tambussi, C.P., M.A. Reguero, S.A. Marenssi, and S.N. Santillana. 2005. *Crossvalia unienwillia*, a new Spheniscidae (Sphenisciformes, Aves) from the late Paleocene of Antarctica. Geobios 38: 667–675.

Thompson, J.D., T.G. Gibson, F. Plewniak, F. Jeanmougin, and D.G. Higgins. 1997. The ClustalX windows interface: flexible strategies for multiple sequence alignment aided by quality analysis tools. Nucleic Acids Research 25: 4876–4882.

Uhen, M.D., and N.D. Pyenson. 2007. Diversity estimates, biases, and historographic effects: resolving cetacean diversity in the Tertiary. Palaeontologia Electronica 10 (2): 11A: 22 pp. (available at http://www.palaeo-electronica.org/2007_2/00123/index.html).

van Tets, G.F., and S. O'Conner. 1983. The Hunter Island penguin, an extinct new genus and species from a Tasmanian midden. Records of the Queen Victoria Museum 81: 1–12.

van Tuinen, M., and S.B. Hedges. 2001. Calibration of avian molecular clocks. Molecular Biology and Evolution 18: 206–213.

van Tuinen, M., C.G. Sibley, and S.B. Hedges. 2000. The early history of modern birds inferred from DNA sequences of nuclear and mitochondrial genes. Molecular Biology and Evolution 17: 451–457.

Walsh, S.A., and M.E. Suárez. 2006. New penguin remains from the Pliocene of Northern Chile. Historical Biology 18: 115–126.

Warheit, K.I., and D.R. Lindberg. 1988. Interactions between seabirds and marine mammals through time: interference competition at breeding sites. *In* J. Burger (editor), Seabirds and Other marine vertebrates. competition, predation and other interactions: 292–328. New York: Columbia Univerity Press.

Watanabe, M., et al. 2006. New candidate species most closely related to penguins. Gene 378: 65–73.

Watson, M. 1883. Report on the anatomy of the Spheniscidae collected during the voyage of H.M.S. Challenger. *In* J. Murray (editor), Report of the scientific results of the voyage of *H.M.S. Challenger* during the years 1873–1876, Zoology. Vol. 7: 1–244. Edinburgh: Neill and Company.

Wiens, J.J. 1998. Incomplete taxa, incomplete characters, and phylogenetic accuracy: is there a missing data problem? Journal of Vertebrate Paleontology 23: 297–310.

Wilkinson, M. 1995. Coping with abundant missing data entries in phylogenetic inference using parsimony. Systematic Biology 44: 501–514.

Williams, T.D. 1995. The penguins. Oxford: Oxford University Press.

Wiman, C. 1905a. Vorfläufige Mitteilung über die alttertiären Vertebraten der Seymourinsel. Bulletin of the Geological Institute of Uppsala 6: 247–253.

Wiman, C. 1905b. Uber die alttertiären Vertebraten der Seymourinsel. Wissenschaftliche Ergebnisse der Schwedischen Südpolar-Expedition 1901–1903 3: 1–37.

Worthy, T.H. 1997. The identification of fossil *Eudyptes* and *Megadyptes* bones at Marfels Beach, Marlborough, South Island. New Zealand Natural Science 23: 71–85.

Worthy, T.H., and J.A. Grant-Mackie. 2003. Late-Pleistocene avifaunas from Cape Wanbrow, Otago, South Island, New Zealand. Journal of the Royal Society of New Zealand 33: 427–485.

Zusi, R.L. 1975. An interpretation of skull structure in penguins. *In* B. Stonehouse (editor), The biology of penguins: 55–84. Baltimore, MD: University Park Press.

APPENDIX 1

Sources for Character Codings of Fossil Taxa

Recently, Otago Museum (OM) penguin specimens were renumbered (Cody Fraser, personal commun.). Older specimen numbers are listed in parentheses to aid comparisons with previous work (e.g., Marples, 1952; Simpson 1971b; Ksepka et al., 2008).

Taxon	Specimens Examined/References for Codings
Anthropodyptes gilli	AMNH 7609 (cast of holotype)
Anthropornis grandis	Simpson (1971a), Myrcha et al. (2002), Jadwiszczak (2006a)
Anthropornis nordenskjoeldi	OU unnumbered (cast of holotype), USNM 402486, UCMP uncataloged
Anthropornis sp.	UCMP 321023
Aptenodytes ridgeni	CM zfa-6 (holotype)
Archaeospheniscus lopdelli	OM GL428 (=C47.21) (holotype)
Archaeospheniscus lowei	OM GL407 (=C47.20) (holotype)
Arthrodytes andrewsi	Ameghino (1905), Acosta Hospitaleche (2005)
Burnside *"Palaeeudyptes"*	OM GL435 (=C48.73–81)
CADIC P-21	CADIC P-21
Crossvallia unienwillia	Tambussi et al. (2005)
Dege hendeyi	Simpson (1979a)
Delphinornis arctowskii	Myrcha et al. (2002)
Delphinornis gracilis	Myrcha et al. (2002)
Delphinornis larseni	OU 22182 (cast of holotype), USNM 404467
Delphinornis wimani	Marples (1953), Myrcha et al. (2002)
Duntroon "*Palaeeudyptes*"	OM GL427 (C47.23), OM GL432 (=C47.25)
Duntroonornis parvus	OM GL462 (=C47.31) (holotype)
Eretiscus tonnii	Simpson (1981), Acosta Hospitaleche et al. (2004)
Icadyptes salasi	MUSM 897 (holotype)
Inguza predemersus	Simpson (1971c, 1975)
Korora oliveri	OM GL433 (=C50.63) (holotype)
Madrynornis mirandus	Acosta Hospitaleche et al. (2007)
Marambiornis exilis	Myrcha et al. (2002)
Marplesornis novaezealandiae	CM zfa16527 (holotype), Marples (1960)
Mesetaornis polaris	Myrcha et al. (2002)
MNZS 1449	MNZS 1449
NMV P2669	Simpson (1970)
Nucleornis insolitus	Simpson (1979b)
Pachydyptes ponderosus	MNZS 1450 (holotype), OM GL1600 (=C47.16)
Palaeeudyptes antarcticus	OU 22127 (cast of holotype)
Palaeeudyptes gunnari	OU uncataloged (cast of holotype), UCMP 321826
Palaeeudyptes klekowskii	UCMP 321023, 321486 Myrcha et al. (1990)
Palaeeudyptes marplesi	OM GL429 (C50.25–47) (holotype)
Palaeospheniscus bergi	AMNH 3322, 3326, 3345, 3347
Palaeospheniscus biloculata	AMNH 3341, 3346 (holotype), Acosta Hospitaleche (2007)
Palaeospheniscus patagonicus	AMNH 3274, 3276, 3285, 3287, 3289, 3295, 3297–3298, 3316, 3321, 3323, 3330, 3336, 3340, 3343–3344, 3349, 3352, 3355, 3358; MUSM 257, Acosta Hospitaleche et al. (2008).
Paraptenodytes antarcticus	AMNH 3338
Paraptenodytes brodkorbi	Ameghino (1905)
Paraptenodytes robustus	OU 2251 (cast of holotype)
Perudyptes devriesi	MUSM 889 (holotype)
Platydyptes amiesi	OM GL434 (C50.61–62) (holotype)
Platydyptes marplesi	OM GL2317 (C47.15) (holotype)
Platydyptes novaezealandiae	MNZS 1451 (holotype)
Pseudaptenodytes macraei	Simpson (1970)
Pygoscelis calderensis	Acosta Hospitaleche et al. (2006)
Pygoscelis grandis	Walsh and Suárez (2006)

APPENDIX 1
(Continued)

Taxon	Specimens Examined/References for Codings
Pygoscelis tyreei	CM zfa22631 (holotype)
SAM Q1882	Simpson (1973, 1975)
SAMA P7158	AMNH 7201 (cast of SAMA P7158)
SAMA P14157	Jenkins (1974)
Seal Rock "*Palaeeudyptes*"	MNZS 1449
Spheniscus chilensis	Emslie and Guerra Correa (2003)
Spheniscus megaramphus	MUSM 175 (holotype), 362–365
Spheniscus muizoni	Göhlich (2007)
Spheniscus urbinai	MUSM 269, 401 (holotype), 402–405
Tereingaornis moisleyi	CM zfa11 (holotype)
"Tonniornis mesetaensis" MLP 93-X-1-145	Tambussi et al. (2006)
"Tonniornis minor" MLP 93-I-6-3	Tambussi et al. (2006)
Waimanu manneringi	CM zfa35 (holotype)
Waimanu tuatahi	OU 12651 (holotype), CM zfa33-34

APPENDIX 2

GenBank Accession Numbers and Authorship for Sequences

Taxon	12S rDNA	16S rDNA	COI	Cytochrome *b*	RAG-1
Aptenodytes forsteri	DQ137187	DQ137147	DQ137185	DQ137225	DQ137246
Aptenodytes patagonicus	AY139221	DQ137148	DQ137186	AY 138623	DQ 137247
Daption capense	X82517	—	—	AF076046	—
Diomedea exulans	DQ137205	DQ137165	DQ137168	DQ137208	DQ137229
Eudyptes chrysocome	AY139630	DQ137155	DQ137172	AF076051	DQ137233
Eudyptes chrysolophus	DQ525756	—	DQ525796	—	DQ525776
Eudyptes filholi	DQ525741	—	DQ525781	—	DQ525761
Eudyptes moseleyi	DQ525746	—	DQ525786	—	DQ525766
Eudyptes pachyrhynchus	U88007, X82522	DQ 137152	DQ137170	DQ137210	DQ137231
Eudyptes robustus	DQ137193	DQ137153	DQ137176	DQ137126	DQ137237
Eudyptes schlegeli	DQ137196	DQ137156	DQ137175	DQ137215	DQ137236
Eudyptes sclateri	DQ137194	DQ137154	DQ137169	DQ137309	DQ137230
Eudyptula minor	NC_004538	DQ137164	DQ137174	NC_004538	DQ137235
Gavia immer	AF173577	DQ137166	DQ137167	DQ137207	DQ137288
Gavia stellata	AF173587	AY293618	AY666477	AF158250	—
Macronectes giganteus	X82523	—	—	AF076060	—
Megadyptes antipodes	DQ137198	DQ137158	DQ137184	DQ137224	DQ1372245
Oceanites oceanicus	—	—	DQ433048	AF076062	—
Oceanodroma leucorhoa	—	—	AY666284	AF0706064	—
Pachyptila desolata	—	—	—	AF076068	—
Pelecanoides urinatrix	X82518	—	—	AF076076	DQ881818
Phoebastria immutabilis	—	—	—	PIU48949	—
Phoebetria palpebrata	—	—	—	U48943	DQ881822
Procellaria aequinoctialis	—	—	—	U74350	—
Pterodroma incerta	—	—	—	U74335	—
Puffinus griseus	X82533, U88024	—	—	U74353	—
Pygoscelis adeliae	AF173573	DQ137149	DQ137183	DQ137223	DQ137224
Pygoscelis antarctica	DQ137190	DQ137150	DQ137181	AF076089	DQ137242
Pygoscelis papua	DQ137191	DQ137151	DQ 137182	AF076090	DQ137243
Spheniscus demersus	DQ137199	DQ137159	DQ137177	DQ137217	DQ137238
Spheniscus humboldti	DQ137201	DQ137161	DQ137180	DQ137220	DQ137241
Spheniscus magellanicus	DQ137200	DQ 137160	DQ137178	DQ137218	DQ 137239
Spheniscus mendiculus	DQ137202	DQ137162	DQ137179	DQ137219	DQ137240
Thalassarche melanophrys	AY158677	AY158677	NC_007172	U48955	AY158677

Authorship: **12S rDNA:** Baker et al. (2006): DQ137187, DQ137190–1, DQ137193–4, DQ137196–202, DQ137205; Banks et al. (2006): DQ525741, DQ525746, DQ525756; Cooper and Penny (1997): U88007, U88024; García-Moreno et al. (unpublished): AY139621, AY139623, AY139630; Paterson et al. (1995): X82517–8, X82522–3, X82533; Slack et al. (2006): AY158677; NC_004538; van Tuinen et al. (2000): AF173573, AF173577–8. **16S rDNA:** Baker et al. (2006): DQ137147–62, DQ13714765–6; Slack et al. (2006): AY158677, AY293618. **Cytochrome *b*:** Baker et al. (2006): DQ137207–10, DQ137215–20, DQ13723–5; Banks et al. (2006): DQ525761, DQ525766, DQ525776; Nunn et al. (1996): U48943, U48949, U48955; Nunn and Stanley (1998): AF076051–2, AF076046, AF076060, AF076062, AF076064, AF076068, AF076076, AF076089–90, U74335, U74350, U74353; Slack et al. (2006): NC_004538; Stanley and Harrison (1999): AF158250. **COI:** Baker et al. (2006): DQ137167–72, DQ137174–86; Banks et al (2006): DQ525781, DQ525786, DQ525796; Herbert et al. (2004): AY666477, AY666284; Kerr et al. (2007): DQ433048; Slack et al. (2006): NC_007172. **RAG-1:** Baker et al. (2006): DQ137230–3, DQ137235–47; Ericson et al. (2006): DQ881818, DQ881822.

APPENDIX 3

Character Definitions

The source for the first use of each character in a phylogenetic context is given as an abbreviation. For example, BG40 indicates the character first appeared as character 40 in the matrix of Bertelli and Giannini (2005). The abbreviations for citations are as follows: AH, Acosta Hospitaleche et al., 2007; BG, Bertelli and Gianni, 2005; C, Clarke et al., 2007; GB, Giannini and Bertelli 2004; K, Ksepka et al., 2006; OH, O'Hara, 1989. Myological characters are taken from the comparative study of Schreiweis (1982). English terminology is utilized in the character descriptions, with Latin equivalents (Baumel and Witmer, 1993) provided in parentheses.

Integument

1. Tip of mandibular rhamphotheca, profile in lateral view: pointed (0); slightly truncated (1); strongly truncated, squared off (2); truncated but with a rounded margin (e.g., as seen in Procellariiformes) (3). (GB1)
2. Longitudinal grooves on the base of the culmen: absent (0); present (1). (GB2)
3. Longitudinal grooves on the base of latericorn and ramicorn: absent (0); present (1). (GB3)
4. Feathering of maxilla, extent: totally unfeathered (0); slightly feathered, less than half the length of maxilla (1); feathering that reaches half the length of maxilla (2); feathering surpassing half the length of maxilla (3). Ordered
5. Ramicorn, inner groove at tip: absent (0); present and single (1); present and double (2). Ordered. (GB5)
6. Orange or pink plate on ramicorn: absent (0); present (1). (GB6)
7. Plates of rhamphotheca, inflated aspect: absent (0); present (1). (GB7)
8. Gape: not fleshy (0); margin narrowly fleshy (1); margin markedly fleshy (2). Ordered. (GB8)
9. Ramicorn color pattern: black (0); red (1); pink (2); yellow (3); orange (4); green (5); blue (6). (GB9)
10. Latericorn and ramicorn, light distal mark: absent (0); present (1). (GB10)
11. Latericorn color: black (0); red (1); orange (2); yellow (3); green (4); blue (5). (GB11)
12. Culminicorn color: black (0); red (1); orange (2). (GB12)
13. Maxillary and mandibulary unguis, color: black (0); red (1); yellow (2); green (3); blue-gray (4). (GB13)
14. Ramicorn, ultraviolet color spot (reflectance peak): absent (0); present (1).
    Jouventin et al. (2005) reported ultraviolet markings on the beak of *Aptenodytes forsteri* and *Aptenodytes patagonicus*. These markings are present in both males and females, but absent in juveniles and in other penguin species. (This study)
15. Bill of downy chick, color: dark (0); reddish (1); pale, variably horn to yellow (2); blue (3). (GB14)
16. Bill of immature, color: dark (0); bicolored red and black (1); red (2); yellow (3); gray (4). (GB15)
17. External nares: present (0); absent (1). (GB17)
18. Nostril tubes: absent in adult (0); present in adult (1). (GB16)
19. Nostril tubes: absent in hatchling (0); present in hatchling (1). Kinsky (1960) documented the transient presence of nostril tubes in *Eudyptula minor*. (GB16)
20. External nares: well separated (0); fused at midline (1). (This study)
21. Iris color: dark (0); reddish brown (1); claret red (2); yellow (3); white (4); silvery gray (5). (GB18)
22. Scalelike feathers: absent (0); present (1). (GB19)
23. Rhachis of contour feathers: cylindrical (0); flat and broad (1). (GB20)
24. Rectrices: form a functional fan (0); do not form a fan (1). (GB21)
25. Remiges: differentiated from contour feathers (0); indistinct from contour feathers (1). (GB22)
26. Apteria: present (0); absent (1). (GB23)
27. Molt of contour feathers: gradual (0); simultaneous (1). (GB24)
28. Yellow pigmentation in crown feathers (pileum): absent (0); present (1). (GB25)
29. Head plumes (crista pennae): absent (0); present (1). (GB26)
30. Head plumes, aspect: compact (0); sparse (1). (GB27)
31. Head plumes, aspect: directed dorsally (0); directed posteriorly, not drooping (1); directed posteriorly, drooping (2). (GB28)
32. Head plumes, position of origin: at base of bill close to gape (0); on the recess between latericorn and culminicorn (1); on forehead (2). Ordered. (GB29)
33. Head plumes, color: yellow (0); orange (1). (GB30)
34. Nape (occiput), crest development: absent (0); slight (1); distinct (2). Ordered. (GB31)
35. Periocular area, color: black (0); white (1); yellow (2); bluish gray (3). (GB32)
36. Fleshy eyering: absent (0); present (1). (GB33)
37. White eyering: absent (0); present (1). (GB34)
38. White eyebrow (supercilium): absent (0); narrow, from postocular area (1); narrow, from preocular area (2); wide, from preocular area (3). Ordered. (GB35)
39. Loreal area (lorum), aspect: feathered (0); with spot of bare skin in the recess between latericorn and culminicorn (1); with spot of bare skin contacting eye (2); bare skin extending to the base of bill (3). Ordered. (GB36)
40. Auricular patch (regio auricularis): absent (0); present (1). (GB37)
41. Throat pattern: black (0); white (1); yellow (2); irregularly streaked (3); with chinstrap (4). (GB38)

42. Collar: absent (0); at most, slight notch present (1); present, diffusely demarcated (2); black, strongly demarked (3). Ordered. (GB39)
43. Breast, golden in color: absent (0); present (1). (GB40)
44. Dorsum color: black (0); dark bluish gray (1); light bluish gray (2). (GB41)
45. Black marginal edge of dorsum between lateral collar and axillary patch, contrasting with dorsum: absent (0); present (1). (GB42)
46. Black dots irregularly distributed over white belly: absent (0); present (1). (GB43)
47. Flanks, dark lateral band reaching the breast: absent (0); present (1). (GB44)
48. Distinct dark axillary patch of triangular shape: absent (0); present (1). (GB45)
49. Flanks, extent of dorsal dark cover into the leg: incomplete, not reaching tarsus (0); complete, reaching tarsus (1). (GB46)
50. Rump: indistinct in color from dorsum (0); distinct white patch (1). (GB47)
51. Tail length: short, the quills barely emerge from the rump (0); quills distinctly developed (1). (GB48)
52. Outer rectrices, color: same as inner rectrices (0); lighter than inner rectrices (1). (GB49)
53. White line connecting leading edge of flipper with white belly: absent (0); present (1). (GB50)
54. Flipper, upperside, light notch at base: absent (0); present (1). (GB51)
55. Leading edge of flipper, pattern of upperside: black (0); white (1). (GB52)
56. Leading edge of flipper, pattern of underside: white (0); incompletely dark (1); completely dark and wide (2). (GB53)
57. Flipper, underside, dark elbow patch: absent (0); present (1). (GB54)
58. Flipper, underside, tip pattern: immaculate (0); patchy, in variable extent (1); small circular dot present (2). (GB55)
59. Immature plumage, white eyebrow (supercilium): absent (0); present (1). (GB56)
60. Immature plumage, throat pattern (jugulum): black (0); mottled (1); white (2); brown (3). (GB57)
61. Immature plumage, flanks, dark lateral band: absent (0); present (1). (GB58)
62. Chicks hatch almost naked: no (0); yes (1). (GB59)
63. Dominant color pattern of first down: pale gray (0); distinctly brown (1); bicolored, dark above and whitish bellow (2); uniformly blackish gray (3). (GB 60)
64. Dominant color pattern of second down: pale gray (0); distinctly brown (1); bicolored, dark above and whitish bellow (2); uniformly blackish gray (3). (GB61)
65. Chick, second down, collar: absent (0); present (1). (GB62)
66. Feet, dorsal color: dark (0); pink (1); orange (2); white-flesh (3); blue (4). (GB63)
67. Feet, light dorsal surface of foot with dark sole: absent (0); present (1). (GB64)
68. Feet, unguis digiti: flat (0); compressed (1). (BG65)

Reproductive Biology

69. Clutch size: two eggs (0); one egg (1). (GB65)
70. Incubatory sac: absent (0); present (1). (GB66)
71. Nest: no nest, incubation over the feet (0); nest placed underground, either burrowed in sand or inside natural hollow or crack (1); open nest, a shallow depression on bare ground or in midst of vegetation (2). (GB67)
72. Size of first egg relative to the second egg: similar (0); dissimilar, first smaller (1); dissimilar, second smaller (2). (GB68)
73. Crèche: absent (0); small, three to six birds (1); formed by dozens to hundreds of immatures (2). (GB69)
74. Eggs, shape: oval (0); conical (1); spherical (2). (BG71)
75. Ecstatic display: absent (0); present (1). (BG72)

Osteology

76. Premaxilla, tip (rostrum maxillare): pointed (0); weakly hooked (1); strongly hooked (2). Ordered. (GB0)
77. Internarial bar (pila supranasalis) shape in cross-section: suboval (0); inverted U-shape (1). (C75)
78. Internarial bar (pila supranasalis), profile in lateral view: dorsal edge curves smoothly to tip of beak (0); pronounced step in dorsal edge (1). (This study)
79. Basioccipital, subcondylar fossa (fossa subcondylaris): absent or shallow (0); deep (1). (BG73)
80. Supraoccipital, paired grooves for the exit of v. occipitalis externae (sulcus vena occipitalis externae): poorly developed (0); deeply excavated (1). (BG74)
81. Frontal, shelf of bone bounding salt-gland fossa (fossa glandulae nasalis) laterally: absent (0); present (1). (OH10)
82. Squamosal, temporal fossa (fossa temporalis), size: fossae separated by considerable wide surface (at least the width of the cerebellar prominence) (0); more extensive, fossae meeting or nearly meeting at midline of the skull (1). (BG76)
83. Squamosal, temporal fossa (fossa temporalis), depth of caudal region: flat (0); shallow (1); greatly deepened (2). Ordered. (BG77)
84. Squamosal, development of the opening that transmits the a. ophthalmica externa in the caudoventral area of the temporal fossa (near nuchal crest): small or vestigial (0); well developed (1). (BG78)
85. Orbit, fonticuli orbitocraneales: small or vestigial (0); broad and conspicuous openings (1). (BG79)
86. Ectethmoid: absent (0); weakly developed, widely separate from the lacrimal (1); well developed, contacting or fused to the lacrimal (2). (BG80)
87. Lacrimal: unperforated (0); perforated (1). (OH11)
88. Lacrimal: reduced, concealed in dorsal view (0); small portion exposed in dorsal view (1); well exposed in dorsal view (2). Ordered. (BG82)

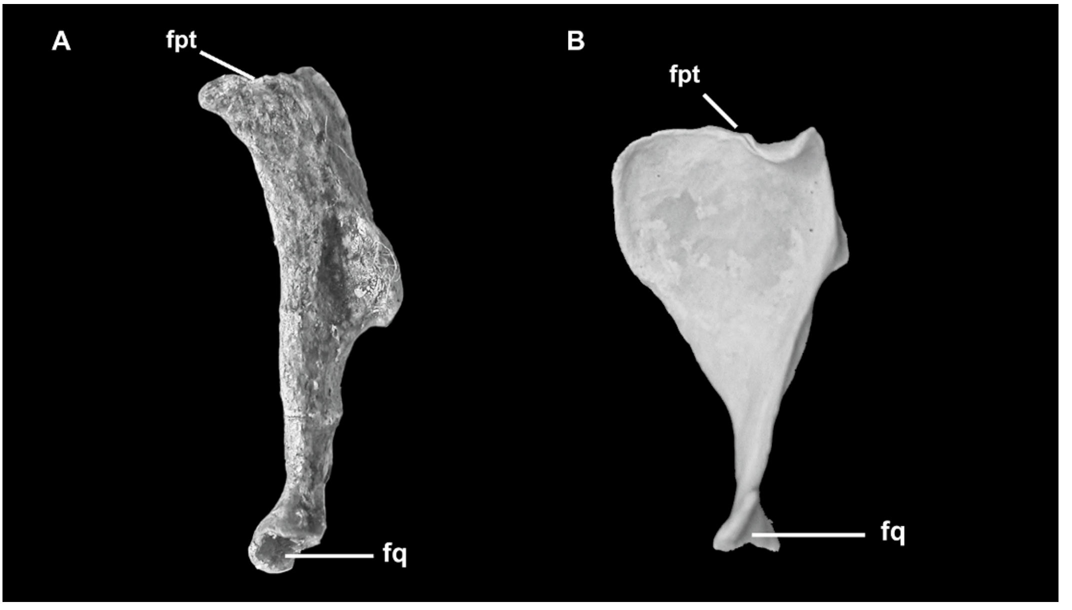

Fig. 22. Pterygoids of selected penguin taxa, illustrating phylogenetic characters: (**A**) the stem penguin *Paraptenodytes antarcticus* (AMNH 3338); (**B**) extant *Spheniscus humboldti* (AMNH 4921). See appendix 5 for abbreviations.

89. Lacrimal, dorsal border: closely applied to the frontal (0); separated by a wide split from the frontal (1). (BG83)
90. Nasal cavity, external naris (cavum nasi, apertura nasi ossea), caudal margin: extended caudal to the rostral margin of the hiatus orbitonasalis (0); not extended caudal to the rostral margin of the hiatus orbitonasalis (1). (OH5)
91. Nasal cavity, internarial bar (pila supranasalis): slender, slightly constricted laterally (0); wide throughout its length (1). (OH6)
92. Basitemporal plate (lamina parasphenoidalis), dorsoventral position with respect to the occipital condyle: ventral to the level of the condyle (0); at the level of the condyle (1); dorsal to the level of the condyle, surface depressed (2). Ordered. (BG86)
93. Basipterygoid process (proccessus basipterygoideus): absent (0); vestigial or poorly developed (1); well developed (2). Ordered. (BG87)
94. Eustachian tubes (tuba auditiva): open or very little bony covering near the caudal end of the tube (0); mostly enclosed by bone (1). (BG88)
95. Pterygoid, shape (fig. 22): elongated (0); slight lateral expansion of rostral end (1); rostal end broad, pterygoid subtriangular (2). Ordered. (BG89)
96. Palatine, lamella choanalis: curved and smooth plate, slightly differentiated from main palatine blade (0); ridged, distinct from main blade by a low keel (1); extended vertically ventrally forming the crista ventralis (2). Ordered. (BG90)
97. Vomer: laterally compressed, vertical laminae and free from palatines (0); horizontally flattened laminae and ankylosed with palatines (1); absent (2). (BG91)
98. Facial foramen (foramen n. facialis): absent (0); present (1). (BG92)
99. Jugal arch, bar shape in lateral view: straight (0); slightly curved (1); ventrally bowed (2); strongly curved, sigmoid shape (3). Ordered. (BG93)
100. Jugal arch, dorsal process: absent (0); present (1). This pointed process is located on the caudal end of the jugal, adjacent to the condyle for articulation with the quadrate. (BG94)
101. Premaxilla, frontal process, nasopremaxillary suture: visible (0); obliterated (1). (BG95)
102. Quadrate, relative lengths of otic and orbital processes (processus oticus and processus orbitalis): otic process longest (0); orbital process longest (1). (This study)
103. Quadrate, otic process, rostral border, tubercle for m. adductor mandibulae externus, pars profunda: absent (0); present, as a ridge (1); present, as a tubercle (2). (BG96)
104. Quadrate, otic process, rostral border, tubercle for m. adductor mandibulae externus, pars profunda (fig. 23): contiguous with squamosal capitulum (0); separated from squamosal capitulum (1). (This study)
105. Tomial edge (crista tomialis): plane of tomial edge approximately at the level of the basitemporal plate (lamina parasphenoidalis) (0); dorsal to the level of the basitemporal plate (1). (BG97)
106. Mandible, symphysis: extensive bony connection (0); short terminal bony connection (1). (C101)

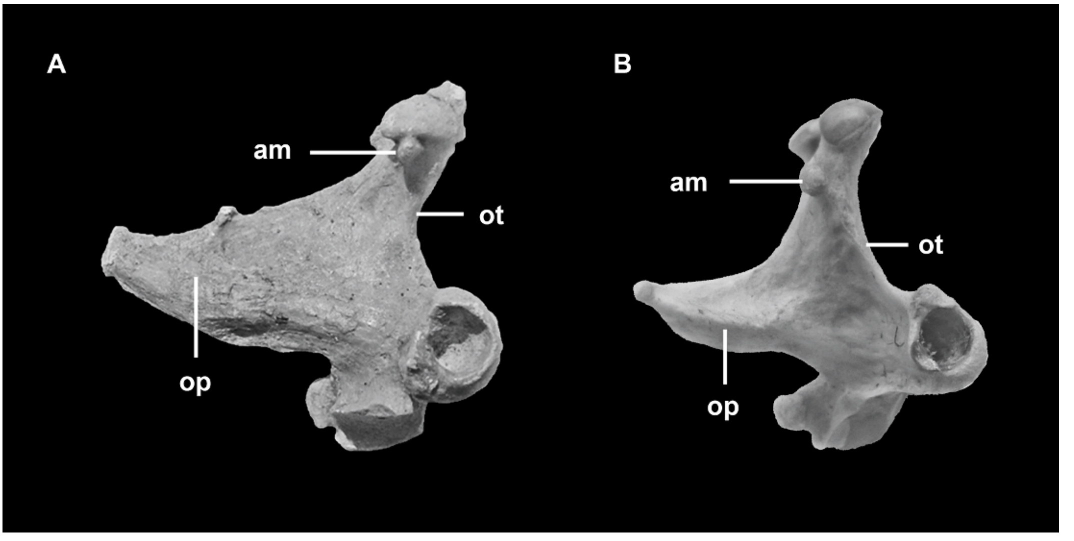

Fig. 23. Quadrates of selected penguin taxa, illustrating phylogenetic characters: (**A**) the stem penguin *Icadyptes salasi* (MUSM 897); (**B**) extant *Spheniscus demersus* (NSM 6294). See appendix 5 for abbreviations.

107. Mandible, posteriorly projected midline spur from dentary underlying symphysis: absent (0); present (1). (This study)
108. Mandible, coronoid process (processus coronoideus), position on the dorsal margin of the mandible with respect to caudal mandibular fenestra (fenestra mandibulae caudalis): markedly rostral (0); on the rostral end of the fenestra (1); caudal to fenestra (2). Ordered. (BG98)
109. Mandible, rostral fenestra (fenestra mandibulae rostralis): imperforate or small opening (0); large opening (1). (OH8)
110. Mandible, caudal fenestra (fenestra mandibulae caudalis): open, can be seen through the medial or lateral aspects (0); nearly or completely concealed by the splenial medially (i.e., fenestra not visible in the medial aspect) (1). (OH9)
111. Mandible, mandibular ramus: depth subequal over entire ramus (0); pronounced deepening at midpoint (1). (BG101)
112. Mandible, mandibular ramus: essentially straight or gently sloping (0); pronounced ventral deflection near midpoint (1). (This study)
113. Mandible, dentary, length of dorsal edge relative to mandibular ramus length in lateral view: markedly more than half the length of ramus (0); approximately half the length of ramus (1). (BG103)
114. Mandible, articular, medial process (processus medialis): not hooked (0); hooked (1). (BG104)
115. Mandible, angular, retroarticular process (processus retroarticularis), aspect in dorsal view in relation to the articular area for the quadrate between the lateral and medial condyles (condylus lateralis and condylus medialis): broad, approximately equal to the articular area (0); moderately long, narrower than the articular area (1); very long, longer and narrower than the articular area (2). Ordered. (BG105)
116. Mandible, angular, aspect in dorsal view: sharply truncated caudally (0); caudally projected, forming retroarticular process (processus retroarticularis) (1). (BG106)
117. Mandible, medial emargination between medial and retroarticular processes: absent (0); weak concavity (1); strong concavity (2). Ordered. (K108)
118. Atlas, processus ventralis: absent or slightly developed (0); well developed, high and prominent ridge on the dorsal surface of the arcus atlantis (1). (BG108)
119. Transition to free cervicothoracic ribs begins at: 13th cervical vertebra: (0); 14th cervical vertebra (1); 15th cervical vertebra (2). Ordered. (BG109)
120. Cervical vertebrae, elongated neural spine (processus spinosus) on the sixth cervical vertebra: absent (0); present (1). (BG110)
121. Cervical vertebrae, transverse process (processus transversus) in last five cervical vertebrae: not elongated laterally (0); greatly elongated laterally (1). (BG111)
122. Cervical vertebrae, transverse process (processus transversus) of vertebrae 12–13: laterally oriented (0); deflected dorsally (1). (BG112)
123. Thoracic vertebrae, posteriormost vertebrae: heterocoelous (0); weakly opisthocoelous; (1); strongly opisthocoelous (2). Ordered. (K114)
124. Thoracic vertebrae, deep excavation on lateral face of posterior thoracic vertebrae: absent (0); present (1). Slack et al. (2006) noted these excavations as one of the distinguishing characters of *Waimanu*. (This study)

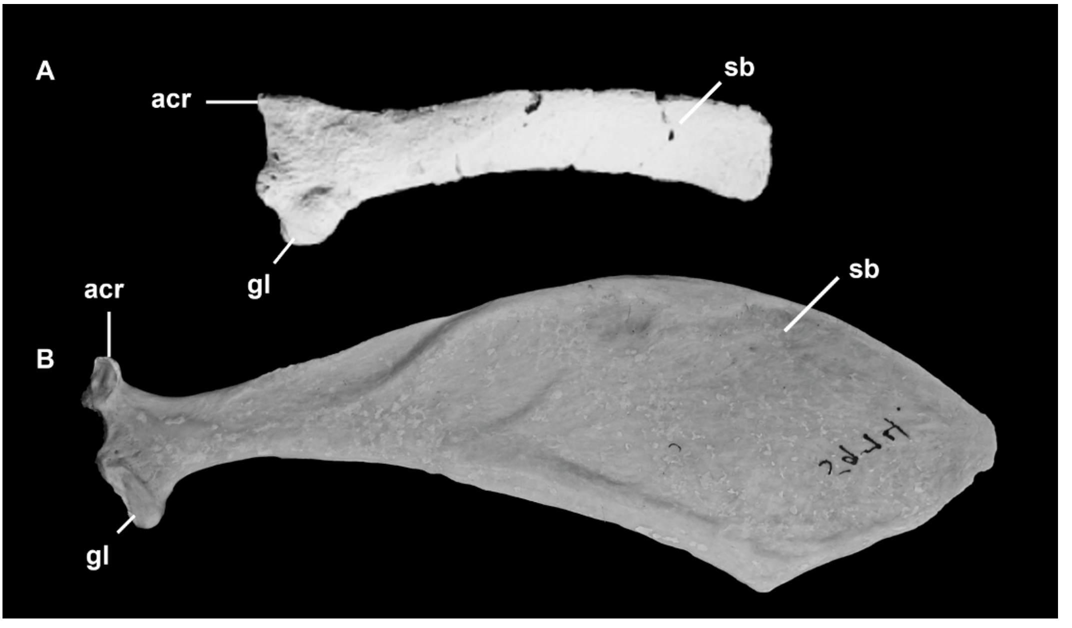

Fig. 24. Scapulae of selected penguin taxa, illustrating phylogenetic characters: (**A**) the stem penguin *Waimanu tuatahi* (CM zfa34); (**B**) extant *Eudyptes chrysolophus* (AMNH 5974). Image **A** reprinted with permission from Slack et al. (2006). See appendix 5 for abbreviations.

125. Synsacrum, number of incorporated vertebrae: nine (0); eleven (1); twelve (2); thirteen (3); fourteen (4), fifteen or more (5). (C117)
126. Synsacrum, height of crista synsacri between acetabuli: flat or weakly projected (0); strongly projected (1). (This study)
127. Caudal vertebrae: seven (0); eight (1); nine (2). Ordered. (BG113)
128. Thoracic ribs, uncinate processes (costae, processes uncinati): elongate, narrow (0); wide at base, spatulate (1); extremely wide at base (2). Reference to bifurcation of the processes in state 2 from previous formulations of this character has been removed, as bifurcation shows individual variation in all species of *Pygoscelis*. (BG114)
129. Thoracic ribs, uncinate processes (costae, processes uncinati): fused to ribs (0); unfused (1). (This study)
130. Sternum, external spine (spina externa rostri): absent (0); present (1). (OH13)
131. Sternum, facies articularis furculae projects as a distinctive process: absent (0); present (1). (BG116)
132. Sternum, articular facets for coracoids (sulcus articularis coracoideus): meet or overlap one another at midline (0); separated by wide nonarticulatory surface (1). (C122)
133. Sternum, labrum internum: continues as sharp ridge onto the base of the spina externa (0); fades away without continuing onto the base (1). (C123)
134. Sternum, caudal incisurae: absent (0); two (1); four (2). (This study)
135. Furcula, hypocleidium (apophysis furculae): absent or low knoblike process (0); long, bladelike process (1). (BG117)
136. Scapula, blade, caudal half (corpus scapulae, extremitas caudalis) (fig. 24): bladelike (0); expanded and paddle-shaped (1). (BG118)
137. Coracoid, length: shorter than humerus (0); greatly elongated, longer than humerus (1). (This study)
138. Coracoid, medial margin, coracoidal fenestra: complete (0); incomplete (1); absent (2). The previous coding of *Pygoscelis papua* is changed to (0/1) reflecting variability in ossification of the ligament forming this fenestra, as described by Olson (1985). (OH14)
139. Coracoid, foramen nervi supracoracoidei: absent (0), present (1). Mayr (2005) cited ontogenetic evidence that this foramen is not homologous to the coracoidal fenestra of penguins. (K122)
140. Coracoid, sternal margin (extremitas sternalis coracoidei): greatly expanded (0); moderate expansion (1). (BG120)
141. Coracoid, sternal margin (extremitas sternalis coracoidei) (fig. 25): convex (0); concave (1); flat (2). (K124)
142. Coracoid, lateral process (processus lateralis): absent or highly reduced (0); well developed (1).
143. Forelimb elements: subcircular in cross-section (0); flattened (1). (BG121)

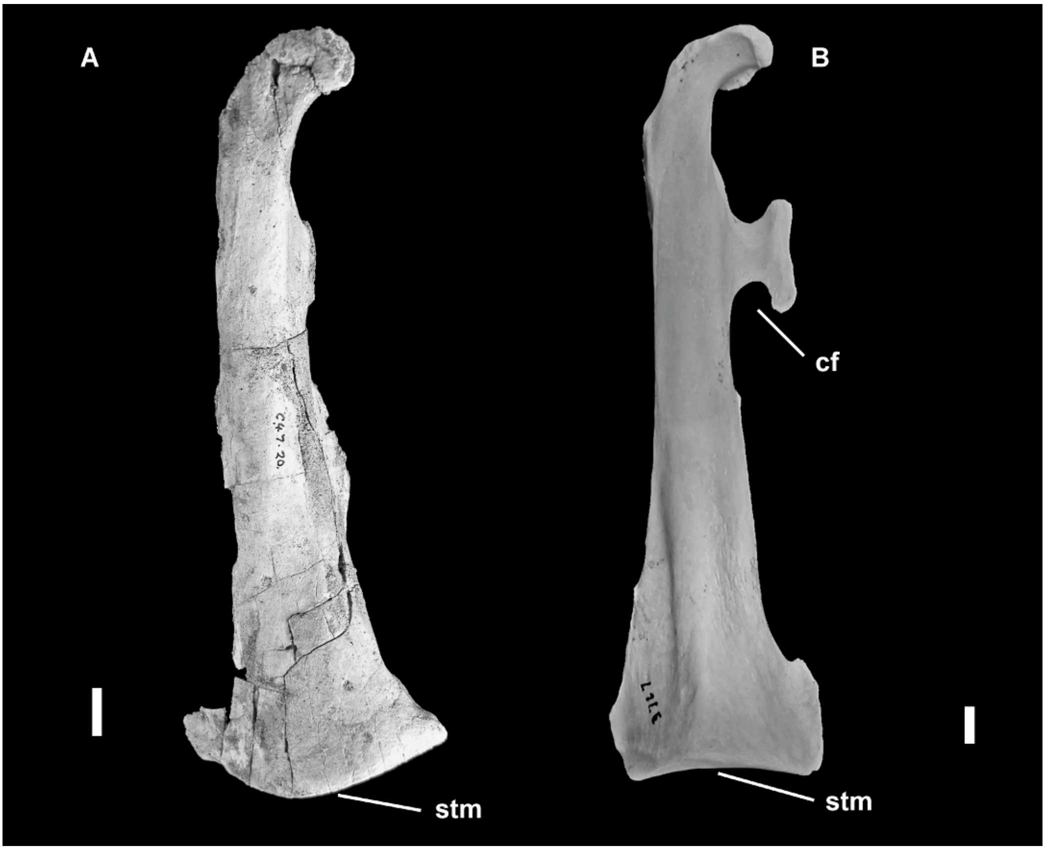

Fig. 25. Coracoids of selected penguin taxa, illustrating phylogenetic characters: (**A**) the stem penguin *Archaeospheniscus lowei* (OM GL407); (**B**) extant *Aptenodytes forsteri* (AMNH 3767). The bone is incomplete in **A**, causing the proximal end to appear less widened. Broken edges suggest that the coracoid fenestra was originally completely enclosed in **A**. Scale bars = 1 cm. See appendix 5 for abbreviations.

144. Humerus, head: very developed and reniform, continuous with tuberculum dorsale: absent (0); present (1). (BG122)
145. Humerus, head in posterior view: apex of humeral head located near midline (0); humeral head slopes so that apex of humeral head located ventrally (1). (C132)
146. Humerus, incisura captius: essentially confluent with sulcus transversus (0); clearly separated from sulcus transversus (1). (K127)
147. Humerus, pit for ligament insertion on proximal surface adjacent to head: absent or very shallow (0); deep (1). (K128)
148. Humerus, orientation of intumenscentia humeri and tuberculum ventrale: intumenscentia projects ventrally from shaft, tuberculum oriented posteriorly (0); intumenscentia projects ventrally from shaft, tuberculum oriented ventrally (1); intumenscentia projected more anteroventrally (so as to be partially obscured in posterior view), tuberculum oriented anteroventrally (2). (K129)
149. Humerus, tricipital fossa (fossa tricipitalis), aspect: small with penetrating pneumatic foramina (0); moderate fossa without pneumatic foramen (1); deep fossa without pneumatic foramen. (BG123)
150. Humerus, tricipital fossa (fossa tricipitalis): single (0); bipartite (1). In some birds (e.g., many oscine Passeriformes) the tricipital fossa is double, with a pars ventralis fossa and a pars dorsalis fossa. Some previous authors discussed the relative sizes of the pars dorsalis fossa and pars ventralis fossa of the humerus in some fossil penguins. However, the bipartite tricipital fossa in penguins is homologous solely to the pars ventralis fossa, which is divided by a septum in some species. (BG124)
151. Humerus, deltoid crest, insertion of m. pectoralis major (impressio m. pectoralis): superficial poorly defined groove (0); shallow, well-defined oblong fossa (1); deep, well-defined oblong fossa (2). Ordered (BG125)
152. Humerus, scar for m. supracoracoideus (impressio insertii m. supracoracoideus): small, semicircular scar (0); greatly elongated with long axis subparallel to main axis of humeral shaft (1).

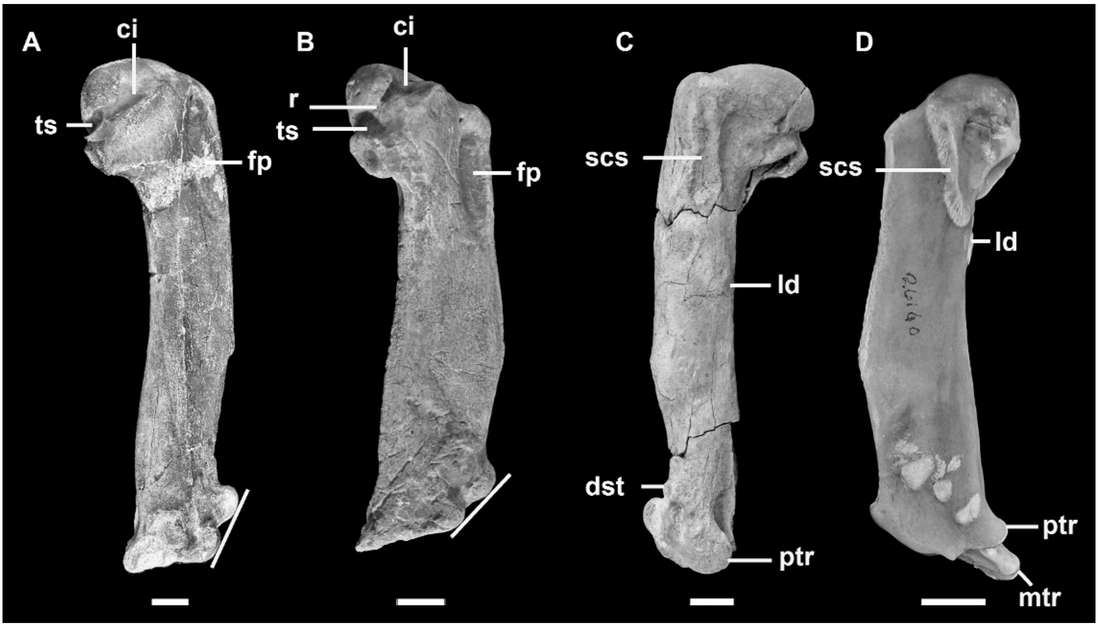

Fig. 26. Humeri of selected penguin taxa, illustrating phylogenetic characters: the stem penguins (**A**) *Palaeeudyptes gunnari* (UCMP 321826), (**B**) *Palaeospheniscus patagonicus* (AMNH 3361), and (**C**) *Perudyptes devriesi* (MUSM 889), and (**D**) extant *Pygoscelis antarctica* (AMNH 2610). Lines illustrate the tangent to the radial and ulnar condyles. See appendix 5 for abbreviations. Scale bars = 1cm. Images **A** and **B** reversed to aid comparison.

This character was previously divided into three states. However, upon consideration of more taxa and larger sample size, we think that the distinction between parallel and oblique orientation of this scar is difficult to score consistently in penguins due to continuous variation in orientation of the scar and variation in shaft shape. (K133)

153. Humerus, scars for m. supracoracoideus and m. latissimus dorsi (impressio insertii m. supracoracoideus and m. latissimus dorsi) (fig. 26): separated by a wide gap (0); separated by a moderate gap (1); separated by small gap or confluent (2). Ordered. (K134)
154. Humerus, proximal margin of tricipital fossa (fossa tricipitalis): weak projection (0); projects so as to be well exposed in proximal view (1). (K135)
155. Humerus, shaft, dorsoventral width: shaft thins or maintains width distally (0); shaft widens distally (1). (K136)
156. Humerus, nutrient foramen (foramen nutricum): situated on ventral face of shaft (0); situated on anterior face of shaft (1). (C143)
157. Humerus, anterior face of shaft elongate depression near ventral margin: absent (0); present (1). This depression is present only in certain fossil taxa and is not to be confused with the vascular depression that runs distally from the ventral to the dorsal margin of the shaft in all penguins. (C144)
158. Humerus, shaft, sigmoid curvature: absent or weak (0); strong (1). (K137)
159. Humerus, development of dorsal supracondylar tubercle (processus supracondylar dorsalis): absent (0); compact tubercle (1); elongate process (2). (BG126)
160. Humerus, demarcation of sulcus scapulotricipitalis: not demarcated (0); passage a well-marked groove (1); development of trochlear ridge for articulation with os sesamoideum m. scapulotricipitis (2). Ordered. (BG127)
161. Humerus, middle trochlear ridge: does not project distal to posterior trochlear ridge (0); projects distal to posterior trochlear ridge (1).
162. Humerus, posterior trochlear ridge: extends beyond ventral margin of the humeral shaft (0); does not extend beyond the humeral shaft (1). (BG128)
163. Humerus, angle between main axis of shaft and tangent of ulnar and radial condyles (condylus dorsalis and condylus ventralis) (fig. 26): less than 45° (0); more than 45° (1); nearly 90° (2). (K141)
164. Humerus, ulnar condyle (condylus ventralis): condyle projected and rounded (0); condyle flattened (1). Ksepka et al. (2006) erroneously reversed the labeling of the ulnar and radial condyles in figure 12 of that study illustrating this character. (K142)
165. Humerus, shelf adjacent to condylus ventralis: large, ratio of condyle width:shelf width >1.3

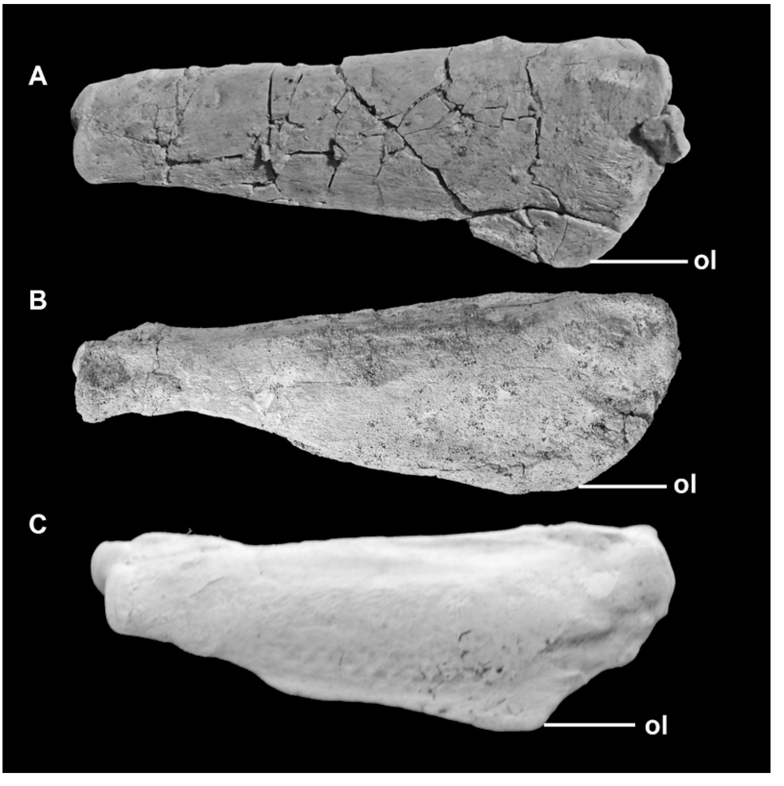

Fig. 27. Ulnae of selected penguin taxa, illustrating phylogenetic characters: the stem penguins (**A**) *Icadyptes salasi* (MUSM 897) and (**B**) *Archaeospheniscus lopdelli* (OM GL428), and (**C**) extant *Spheniscus demersus* (NSM 6294). See appendix 5 for abbreviations.

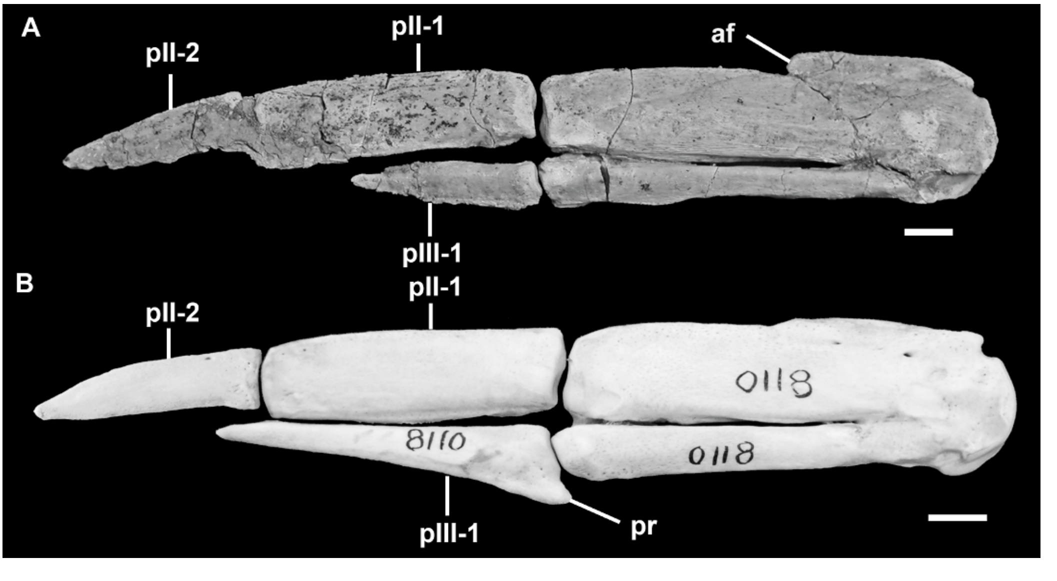

Fig. 28. Carpometacarpi and phalanges of selected penguin taxa, illustrating phylogenetic characters: (**A**) the stem penguin *Icadyptes salasi* (MUSM 897) and (**B**) extant *Aptenodytes forsteri* (AMNH 8110). See appendix 5 for abbreviations. Scale bars = 1 cm.

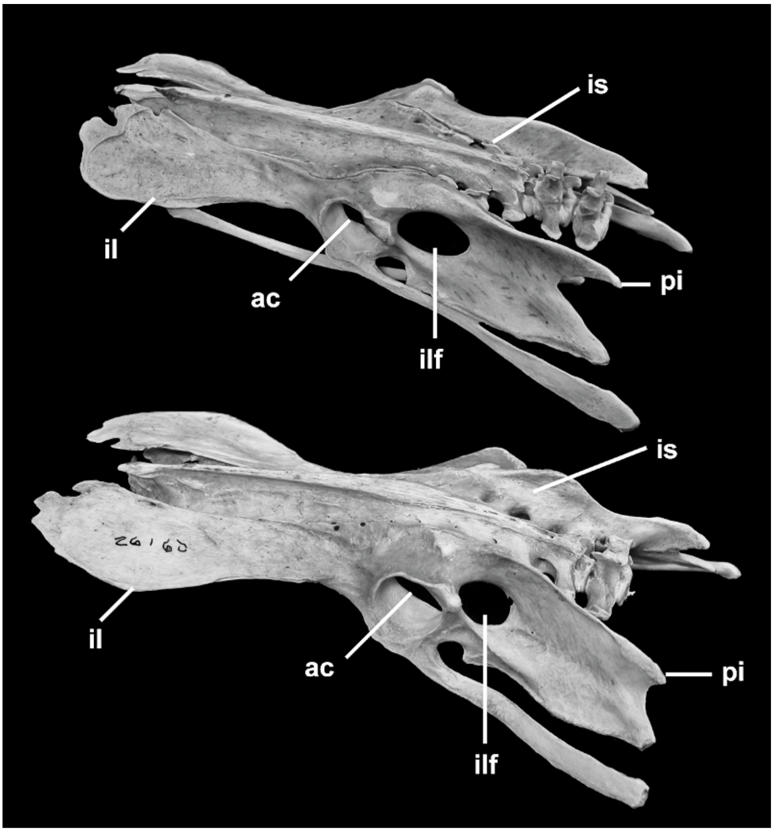

Fig. 29. Pelves of selected penguin taxa, illustrating phylogenetic characters: the extant penguins (**A**) *Spheniscus humboldti* (AMNH 26165) and (**B**) *Pygoscelis antarctica* (AMNH 26160). See appendix 5 for abbreviations.

(0); moderate, ratio of condyle width:shelf width 1.3–2.0 (1); greatly reduced, less than half condyle width (2). Ordered (K143)

166. Radius, shaft: narrow (0); broad and flattened (1). (This study)
167. Ulna, olecranon and posterior border (fig. 27): border forms smooth curve with apex located one-fourth of length to distal end (0); well-developed tablike projection arises proximally, very close to humeral articulation (1); acute projection, distally displaced from humeral facet (2); rounded (3). (K144)
168. Ulna, distinct process extending toward sulcus humerotricipitalis of humerus: absent (0); present (1). (K145)
169. Ulnare: U-shaped (0); triangular, fan-shaped wedge (1). (This study)
170. Carpometacarpus, pisiform process (processus pisiformis): well-projected round tubercle (0); reduced to a low ridge (1). (C155)
171. Carpometacarpus, distal facet on metacarpal I (fig. 28): absent (0); present (1). (C156)
172. Carpometacarpus, metacarpal II, distinct anterior bowing: absent (0); present (1). (C157)
173. Carpometacarpus, extension of metacarpals II and III: subequal (0); metacarpal III projects markedly distal of metacarpal II. (C158)
174. Carpometacarpus, metacarpal III, distal articular surface (facies articularis digitalis major): wedge-shaped or broadens anteriorly in distal view (0); slightly depressed ovoid surface (1). (C159)
175. Carpometacarpus, extensor process (processus extensorius): present (0); absent (1). (This study)
176. Carpometacarpus, metacarpal II, distal expansion: absent (0); present (1). (This study)
177. Phalanges of manus, phalanx digit III proximal process (fig. 28): absent (0); present (1). (BG130)
178. Phalanges of manus, relative length of phalanx III-1 and phalanx II-1: phalanx III-1 shorter (0); subequal (1). (C161)
179. Phalanges of manus, length relative to carpometacarpus: long (0); short (1). (BG131)
180. Fusion of ilia to synsacrum (fig. 29): unfused (0); partially fused (1); well fused (2). Ordered. (K149)
181. Pelvis, preacetabular ilia: flat, well separated (0); approach one another, but do not contact at

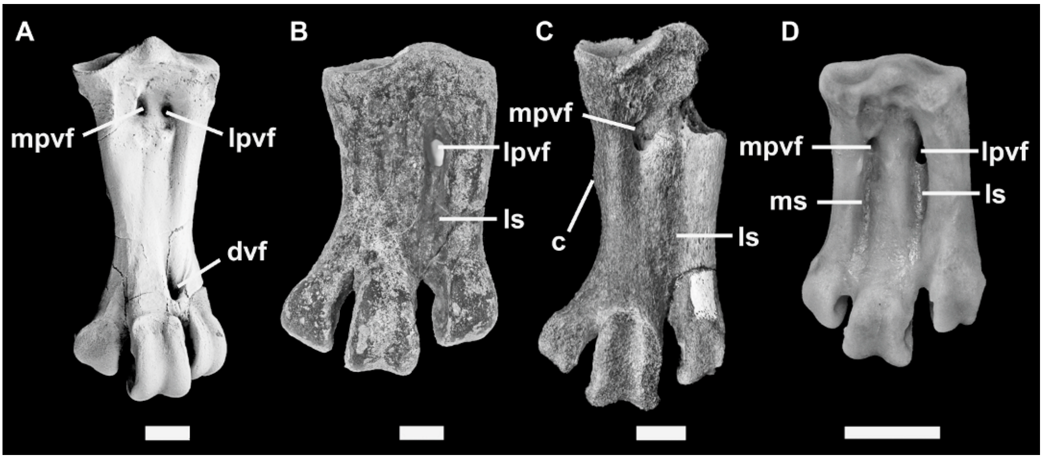

Fig. 30. Tarsometatarsi of selected penguin taxa, illustrating phylogenetic characters: the stem penguins (**A**) *Waimanu manneringi* (CM zfa35), (**B**) *Palaeeudyptes klekowskii* (UCMP 321486), and (**C**) *Anthropornis* sp. (UCMP 321023), and (**D**) extant *Spheniscus magellanicus* (AMNH 24679). Scale bars = 1 cm. See appendix 5 for abbreviations.

midline (1); contact at midline forming canalis iliosynsacralis (2). (This study).

182. Pelvis, foramina intervertebralia large, forming wide openings on dorsal surface of pelvis: absent (0); present (1). (This study)
183. Ilium, projected postiliac spine: absent (0); present (1).
184. Pelvis, relative size of ilioischiadic foramen and acetabulum (foramen ilioischiadicum and foramen acetabuli) (fig. 29): smaller (0); similar or larger (1). (OH16)
185. Pelvis, fenestra ischiopubica: very wide and closed at its caudal end (0); slitlike and open at its caudal end (1). (BG133)
186. Ischium, most caudal extent in relation to postacetabular ilium: ischium shorter than ilium (0); ischium projects slightly beyond the ilium (1); ischium produced far caudal to ilium (2). (BG134)
187. Patella: absent or unossified (0); present (1). (This study)
188. Patella, sulcus m. ambiens: shallow groove (0); deep groove (1); perforated (2). (BG135)
189. Tibiotarsus, crista patellaris: greatly enlarged (0); slightly developed (1). (BG136)
190. Tibiotarsus, shaft, anteroposterior flattening: weak, midshaft anteroposterior depth >75% mediolateral width (0); strong, midshaft anteroposterior depth equal to or <75% mediolateral width (1). (C169)
191. Tibiotarsus, notch in distal edge of medial condyle (condylus medialis): present (0); absent (1). (AH38)
192. Tibiotarsus, lateral condyle (condylus lateralis) in lateral profile: ovoid (0); subcircular (1). (AH37)
193. Tibiotarsus, sulcus extensorius: placed medially or close to midline of the anterior face of the tibiotarsus (0); placed laterally (1). Variation of this feature in penguins was noted by Clarke et al. (2003). (This study).
194. Tarsometatarsus, elongation index (EI; proximodistal length/mediolateral width at proximal end): slender, EI > 3 (0); shortened, 2.5 < EI < 3 (1); greatly shortened EI < 2.5 (2). Values for some Antarctic fossils were obtained from the table of measurements in Myrcha et al. (2002). Ordered. (BG139)
195. Tarsometatarsus, medial margin, pronounced convexity: absent (0); present (1). (K157)
196. Tarsometatarsus, intermediate hypotarsal crests (crista intermediae hypotarsi): distinct, separated by groove (0); no distinct separation of crests (0);. (K158)
197. Tarsometatarsus, dorsal sulcus between metatarsals II and III (sulcus longitudialis dorsalis medialis) (fig. 30): absent or barely perceptible (0); shallow groove (1); deep groove (2). Ordered. (K159)
198. Tarsometatarsus, os metatarsale IV: distal end projects laterally (0); straight (1); distal end deflected medially (2). (K160)
199. Tarsometatarsus, foramen vascularia proximalia medialis opening on fossa para hypotarsalis medialis: present (0); absent (1). (BG140)
200. Tarsometatarsus, proximal vascular foramina on plantar surface (fig. 30): foramen vasculare proximale mediale present, foramen vasculare proximale laterale absent or vestigial (0); both foramina present (1); foramen vasculare proximale laterale present, foramen vasculare proximale mediale absent or vestigial (2). (K162)
201. Tarsometatarsus, distal vascular foramen (foramen vasculare distale) (fig. 30): present, separated from incisura intertrochlearis lateralis by osseous bridge (0); present, open distally (1); absent (2). Ordered. (K163)

202. Tarsometatarsus, enclosed hypotarsal canals (canales hypotarsi): present (0); absent (1). (BG141)

Myology

203. M. latissimus dorsi, pars cranialis, accessory slip: absent (0); present (1). (BG143)
204. M. latissimus dorsi, pars cranialis and pars caudalis: separated (0); fused (1). (BG144)
205. M. latissimus dorsi, pars metapatagialis, development: wide (0); intermediate (1); narrow (2). Ordered. (BG145)
206. M. serratus profundus, cranial fascicle: absent (0); present (1). (BG146)
207. M. deltoideus, pars propatagialis, subdivision in superficial and deep layers: undivided (0); divided (1). (BG147)
208. M. deltoideus, pars major: triangular or fan-shaped (0); strap-shaped (1). (BG148)
209. M. deltoideus, pars major, caput caudale: short (0); intermediate (1); long (2). Ordered. (BG149)
210. M. deltoideus, pars minor, origin on the clavicular articulation of the coracoid: absent (0); present (1). (BG150)
211. M. ulnometacarpalis ventralis: absent (0); present (1). (BG151)
212. M. iliotrochantericus caudalis: narrow (0); wide (1). (BG152)
213. M. iliofemoralis, origin: tendinous (0); partially tendinous and partially fleshy (1); totally fleshy (2). This character previously included four states. I have lumped the states "mostly tendinous" and "mostly fleshy" into a single state to avoid overweighing this ordered character. Ordered. (BG153)
214. M. flexor perforatus digitis IV, rami II–III: free (0); fused (1). (BG154)
215. M. flexor perforatus digitis IV, rami I–IV: free (0); fused (1). (BG155)
216. M. flexor perforatus digitis IV, insertion of middle rami: on phalanx 3 (0); on phalanx 4 (1). (BG156)
217. M. latissimus dorsi, pars caudalis, additional origin from dorsal process of vertebrae: absent (0); present (1). (BG157)

Tongue

218. Oral mucosa (bucca, tunica mucosa oris), buccal papillae group on the medial surface of the lower jaw (ramus mandibularis) at the level of the rictus: small number of rudimentary papillae with no clear arrangement (0); two clear rows of short conical papillae (1); large, elongated papillae with no clear arrangement (2). (BG158)

Trachea

219. Tracheal rings: single (0); bifurcated (1). (This study)

APPENDIX 4

Phylogenetic Matrix: A = 0/1, B = 1/2, C = 3/4, D = 0/1/2/3

Character	.........10.........20.......30.......40
Gavia immer	0001000000000???00002000000?????????????
Gavia stellata	0001000000000?D00000200000?????????????
Daption capense	3001000000000?0001110000000?????????????
Diomedea exulans	30000000402 2????01100000000?????????????
Macronectes giganteus	3001000030 3?2?2301115000000?????????????
Oceanites oceanicus	3000000000000?0001110000000?????????????
Oceanodroma leucorhoa	3000000000000?0001110000000?????????????
Pachyptila desolata	3000000060504?3401110000000?????????????
Pelecanoides urinatrix	3000000000?0?0001110000000?????????????
Phoebastria immutabilis	3000000020220?0?0110000000?????????????
Phoebetria palpebrata	3000000000000?0001100000000?????????????
Procellaria aequinoctialis	3000000050403??001110000000?????????????
Pterodroma incerta	3000000000000?0001110000000?????????????
Puffinus griseus	3000000000000?0001110000000?????????????
Thalassarche melanophrys	3000000020221?0001100000000?????????????
Aptenodytes forsteri	000201000000100100?011111100????0000001
Aptenodytes patagonicus	000101000000100100?011111100????0000001
Pygoscelis adeliae	100310001010001 1100?411111100????1001000
Pygoscelis antarctica	100210000000000100?211111100????0100000
Pygoscelis papua	1002100010100011100?111111100????0001000
Megadyptes antipodes	1001200020111000100?311111110????0210000
Eudyptes chrysocome	1001201110111?02100?211111111121020 00000
Eudyptes chrysolophus	1001201210111002100?211111111122100 00000
Eudyptes filholi	1001201210111?02100?211111111121020 00000
Eudyptes moseleyi	1001201110111?02100?211111111021020 00000
Eudyptes pachyrhynchus	1001201010111?02100?211111111011000 00000
Eudyptes robustus	1001201210111?02100?211111111011000 00000
Eudyptes schlegeli	1001201210111?02100?211111111122101 00000
Eudyptes sclateri	1001201210111002100?011111111000000 00000
Eudyptula minor	110120000000000001005111111 00????0300000
Madrynornis mirandus	??
Spheniscus demersus	2110100001000000000001111111 00????0010320
Spheniscus humboldti	211010000100000000001111111 00????0010230
Spheniscus magellanicus	211010000100000000000 1111111 00????0010210
Spheniscus mendiculus	21101000310 00?000000011111100????0010130
Anthropornis grandis	??
Anthropornis nordenskjoeldi	??
Anthropornis sp. UCMP 321023	??
Archaeospheniscus lopdelli	??
Archaeospheniscus lowei	??
Burnside "*Palaeeudyptes*"	??
Dege hendeyi	??
Delphinornis arctowskii	??
Delphinornis larseni	??
Delphinornis gracilis	??
Delphinornis wimani	??
Duntroon "*Palaeeudyptes*"	??
Duntroonornis parvus	??
Eretiscus tonnii	??
Icadyptes salasi	??
Madrynornis mirandus	??
Marambiornis exilis	??
Marplesornis novaezealandiae	??

APPENDIX 4
(Continued)

Character	.........10.........20.......30.......40
Mesetaornis polaris	??
Pachydyptes ponderosus	??
Palaeeudyptes gunnari	??
Palaeeudyptes klekowskii	??
Palaeospheniscus bergi	??
Palaeospheniscus biloculata	??
Palaeospheniscus patagonicus	??
Paraptenodytes antarcticus	??
Perudyptes devriesi	??
Platydyptes marplesi	??
Platydyptes novaezealandiae	??
Pygoscelis grandis	??
Spheniscus chilensis	??
Spheniscus megaramphus	??
Spheniscus muizoni	??
Spheniscus urbinai	??
Waimanu manneringi	??
Waimanu tuatahi	??
IB/P/B-0382	??
"*Tonniornis*"	??

Character	.........50.........60.......70.......80
Gavia immer	?????????????????????0?100?0002000000010
Gavia stellata	?????????????????????0110000002000000011
Daption capense	?????????????????????0000001102?00020111
Diomedea exulans	?????????????????????0?????0?02???021010
Macronectes giganteus	?????????????????????0330D00102?00020111
Oceanites oceanicus	?????????????????????0110001101?00020001
Oceanodroma leucorhoa	?????????????????????0000001101?00020001
Pachyptila desolata	?????????????????????0A00401101?00020101
Pelecanoides urinatrix	?????????????????????0000401101?00020101
Phoebastria immutabilis	?????????????????????0??0100?02???021010
Phoebetria palpebrata	?????????????????????0000300102?00021010
Procellaria aequinoctialis	?????????????????????0110001101?00020111
Pterodroma incerta	?????????????????????0??0101101?00020101
Puffinus griseus	?????????????????????0000101101?00020111
Thalassarche melanophrys	?????????????????????0000300102?00021010
Aptenodytes forsteri	0011100010100000000001000000110?21100001
Aptenodytes patagonicus	0011100010100001110001110000110?21100001
Pygoscelis adeliae	0000000100100001010200010110002222110001
Pygoscelis antarctica	4000000100110001110100000100002022110001
Pygoscelis papua	000000010111001101000002020000222211000A
Megadyptes antipodes	2000000010101010100200110101002000110000
Eudyptes chrysocome	0000000010100001110100220111002120110000
Eudyptes chrysolophus	0000000011100001110100220111002120110000
Eudyptes filholi	0000000010100001110100220111002120110000
Eudyptes moseleyi	0000000010100002110100220111002120110000
Eudyptes pachyrhynchus	0000000010100001110200220111002120110000
Eudyptes robustus	0000000010100002110200220111002120110000
Eudyptes schlegeli	1000000011100001110100220111002120110000
Eudyptes sclateri	0000000011100002110200220111002120110000
Eudyptula minor	1002000010001010020200121301001010110001
Spheniscus demersus	0100011010000000111110022100100101011100 1

APPENDIX 4
(Continued)

Character	.........50.........60.......70.......80
Spheniscus humboldti	3000011010000101110300?210010010?0111001
Spheniscus magellanicus	0300011010000100111110?21001001020111001
Spheniscus mendiculus	3200011010000001110310?2?001001000111001
Anthropornis grandis	??
Anthropornis nordenskjoeldi	??
Anthropornis sp. UCMP 321023	??
Archaeospheniscus lopdelli	????????????????????????????????????0???
Archaeospheniscus lowei	??
Burnside “*Palaeeudyptes*”	??
Dege hendeyi	??
Delphinornis arctowskii	??
Delphinornis larseni	??
Delphinornis gracilis	??
Delphinornis wimani	??
Duntroon “*Palaeeudyptes*”	????????????????????????????????????0???
Duntroonornis parvus	??
Eretiscus tonnii	??
Icadyptes salasi	???????????????????????????????????0?00?
Madrynornis mirandus	?????????????????????????????????????0?0
Marambiornis exilis	??
Marplesornis novaezealandiae	??????????????????????????????????????01
Mesetaornis polaris	??
Pachydyptes ponderosus	??
Palaeeudyptes gunnari	??
Palaeeudyptes klekowskii	??
Palaeospheniscus bergi	??
Palaeospheniscus biloculata	??
Palaeospheniscus patagonicus	??
Paraptenodytes antarcticus	??????????????????????????????????????10
Perudyptes devriesi	????????????????????????????????????0?0?
Platydyptes marplesi	??
Platydyptes novaezealandiae	??
Pygoscelis grandis	??
Spheniscus chilensis	??
Spheniscus megaramphus	???????????????????????????????????210?1
Spheniscus muizoni	??
Spheniscus urbinai	???????????????????????????????????210??
Waimanu manneringi	??
Waimanu tuatahi	??
IB/P/B-0382	??
“*Tonniornis*”	??

Character	.........90........100......110......120
Gavia immer	111000020011000201001000000000000??0?111
Gavia stellata	11100002001100020100100?000000000??0?111
Daption capense	011012120010200211000?0?0100000000?0?000
Diomedea exulans	10000212010200021100100?0110000000?0?000
Macronectes giganteus	01101212011020021100000?0100000000?0?000
Oceanites oceanicu	00001212101110021100010?010?010100?0?000
Oceanodroma leucorhoa	00001212101110021100010?010?010100?0?000
Pachyptila desolata	01101212001120021100010?0100010000?0?000
Pelecanoides urinatrix	01100212001120021100010?0101010000?0?000
Phoebastria immutabilis	10000212010200021100100?0111000000?0?0?0

APPENDIX 4
(Continued)

Character	.........90........100......110......120
Phoebetria palpebrata	100002120102000211001 00?0111000000?0?000
Procellaria aequinoctialis	0111121200102002110000?0?010001000 0?0?000
Pterodroma incerta	0110121200102002110001 0?010001000 0?0?000
Puffinus griseus	0111121200102002110000?0?01000A0000?0?001
Thalassarche melanophrys	100002120102000211001 00?0111000000?0?000
Aptenodytes forsteri	0011110200120120012A0111100110 0001012111
Aptenodytes patagonicus	00111102001201200120011110011 00001012111
Pygoscelis adeliae	1011010100120120003001111102001011011010
Pygoscelis antarctica	1010010100120A200030011111020100110 11010
Pygoscelis papua	1011011100120A20002A0111110100001 1011010
Megadyptes antipodes	1020011200120120002101110102010011112011
Eudyptes chrysocome	102??1120012012?0031 0121010?0?10111120?0
Eudyptes chrysolophus	1020011200120120003101210102011011112000
Eudyptes filholi	102??1120012012?0031 0121010?0?10111120?0
Eudyptes moseleyi	1020011200120120003101210102001011112010
Eudyptes pachyrhynchus	A020011200120120003101210102001011112020
Eudyptes robustus	1020011200120121003101210102001011112000
Eudyptes schlegeli	1020011200120120003101210102011011112010
Eudyptes sclateri	10200112001201200031012101020110111120??
Eudyptula minor	0020011200120121001011110101000001112010
Spheniscus demersus	0120011001020121001011210100000011212011
Spheniscus humboldti	0120011001020121001011210100000011212011
Spheniscus magellanicus	0120011001020121001011210100000011212011
Spheniscus mendiculus	0120011001020121001011210100000011212011
Anthropornis grandis	??
Anthropornis nordenskjoeldi	??
Anthropornis sp. UCMP 321023	??
Archaeospheniscus lopdelli	??
Archaeospheniscus lowei	?????????????????????????0??????????????
Burnside "*Palaeeudyptes*"	??
Dege hendeyi	??
Delphinornis arctowskii	??
Delphinornis larseni	??
Delphinornis gracilis	??
Delphinornis wimani	??
Duntroon "*Palaeeudyptes*"	??
Duntroonornis parvus	??
Eretiscus tonnii	??
Icadyptes salasi	012??????002??01??001020001?0?0000?1????
Madrynornis mirandus	?020??1??0??0?2???B??121???200?0?121B0??
Marambiornis exilis	??
Marplesornis novaezealandiae	?1210??????201110????120???2?0???00100??
Mesetaornis polaris	??
Pachydyptes ponderosus	??
Palaeeudyptes gunnari	??
Palaeeudyptes klekowskii	??
Palaeospheniscus bergi	??
Palaeospheniscus biloculata	??
Palaeospheniscus patagonicus	??????????1????????????????????0????????
Paraptenodytes antarcticus	012?0??????2010??????020???2?0???00101??
Perudyptes devriesi	0120???????20???????1????1??0?0?0???????
Platydyptes marplesi	??
Platydyptes novaezealandiae	??
Pygoscelis grandis	??

APPENDIX 4
(Continued)

Character	.........90........100......110......120
Spheniscus chilensis	??
Spheniscus megaramphus	0120?????102?1??????1???0?00000001112???
Spheniscus muizoni	??
Spheniscus urbinai	012??????10?????????1???0?0?0?00????????
Waimanu manneringi	??
Waimanu tuatahi	012????20?????????0??????0????00????????
IB/P/B-0382	??
"*Tonniornis*"	??

Character	.........130........140......150.....160
Gavia immer	000051001011010002101100010010000?000011
Gavia stellata	000051001001011002101100010010000?000011
Daption capense	000120100110020002102100010010000?000020
Diomedea exulans	000030?00110000002102100010000000?000020
Macronectes giganteus	000130100110000002102100010011000?000020
Oceanites oceanicus	00?10010011000100210110001001001??000021
Oceanodroma leucorhoa	00010010011000100210110001001001??000020
Pachyptila desolata	00012010011002000210210001001000??000020
Pelecanoides urinatrix	000110101111000002101100010010010?000021
Phoebastria immutabilis	000030100110000002102100010000000?000020
Phoebetria palpebrata	000?30100110000002102100010000000?000020
Procellaria aequinoctialis	0001?010011002000210210001001000??000020
Pterodroma incerta	0001?0?0011002000210210001001000 0?000020
Puffinus griseus	000130100110020002102100010000000?000020
Thalassarche melanophrys	000?30100110000002102100010000000?000020
Aptenodytes forsteri	1120311110011101110110111112212120100002
Aptenodytes patagonicus	11203111100111011101101111A2212120100002
Pygoscelis adeliae	1120301111011101110110111102212120100002
Pygoscelis antarctica	1120301211011101110110111102212120100002
Pygoscelis papua	11204012110111011A0110111112212120100002
Megadyptes antipodes	1020301111011101100110111112212120100002
Eudyptes chrysocome	1020?0?111011101100110111112212120100002
Eudyptes chrysolophus	1020301111011101100110111112212120100002
Eudyptes filholi	1020?0?111011101100110111112212120100002
Eudyptes moseleyi	1020301111011101100110111112212120100002
Eudyptes pachyrhynchus	10203011110111011A0110111112212120100002
Eudyptes robustus	1020C01111011101100110111112212120100002
Eudyptes schlegeli	1020?01111011101100110111112212120100002
Eudyptes sclateri	1?20301111011101100110111112212120100002
Eudyptula minor	1020202111011101110110111112212120100002
Spheniscus demersus	1020312111011101100110111112212121100002
Spheniscus humboldti	1020312111011101100110111112212121100002
Spheniscus magellanicus	1020312111011101100110111112212121100002
Spheniscus mendiculus	1020?12111011101100110111112212121100002
Anthropornis grandis	??????????????????????1100?120210????1??
Anthropornis nordenskjoeldi	??
Anthropornis sp. UCMP 321023	??
Archaeospheniscus lopdelli	??2????????????????00?1?????????????1?02
Archaeospheniscus lowei	????????????????1??00?110001202110111102
Burnside "*Palaeeudyptes*"	??????????????????????110001202100011002
Dege hendeyi	??????????????????????1111??21211?10?00?
Delphinornis arctowskii	??
Delphinornis larseni	??

APPENDIX 4
(Continued)

Character	.........130........140......150.....160
Delphinornis gracilis	??
Delphinornis wimani	??
Duntroon "*Palaeeudyptes*"	??20????????????1??00?110001202100011002
Duntroonornis parvus	??
Eretiscus tonnii	??????????????????????1111?221211?1??002
Icadyptes salasi	??????????????????????110?0120210?011002
Madrynornis mirandus	??2??????1?1????1001101111??2121?01?0002
Marambiornis exilis	??
Marplesornis novaezealandiae	??2??????1010?0110?11?111?1?212???10?00?
Mesetaornis polaris	??
Pachydyptes ponderosus	????????????????1?000?11000120210000A1002
Palaeeudyptes gunnari	??????????????????????11000120210001?10?
Palaeeudyptes klekowskii	??????????????????????11000120210?01?102
Palaeospheniscus bergi	??2?21????????????????1111A2212110100002
Palaeospheniscus biloculata	??????????????????????111?A?21211?1000??
Palaeospheniscus patagonicus	???????????????1???11?1111A2212110100002
Paraptenodytes antarcticus	??????????????????0???110001202110110002
Perudyptes devriesi	??????????????????????11000120110001?112
Platydyptes marplesi	?????????1?00?0110010?1101022021?01??002
Platydyptes novaezealandiae	??????????????????????11?1022?2??01??00?
Pygoscelis grandis	?????0????????????????1?????21???????0?2
Spheniscus chilensis	???????????????????11?111????121?01??002
Spheniscus megaramphus	??
Spheniscus muizoni	??20?????????????0?11?1111?22121?01??002
Spheniscus urbinai	???0?????????1??10011?111112212120100002
Waimanu manneringi	??111???????????????????????????????????
Waimanu tuatahi	??1???????????000??01?11010?2011010?0111
IB/P/B-0382	??????????????????????110???21?1??0??0?2
"*Tonniornis*"	??????????????????????11????2021??0??0?2

Character	.........170........180......190.....200
Gavia immer	??20?03?0010000000102011000?200010000001
Gavia stellata	??20?03?00100000001020?1000?2000?0000001
Daption capense	??20?03?0110000100101111020?1000?0000001
Diomedea exulans	??20?03?0010000100122011020?110000000001
Macronectes giganteus	??20?03?0010000100122111020?100000000001
Oceanites oceanicus	??20?03?0110000100101101020?100000000001
Oceanodroma leucorhoa	??20?03?0010000100101101020?110000000001
Pachyptila desolata	??20?03?0110000100121101020?100000000001
Pelecanoides urinatrix	??20?03?0110000100101111020?100000000001
Phoebastria immutabilis	??20?03?0010000100122011020?1000?0000001
Phoebetria palpebrata	??20?03?001000010012???1020?11???0000001
Procellaria aequinoctialis	??20?03?0010000100101111020?10???0000001
Pterodroma incerta	??20?03?0010000100101111020?100000000001
Puffinus griseus	??20?03?0010000100101111020?200000000001
Thalassarche melanophrys	??20?03?0010000100122011020?110000000001
Aptenodytes forsteri	1011012011011110110010101110001112012101
Aptenodytes patagonicus	1011012011011110110010101110001112012101
Pygoscelis adeliae	1011012011011110110110101112001112011111
Pygoscelis antarctica	1011012011011110110210101112001112011111
Pygoscelis papua	101101201101111011021010111100111201B111
Megadyptes antipodes	1011012011011110110010101111001112012101
Eudyptes chrysocome	1011012011011110110010101111001112012101

APPENDIX 4
(Continued)

Character	.........170........180......190.....200
Eudyptes chrysolophus	1011012011011110110010101111001112012101
Eudyptes filholi	1011012011011110110010101111001112012101
Eudyptes moseleyi	1011012011011110110010101111001112012101
Eudyptes pachyrhynchus	1011012011011110110010101111001112012101
Eudyptes robustus	1011012011011110110010101111001112012101
Eudyptes schlegeli	1011012011011110110010101111001112012101
Eudyptes sclateri	101101201101111011001010111100111201B101
Eudyptula minor	1011012011011110110010111111001112012101
Spheniscus demersus	1A11012011011110110010111111001112012101
Spheniscus humboldti	1111012011011110110010111111001112012101
Spheniscus magellanicus	1111012011011110110010111111001112012101
Spheniscus mendiculus	1111012011011110110010111111001112012101
Anthropornis grandis	?????????????????????????????????11?0110
Anthropornis nordenskjoeldi	??0??????????????????????????????11?0110
Anthropornis sp. UCMP 321023	?????????????????????????????????11?0110
Archaeospheniscus lopdelli	1?10110??????????????????????????20?0211
Archaeospheniscus lowei	1110110???????????????????12????????????
Burnside "*Palaeeudyptes*"	1?002?10?111??1?????????????0??102??01?2
Dege hendeyi	??1??????????????????????????????20?21??
Delphinornis arctowskii	?????????????????????????????????2010111
Delphinornis larseni	?????????????????????????????????1010111
Delphinornis gracilis	?????????????????????????????????1010111
Delphinornis wimani	?????????????????????????????????2010??1
Duntroon "*Palaeeudyptes*"	1?002110?1011110????????????????????????
Duntroonornis parvus	?????????????????????????????????20?02?1
Eretiscus tonnii	1?1??????????????????????????????10111?2
Icadyptes salasi	1?00211011110110000?????????????????????
Madrynornis mirandus	101??12????11?10???????0??110?111201?101
Marambiornis exilis	?????????????????????????????????1000111
Marplesornis novaezealandiae	??11012?1???????????????????????????????
Mesetaornis polaris	?????????????????????????????????1000111
Pachydyptes ponderosus	11002????1?10?10????????????????????????
Palaeeudyptes gunnari	11002????????????????????????????20?0112
Palaeeudyptes klekowskii	??002????????????????????????????2000112
Palaeospheniscus bergi	101?01???1011110???0?0???????????20111?2
Palaeospheniscus biloculata	??????????????????????????????11???????2
Palaeospheniscus patagonicus	10100120?1011110??????????110?11120111?2
Paraptenodytes antarcticus	10101?????????????????????12?111120?0?11
Perudyptes devriesi	0????????1?100?0???010?????????1?B0?01??
Platydyptes marplesi	??101101??011110????????????????????????
Platydyptes novaezealandiae	1?101101????????????????????????????????
Pygoscelis grandis	10???1??1??????????0???0????????1201?111
Spheniscus chilensis	111??12???011?10????????????????1???2???
Spheniscus megaramphus	??
Spheniscus muizoni	111?012??1?11?10????????????????1201210?
Spheniscus urbinai	111101??11011110???0???1??1??????2012101
Waimanu manneringi	???????????????????0??11????01??01000001
Waimanu tuatahi	0??0?010?0100011?????????????????10?00?1
IB/P/B-0382	??0?????????????????????????????????????
"*Tonniornis*"	110?????????????????????????????????????

APPENDIX 4
(Continued)

Character	.........210....219
Gavia immer	00?????????????????
Gavia stellata	00?021?1?01????????
Daption capense	00?????????????????
Diomedea exulans	00?????????????????
Macronectes giganteus	00????????????????0
Oceanites oceanicus	00?????????????????
Oceanodroma leucorhoa	00?????????????????
Pachyptila desolata	00?????????????????
Pelecanoides urinatrix	00?????????????????
Phoebastria immutabilis	00?????????????????
Phoebetria palpebrata	00?????????????????
Procellaria aequinoctialis	00?????????????????
Pterodroma incerta	00?????????????????
Puffinus griseus	00????????????????0
Thalassarche melanophrys	00?????????????????
Aptenodytes forsteri	21110110110110011?1
Aptenodytes patagonicus	211101101101100112?
Pygoscelis adeliae	21112100211100111?1
Pygoscelis antarctica	21112100211100111??
Pygoscelis papua	211121102111001112?
Megadyptes antipodes	21001010211001110??
Eudyptes chrysocome	21?????????????????
Eudyptes chrysolophus	210011100000111001?
Eudyptes filholi	21?????????????????
Eudyptes moseleyi	21???????????????1?
Eudyptes pachyrhynchus	210011A0000011100??
Eudyptes robustus	21?????????????????
Eudyptes schlegeli	21001110000011100??
Eudyptes sclateri	21?????????????????
Eudyptula minor	210021001001000000?
Spheniscus demersus	210010110110211000?
Spheniscus humboldti	21001011011021100?1
Spheniscus magellanicus	210010110110211000?
Spheniscus mendiculus	210010110110211000?
Anthropornis grandis	21?????????????????
Anthropornis nordenskjoeldi	2??????????????????
Anthropornis sp. UCMP 321023	2??????????????????
Archaeospheniscus lopdelli	21?????????????????
Archaeospheniscus lowei	???????????????????
Burnside "*Palaeeudyptes*"	2??????????????????
Dege hendeyi	2??????????????????
Delphinornis arctowskii	01?????????????????
Delphinornis larseni	01?????????????????
Delphinornis gracilis	A1?????????????????
Delphinornis wimani	A1?????????????????
Duntroon "*Palaeeudyptes*"	???????????????????
Duntroonornis parvus	?1?????????????????
Eretiscus tonnii	?1?????????????????
Icadyptes salasi	???????????????????
Madrynornis mirandus	21?????????????????
Marambiornis exilis	11?????????????????
Marplesornis novaezealandiae	???????????????????
Mesetaornis polaris	11?????????????????
Pachydyptes ponderosus	???????????????????

APPENDIX 4
(Continued)

Character	.........210....219
Palaeeudyptes gunnari	21?????????????????
Palaeeudyptes klekowskii	21?????????????????
Palaeospheniscus bergi	21?????????????????
Palaeospheniscus biloculata	?1?????????????????
Palaeospheniscus patagonicus	21?????????????????
Paraptenodytes antarcticus	21?????????????????
Perudyptes devriesi	2??????????????????
Platydyptes marplesi	???????????????????
Platydyptes novaezealandiae	???????????????????
Pygoscelis grandis	21?????????????????
Spheniscus chilensis	???????????????????
Spheniscus megaramphus	???????????????????
Spheniscus muizoni	21?????????????????
Spheniscus urbinai	21?????????????????
Waimanu manneringi	01?????????????????
Waimanu tuatahi	01?????????????????
IB/P/B-0382	??0????????????????
"*Tonniornis*"	???????????????????

APPENDIX 5

Anatomical Abbreviations

ac	acetabulum
acr	acromion
af	articular facet for alular phalanx
am	adductor mandibulae externus, pars profundus tubercle
art	articular surface for antitrochanter
at	antitrochanter
c	convexity on metatarsal II
cf	coracoid fenestra
ci	capital incisure
d	ovoid depression (see text)
de	lateral epicondylar depression
dst	dorsal supracondylar tubercle
dt	dorsal tubercle
dvf	distal vascular foramen
f	proximal end of left femur
fc	fibular crest
fp	fossa for insertion of m. pectoralis
fpt	articular facet for pterygoid
fq	articular facet for quadrate
gl	glenoid facet
if	infracotylar fossa
il	iliac blade
ilf	ilioischiadic foramen
is	contact between ilium and synsacrum
lc	lateral cnemial crest
ld	m. latissimus dorsi insertion scar
lpvf	lateral proximal vascular foramen
ls	lateral intermetatarsal sulcus
m	matrix encrusted onto bone (does not represent extent of cranial cnemial crest)
mcI	intact portion of metacarpal I
mcII	metacarpal II
mcIII	metacarpal III
mpvf	medial proximal vascular foramen
ms	medial intermetatarsal sulcus
mtr	middle trochlear ridge
nc	nuchal crest
nf	nutrient foramen
oc	occipital condyle
ol	olecranon
or	orbital process
ot	otic process
pa	preaxial angle
pi	postiliac spine
pm	fragment of left and right premaxillae
po	postorbital process
pp	pisiform process
pr	proximal process
ps	parasphenoid
ptr	posterior trochlear ridge
pII-1	manual phalanx II-1
pII-2	manual phalanx II-2
pIII-1	manual phalanx III-1
r	ridge
rc	radial condyle
s	mandibular symphysis
sb	scapular blade
sc	sagittal crest
scr	m. supracoracoideus insertion scar
sf	salt gland fossa
sp	synsacral spine
stf	secondary tricipital fossa
stm	sternal margin
su	supratendinal bridge
t	tubercle at intersection of supracondylar crests
tf	temporal fossa
tr	trochanteric crest
trf	tricipital fossa
ts	transverse ligament sulcus
tII	trochlea II
tIII	trochlea III
tIV	trochlea IV
uc	ulnar condyle (distal surface missing)
II	articular facet for phalanx II-1
III	articular facet for phalanx III-1